Summer 2021

Rainfall-Runoff Mechanisms and Flood Mitigation in a Coastal Watershed with Numerous Wetlands and Ponds

Homa Jalaeian Taghadomi
Old Dominion University, hjala001@odu.edu

RAINFALL-RUNOFF MECHANISMS AND FLOOD MITIGATION IN A COASTAL WATERSHED WITH NUMEROUS WETLANDS AND PONDS

by

Homa Jalaeian Taghadomi
B.S. June 2007, Birjand University, Iran
M.E. January 2012, University of Putra, Malaysia

A Dissertation Submitted to the Faculty of
Old Dominion University in Partial Fulfillment of the
Requirements for the Degree of

DOCTOR OF PHILOSOPHY

CIVIL AND ENVIRONMENTAL ENGINEERING

OLD DOMINION UNIVERSITY
August 2021

Approved by:

Xixi Wang (Director)

Tom Allen (Member)

Mujde Erten-Unal (Member)

ABSTRACT

RAINFALL-RUNOFF MECHANISMS AND FLOOD MITIGATION IN A COASTAL WATERSHED WITH NUMEROUS WETLANDS AND PONDS

Homa Jalaeian Taghadomi
Old Dominion University, 2021
Director: Xixi Wang

This study analyzed mechanisms of flooding in Blackwater River Watershed, located in coastal Virginia and hydraulically connected with mid-Atlantic Ocean. The analysis was based on the examination and simulation of the rainfall-runoff relationship, and such an analysis is very important for conventional water resource management and dealing with hydrologic extremes (e.g., floods and droughts, as well as ecological and pollution discharges). The rainfall-runoff relationship is a quantitative description of the hydrologic cycle, a dynamic process that can be interactively influenced by various factors, namely climate, topography, soils, land use and land cover, and land management practice.

In the past 60 years, there is no significant changes in precipitation patterns, so climate change can be downplayed. The rainfall-runoff relationship has not been changed by human activities and was found to be independent of drainage areas within the watershed. The overall storage capacity tended to be smaller in an upstream than a downstream drainage area. The drainage area above Dendron, Virginia, had a runoff coefficient of zero to 0.6, while the drainage area above Franklin had a runoff coefficient of 0.05 to 0.32.

The observed data at Dendron and Franklin, Virginia, indicated that baseflow accounted for more than 50% of the total streamflow at the annual scale and in spring and winter. Such a percentage was smaller in summer and fall because a higher evapotranspiration lowered the water table. Regardless of the seasons, the shallow aquifer beneath the watershed was discharging groundwater into the Blackwater River all the time.

Although the current Soil and Water Assessment Tool (SWAT) model had limitations in mimicking the baseflow variations and representing the storages across the study watershed, it was judged to be good enough for the model to be used for screening possible flood-mitigation scenarios. Moreover, the historical floods incurred by the study watershed were primarily caused by storms with an above-normal intensity and/or duration.

Using gated outlet structures to regulate the water levels in the storages can be a cost-effective flood-mitigation measure for the Blackwater River Watershed.

ACKNOWLEDGEMENTS

I would like to express the deepest appreciation to my academic advisor, Professor Xixi Wang, who has the attitude and the substance of a genius; he continually and convincingly conveyed a spirit of adventure in regard to research, and an excitement in regard to teaching. Without his guidance and persistent help this dissertation would not have been possible. It has been an honor to be his student.

I would like to thank my committee members, Professor Tom Allen, for his guidance, dedications of time and services, and Dr. Mujde Erten-Unal for all her support and mindful encouragements. Also, I appreciate all faculty and staff members in the Department of Civil and Environmental Engineering (CEE) at ODU.

I would like to thank my family from my heart. My husband, Turaj, gives me all love, encouragement, and support. I feel lucky to have him, his love, friendship, and support. My little three years old daughter, Hilla, for all her love and joy. My parents and siblings give me love, encouragement, and support. Finally, I would like to express my extreme sincere gratitude and appreciation to my brother Reza, for all his support since I graduated from high school and encouraged me to pursue higher education abroad.

NOMENCLATURE

A	Amplitude Ratio, (No Units)
C	Centroid of pipe, inches
Do	Outside Diameter of Pipe, inches
E	Modulus of Elasticity, lb/in2
EH	Elastic Modulus at Operating Temperature, lb/in2
f	Stress-Range Reduction Factor, (No Units)
F	Force, lbs
I	Moment of Inertia of Pipe, in4
N	Number of Cycles, cycles
P	Pressure, lb/in2
R	Stress Ratio, (No Units)
Sa	*Sh* = Allowable Static Stress, lb/in2
Sc	Allowable stress at Minimum Temperature (70°), lb/in2
Se	Endurance Limit, lb/in2
SY	Yield Strength, lb/in2
V	Shear, lbs
ZNom	Section Modulus, in3

TABLE OF CONTENTS

Page

LIST OF TABLES

LIST OF FIGURES

Figure Page

Figure Page

CHAPTER 1

INTRODUCTION AND LITERATURE REVIEW

1.1 Background

Coastal watersheds are characterized by their special features, including hydraulically connected to the ocean, more wetlands and depressions, more permeable soils (DeCatanzaro *et al.*, 2009), high water table (H. Kang and Nielsen, 1997), low topographic gradients (Magilligan *et al.*, 2008), large spatiotemporal fluctuations of precipitation (Castillo *et al.*, 2014), diverse vegetation coverages (Caris *et al.*, 2013; Luna *et al.*, 2011), and poorly-defined drainage geomorphology (Fares and El-Kadi, 2008). Coastal watersheds start up with the streams and rivers that flow downstream to the coastal plains and ultimately into the ocean (EPA, 1998). They are already influenced by sea level rise, climate change, and adverse effects from a variety of human activities (Mallin *et al.*, 2000).

Because coastal watersheds are generally in low-gradient areas with moderate slopes (Magilligan *et al.*, 2008) and a massive volume of storage capability, streams are not straightforward in coastal plains and water is regarded in the channels (Shen *et al.*, 2019). When soils are saturated during rainy seasons, runoff is mostly produced as the surface flow (Lu *et al.*, 2006). Moreover, the absence of adaptation, rapid development, and human population (DeCatanzaro *et al.*, 2009) in the coastal plains, accompanied with more sea level rise incidents (Tahvildari and Castrucci, 2020), increases the frequency and magnitude of the annual flooding (Oppenheimer. *et al.*, 2016). Therefore, extreme storm events in coastal watersheds due to urbanization, land use and human population and activities over the last 40 years have led to increase levels of flood damage in flood prone areas (Crossett *et al.*, 2013). Nevertheless, the impact of the variability in annual rainfall was discovered to be more important than the land use form on annual outflows drained out of coastal watersheds (Amatya *et al.*, 2002).

In the context of climate change and sea level rise in coastal watersheds, flooding is the most common natural hazard (Hallegatte *et al.*, 2013; Tahvildari and Castrucci, 2020; Woodruff *et al.*, 2013). Floods are hydrological events categorized by significant magnitudes of water levels and discharges, leading to inundation of residential areas and/or lands adjacent to streams, rivers, lakes, and reservoirs (Marsalek *et al.*, 2000). Flooding adversely impacts the society, economy, and environment. The impacts on society and economy include losses of lives and properties and damages of infrastructure, while the impacts on environmental, such as sedimentation, pollution, and destroying of natural habitats, to just name a few, can be comprehensive and extensive (Marsalek *et al.*, 2000). The process of generating runoff depends on precipitation, interception, evaporation, infiltration, soil moisture conditions, land gradient and water storages.

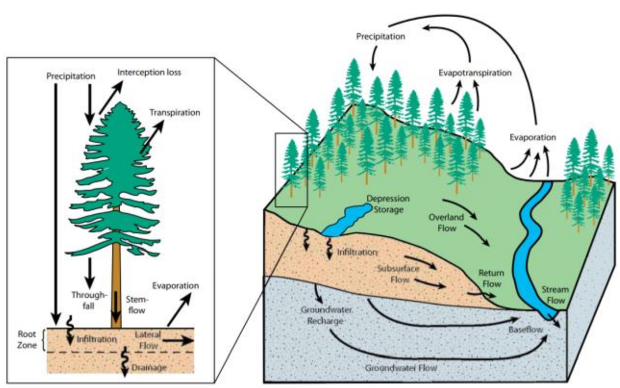

Figure 1.1. The hillslope hydrologic cycle and stand water balance (Winkler *et al.*, 2010).

Intense rainfall and severe storm tide are critical factors for flooding (Bilskie and Hagen, 2018; Dawson *et al.*, 2008); and if they occur at a same time, their combined effects exacerbated flooding (Castrucci and Tahvildari, 2018; Shen *et al.*, 2019; K. Xu *et al.*, 2014). Although, in coastal watersheds stormwater collected by drainage system is led into the sea, during high tide events, the drainage capacities are decreased with groundwater flows (Shen *et al.*, 2019) and severe storm surge events can generate widespread coastal flooding (Castrucci and Tahvildari, 2018). As a result, flooding occurs when the conveyance capacity of the waterways is exceeded by the runoff flowing downstream, which can be resulted from reduction in the natural ground and/or soil capacity that can absorb surface runoff, as well as from storms with a large rainfall intensity and/or a long-lasting duration. Heavy storm, failure of dam and/or rapid snowmelt can cause the inundation from hours to days and riverine flooding, which is very common in the contiguous United States of America (USA) (FEMA, 1992). Then, coastal watersheds experience mild and severe tidal flooding which naturally happen due to high tides and heavy rainfall causing backwater to the low-lying areas in coastal watersheds (CDC, 2017; NOAA, 2017). Unlike riverine flooding, coastal flooding is caused by backwater effects and toward-inland storm surges during high tides. Such effects and surges can be resulted from severe storms, hurricanes, or tsunamis. The erosion associated with coastal flooding can be deteriorated by human developments and lacking beach protection measures (FEMA, 1992).

On the other hand, the placement of human property and population in U.S. coastal areas are increasing (Gunn, 2016; Hallegatte *et al.*, 2013). Then residential areas where there is abundance of people and commercial activities, coastal ecosystems face to coastal hazards, such as hurricanes, erosion, and sea level rise (Crossett *et al.*, 2013). Regardless of the type of flood, residential areas that are located in floodplains, flood damage can happen because of deforestation of the coastal area as an important impact on water table (Lu *et al.*, 2006; Winkler *et al.*, 2010). Although the risks and costs of flooding damage are unknown (Kreibich *et al.*, 2005), the economic and financial profits by living in the flood zones are certain (White, 1937) and these advantages lead to the growing of urbanization and population (Burton *et al.*, 1968).

Additionally, natural resources such as water quality and quantity have been influenced by human development, resulting in changes of land use and land cover along the land-seawater interface (Fares, 2008). Urbanization and climate change (Miller and Hutchins, 2017) and also timing of the floods have a large impact on urban flooding and water quality (Howitt *et al.*, 2007). Coastal flooding is raising exposure to health risks (CDC, 2017).

Although essential progresses have been made in planning, designing, and implementing flood mitigation measures, the flooding impacts have been increasing all over the world, including USA (A. Bronstert, 1995; Pielke *et al.*, 2002). Among them, a cost-effective non-engineering measure is to provide timely and consistent information to the public about the risk from flooding (FEMA, 2001). Regardless of its purposes, land use planning and discourse must be coordinated with flood management planning (Marsalek *et al.*, 2000).

In reality, damaging floods are usually dependent on four factors, namely meteorological conditions, catchment characteristics (figure 1.2), stream conveyance capacities, and floodplain managements (A. Bronstert, 1995). In urban environments, both inadequate storm sewer systems and dense properties and infrastructure make it more challenging to mitigate the flooding impacts. The construction of larger-capacity drainage systems to cope with flooding is very expensive (Schmitt *et al.*, 2004). To mitigate flood risk and control stormwater, flood walls and tide gates have been planned (Shen *et al.*, 2019).

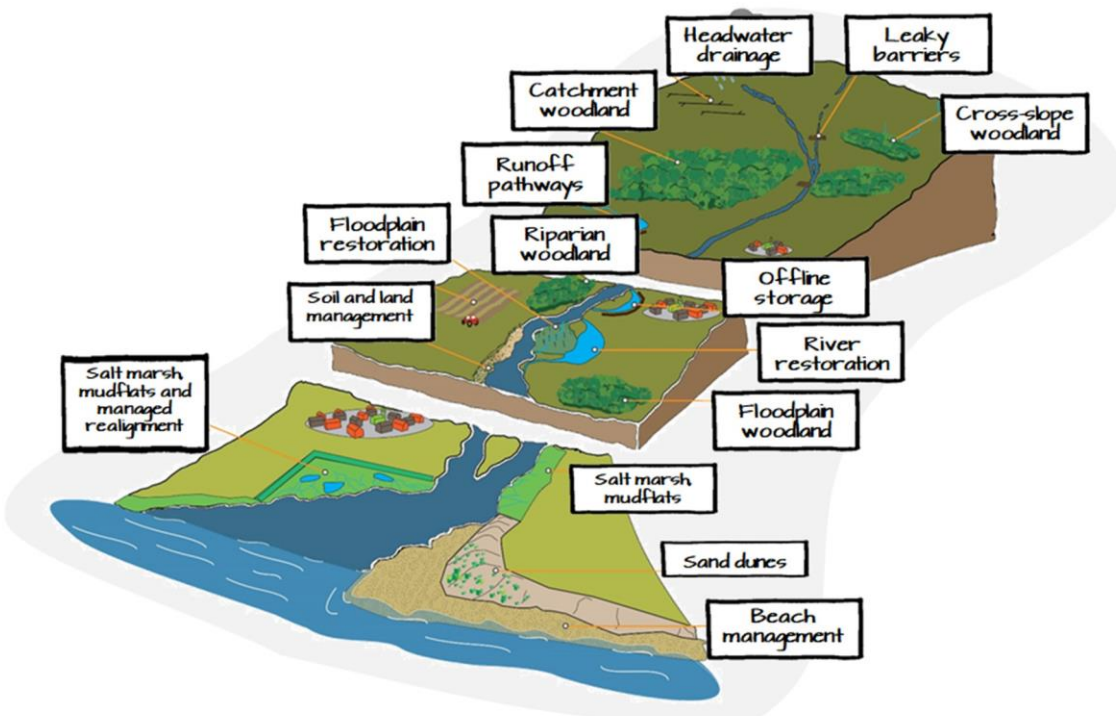

Figure 1.2. Coastal watershed characteristics. (Environment Agency, 2017).

It has been reported that climate change has resulted in, and will continue to result in, more frequent storm events with a larger magnitude, causing flooding, impacting the local economic, and reducing the sustainability of the society (Adam Terando, National Climate Assessment). Climate change is conventionally acknowledged in the global and continental spatial scales. However, flood management must be done at basin, watershed, and/or catchment scales. Currently, tools and data are very limited for planners, center directors, base commanders, local civic and governmental officials, scientists, and engineers to assess impacts of climate change at such management scales. The existing data can only reflect a few of environment conditions that influence wildlife habitat, agriculture, silviculture, and rural and urban population. The global climate change assessments used two primary data sources: National Oceanic and Atmospheric Administration (NOAA) weather data covering large areas and individual rain gauge data in specific areas. These two sources must be assessed for suitability in basins. The flooding is likely to become more severer due to changing climate and rising sea level (Huntington, 2010; Oki and Kanae, 2006).

1.2 Literature Review

One of the most fundamental hydrologic processes to understand is the rainfall-runoff relationship due to the variability of the spatial and temporal watershed characteristics (Tokar and Johnson, 1999). The procedure of transforming rainfall into runoff over a watershed is generally approximate due to the non-linear functionality (ASCE, 2000; Rajurkar *et al.*, 2004). The relationship between rainfall and runoff can be affected by both climate change (Guhathakurta *et al.*, 2011) and human activities (H. Chu *et al.*, 2019), topographic gradients (Wooldridge *et al.*, 2001), duration and intensity of rainfall (Goel *et al.*, 2000), water storage capacity (Darboux *et al.*, 2002), vegetation (Dunne *et al.*, 1991), catchment size and shape (Pilgrim *et al.*, 1982), and land use and land cover characteristics (Wei *et al.*, 2007; Wooldridge *et al.*, 2001). Some ecosystem changes may accompany climate change and affect hydrology, such as shift from forest to marshes in floodplains (Wan *et al.*, 2021). To date, the rainfall and runoff relationship has been extensively studied as one of the fundamental concepts in water resources management, but it is not well understood for coastal watersheds (Areerachakul and Junsawang, 2014). The hydrologic processes that affect the generation of runoff in a watershed include precipitation, infiltration, soil saturation, hillslope, interception, evaporation, and groundwater (Winkler *et al.*, 2010). Hydrologists have studied for many years to find out the transformation of precipitation into the runoff, to predict streamflow in the purposes of water supply, flood control, irrigation, water quality, drainage, recreation, power generation, and fish and wildlife propagation (Tokar and Johnson, 1999). The general relation is that runoff increases with rainfall and vice versa (El-Jabi and Sarraf, 1991; Rafter, 1903; Todini, 1988). High-intensity rainfall decreases the runoff lag time (Mu *et al.*, 2015). Other physiographical aspects that directly affect the amount of rainfall and the volume of runoff have also been widely examined and documented in exiting literature.

The importance of quantifying the rainfall-runoff relationship requires no preamble for hydrologic engineering design and water resources management (Nourani *et al.*, 2009; Sitterson *et al.*, 2017). However, such a relationship can be sophisticated for coastal watersheds, which usually have numerous wetlands and receive rainfall storms with a large spatiotemporal variability (Brocca *et al.*, 2011; Talchabhadel *et al.*, 2015). In this regard, a large variety of models have been developed and applied to understand the rainfall-runoff relationship and forecast flooding (Nayak *et al.*, 2005). One of the studies has conducted a linear regression model for investigating the association between rainfall intensity and runoff during storm events in the White Volta River at Pwalugu (Kasei *et al.*, 2013). Regression analyses were also implemented to understand the rainfall-runoff relationship under different storm scenarios in Beijing, China (L. Yao *et al.*, 2016).

One of the critical environmental challenges is soil erosion during rainfall events causing from soil separation and transport by rainfall-runoff processes. Soil erosion not only can decrease the land productivity but also can decrease slope stability and lead to landslides or debris flow. Slope steepness is an essential topographic aspect, which can control the infiltration and runoff directly (S. Wu *et al.*, 2017).

Several attempts have been made to model, simulate, and predict flood scenarios by analyzing rainfall-runoff behaviors in different regions (Ahn *et al.*, 2014; Barszcz, 2016; Brocca *et al.*, 2011; Costa and Fernandes, 2017; Orupabo *et al.*, 2015; Zeng *et al.*, 2016). Most of the widely-used hydrologic models, such as HEC-HMS (Hydrologic Engineering Center Hydrologic Modeling System), Artificial Neural Network (ANN), and SWAT (Soil and Water Assessment Tool), have been introduced in literature (S. L. Neitsch *et al.*, 2011). SWAT as a powerful interdisciplinary watershed modeling tool (Gassman *et al.*, 2007) has been rapidly employed to improve runoff predictions for watersheds with varying physical characteristics and management practices (Bingner, 1996; Cheng *et al.*, 2016; Kannan *et al.*, 2007; Manguerra and Engel, 1998; Rostamian *et al.*, 2008; A. Zhang *et al.*, 2012). In the hydrologic simulation, SWAT has been applied in literatures to use the curve number (CN) method for the simplicity of runoff estimation (Tasdighi *et al.*, 2018). To find the relationship between rainfall and runoff, the artificial neural network (ANN) technique, as a non-linear inter-extrapolator and essential prediction tool, have also been used by hydrologists (Areerachakul and Junsawang, 2014;

Rajurkar *et al.*, 2004; Tokar and Johnson, 1999). ANN and multivariate autoregressive moving average method (MARMA) have been compared during wet and dry seasons for daily streamflow discharge prediction (Areerachakul and Junsawang, 2014). It has been concluded that a ANN model can have a good performance (Rajurkar *et al.*, 2004; Sohail *et al.*, 2008) and that it can be applied when the variety of data is small and/or incomplete (Ghumman *et al.*, 2011; Tokar and Johnson, 1999). The ANN model's performance indicates that the size and geographical locations of a catchment of interest (Rajurkar *et al.*, 2004) are important factors for the relationship between rainfall and runoff.

Recent studies reveal that climate change is altering both inter-and intra-annual variations of precipitation and increasing air temperature (Huntington, 2010; Oki and Kanae, 2006). Such climate impacts are relatively more significant for coastal than continental watersheds because coastal watersheds usually have numerous wetlands and waterbodies. Climate change will result in more frequent storm events with a larger magnitude, causing flooding, impacting the local economy, and reducing the sustainability of the community (Dibike and Coulibaly, 2005; Qi *et al.*, 2009; Rahimi *et al.*, 2020). Based on some studies in Three-River Headwaters region, by increasing the temperature and no significant changes to the rainfall, the runoff trend has been declined over the 40 years (S. Zhang *et al.*, 2011). While some studies proved that by rising 1°C global annual temperature, the global runoff rate will be increased by 4% (Labat *et al.*, 2004). The results of (J. Xu, 2011) revealed the critical impacts of climate change and human activities on the relation between precipitation and runoff in Wudinghe River, China. According to (J. Xu, 2011), the impacts of climate change and human activities would compound the influence of precipitation variation on annual runoff generation.

Infiltration and saturation excesses are two different runoff generation mechanisms. When soil becomes nearly saturated, and the infiltration rate is less than the rainfall intensity, the amount of runoff will increase (Yang *et al.*, 2015). When rainfall occurs at a particular time, a portion of the rain known as interception storage and the rest of the rain reaches the land surface, and water begins to infiltrate into the soil (Mu *et al.*, 2015). The time interval used in measuring the two variables and the size of the area being considered can affect this relationship. Vegetation affects the infiltration (Dunne *et al.*, 1991); when infiltration continues for a long time period, the soil will become saturated (Rao *et al.*, 1998). Some studies investigated the effect of land use (Peng and Wang, 2012; Sun *et al.*, 2013) and urbanization on infiltration and runoff (Holman-Dodds *et al.*, 2003; I. S. Kang *et al.*, 1998). Since the 1960s, urbanization started in the On-Cheon Stream watershed in Pusan, South Korea and caused more runoff and flooding (I. S. Kang *et al.*, 1998). In addition, the Peachtree Creek watershed in the state of Georgia of USA has experienced an increase in peak runoff, especially during wet seasons in more urbanized areas compared to the less urbanized areas (Ferguson and Suckling, 1990).

Runoff, as an important component process of the hydrologic cycle, is generated by precipitation to sustain waterbodies and stream systems (Loaiciga *et al.*, 1996) though it can sometime cause flooding (Boardman *et al.*, 1994). For a given location, precipitation intensity, distribution, and duration are essential factors for runoff generation, as measured by peak discharge, volume, and time distribution of flow rates (i.e., flow hydrograph) (Desta, 2006; Goel *et al.*, 2000; B. M. Liu *et al.*, 2008; Van Dijk *et al.*, 2005). In practice, the time interval (Baker *et al.*, 1978) and the drainage area of interest (Line and White, 2007; Seaburn, 1969) can influence the qualification of such a rainfall-runoff relationship. It has been reported by a study in the Whiteoak Bayou watershed, located in the state of Texas, that the annual peak flows and runoff depth depend on the rainfall volume and urban area (Olivera and DeFee, 2007). Besides, other physiographical factors directly influence on the percentage of rainfall that can be converted into runoff. There is a linear relation between rainfall variations over a catchment and variation in runoff from the outlet of the catchment (Rajurkar *et al.*, 2004). Although hydrologists assume an empirical relationship between watershed characteristics and runoff (Brun and Band, 2000), the position of storm for storage of the rainfall relative to the watershed outlet turns out to be more critical (Syed *et al.*, 2003). This observation revealed the importance of coastal watershed position, size, and shape with the rainfall volume in generating runoff (Syed *et al.*, 2003). Further, it has been assumed that groundwater (Sklash and Farvolden, 1979) and watershed infiltration capacity (Betson, 1964) play an important role in producing surface runoff and baseflow into downstream and waterbodies. Also, the impact of soil types and geographical conditions on the rainfall-runoff relationship has been investigated in a coastal area in southern china (Fu *et al.*, 2012). Flooding has affected the economy, agriculture, tourism, and our daily life in diverse ways. Several reasons affect the magnitude of flooding, such as sea level rise (Wang Xixi *et al.*, 2017), precipitation characteristics (Bracken *et al.*, 2008), seasonal variability, and extreme storms (Niroomandi *et al.*, 2018). Changes in precipitation patterns can be associated with severe environmental events (Chen *et al.*, 2017). For instance, the reduction in the number of rainy days can result in drought, while the upward trend in the frequency of days with precipitation can increase the runoff coefficient and the risk of flooding (Kim and Lee, 2008). The critical impact of the extreme events on human life emphasizes the importance of modeling and predicting the number of rainy days.

The results of studies in different geographical areas have revealed that wetlands contribute to the treatment of stormwater runoff and mitigate the risk of flood damage to the downstream (Acreman and Holden, 2013; Hey and Philippi, 1995; Strecker, 1992). Natural wetlands, as intermediate ecosystems between aquatic and terrestrial systems, receive stormwater runoff (Carleton *et al.*, 2000; Mitsch *et al.*, 1989) and then discharge the water slowly to the downstream (Nicholls *et al.*, 1999), while a higher water surface elevation in wetlands and ponds could be resulted from storm events (van der Valk *et al.*, 1994). In the states of Texas and Florida, the relationship between wetlands and watershed flooding has been examined (Brody *et al.*, 2007). Results show that wetland areas have fewer peak flows and wetlands are effective in flood mitigation in the watersheds drained by the Charles River, Neponset River, and Ten Mile River in the state of Massachusetts (Ogawa and Male, 1986).

Climate change (Vörösmarty *et al.*, 2000) and the increase of human activities have significantly changed land use and land cover, which have essential effects on the natural waterbodies such as wetlands and ponds and hydrologic processes (Potter, 1991). The hydrologic processes are influenced by the spatial and temporal distribution of basin physiographic. For instance, the land use change can influence the amount of evapotranspiration and waterbodies as well as water consumption (Zhou *et al.*, 2019). In the state of Virginia, the runoff from rainfall through the urbanized areas might run down to the wetlands, ponds, and stormwater sewers, and ultimately empty into a creek or river, while in rural or undeveloped areas, runoff goes down and recharges groundwater. For example, since 1966, the depth to groundwater monitoring well in Fairy Stone State Park has extended from 5.98 to 27 ft in a dry season. Many monitoring wells show much deeper water tables. Another monitoring well in Accomack County indicates groundwater depth on the Eastern Shore reaching from 71 to 109 ft. Figure 1.3 shows the groundwater level from November 2009 to August 2019 in the city of Franklin, Virginia. There has been a significant increase from 2009 to 2012. While from 2012 to 2019, it increased gradually and no visible fluctuation over the period. In Franklin, the average depth to groundwater at the monitoring well is about 200 ft, much lesser than that in other sites because of the extensive industrial withdrawals. This well is positioned in the Northern Atlantic Coastal Plain aquifer system (S100NATLCP) national aquifer. Figure 1.4 illustrates that groundwater could restore during the cold period (winter), while the depth to groundwater increases during summer because of the higher evapotranspiration. This well is positioned in the Valley and Ridge (N500VLYRDG) national aquifers.

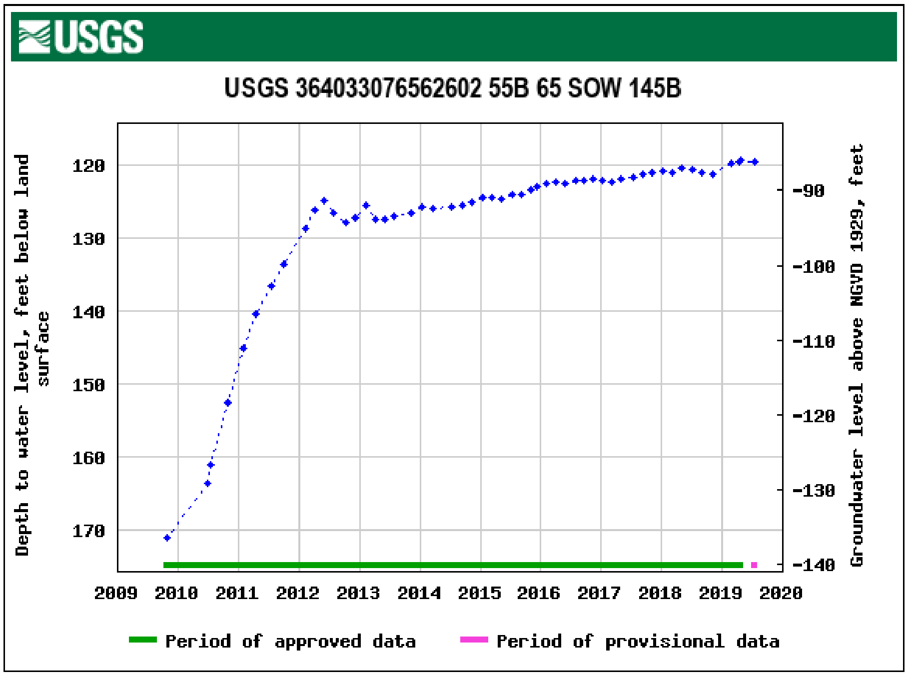

Figure 1.3. The groundwater level in the City of Franklin, Virginia.

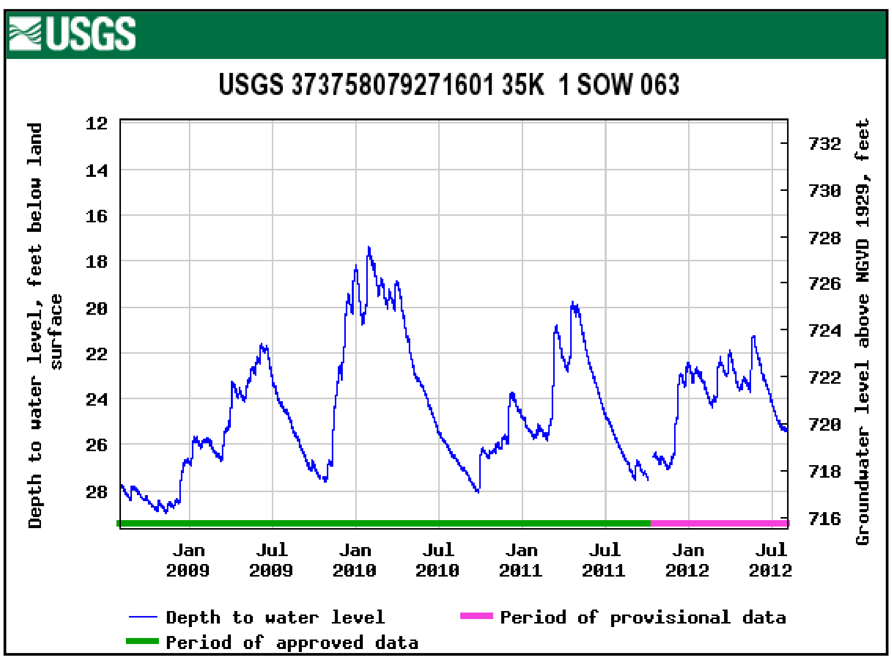

Figure 1.4. The groundwater level in Rockbridge County, Virginia.

Wetlands are wet areas by surface or groundwater recharge that store floodwaters and maintain land surface water flow over the dry period (Acreman and Holden, 2013). One critical factor in increasing the magnitude of flood damage is the river stage and velocity increase. Therefore, rather than enduring to trust real solutions for flood control, it is time to improve a flood management strategy containing wetlands and ponds to capture and hold runoff (Acreman and Holden, 2013; Hey and Philippi, 1995). The Environmental Agency for England and Wales are responsible for assessing and monitoring the runoff, and enhancing the surface water flow management practices, established constructed wetlands for the reduction of flood damage (Shutes *et al.*, 1999). Constructed wetlands can retain short-duration storms for the maximum retention period and accommodate high flows and prevent overland flow. Besides, constructed wetlands must be huge enough to conserve the first flush of the heavy storms. Wetlands and ponds should be designed on a return period of 10-year or larger, where the land availability makes this feasible (Shutes *et al.*, 1999).

Moreover, wetlands and ponds collect stormwater and then discharge the water slowly (Hunt *et al.*, 1999). This function decreases the speed and volume of runoff and reduces the risk of flood damage downstream. Wetlands and ponds usually have higher water surface elevations after storm events. Based on (Windham-Myers *et al.*, 2014), wetlands provide a temporary storage for stormwater runoff and contribute to reducing risks to public safety, decreasing damage to public or private property, promote landscape amenity, and reduce downstream flooding and erosion in the urban area (Acreman and Holden, 2013). They can also store floodwaters during high runoff events analogous to serving as natural sponges that soak up water (Martin and Smoot, 1986). The degradation of wetlands in the watershed areas could cause a dramatic increase in flood peaks in those areas. Wetlands located inside and upstream of rural areas are very valuable for flood mitigation (Wong *et al.*, 1999). The detention period of stormwater wetlands and ponds is highly variable because of the stormwater inflow's alternating and unsteady nature (Wong *et al.*, 1999). Also, wetlands cause discharging groundwater to the land surface or preventing quick drainage of water from the land surface (Winter *et al.*, 1998). A remarkable variety of wetlands are found through the Virginia landscape. Four percent of the Virginia territory has been covered by wetlands and ponds (Dahl, 1990). Wetlands located in the west of the Coastal Plain are mostly small and isolated, and their positions and sizes are dictated principally by topography, precipitation, and groundwater availability (Heath, 1984).

To view America's wetland resources, the Wetland Mapper from U.S. Fish & Wildlife Service (National Wetlands Inventory) website (https://www.fws.gov/wetlands/ data/ mapper.html) has been designed to integrate digital map data and other resource materials to generate current information and functions of wetlands. In the Blackwater River watershed, there are 19,499 wetlands with a total surface area of 311 km^2, including lakes, freshwater ponds, freshwater frosted and shrub wetlands, freshwater emergent wetlands, and riverine. This dissertation investigates the contributing indicators to the rainfall-runoff relationship to forecast flooding in the coastal watershed with numerous wetlands and ponds.

Hydrologists assume that there is a relationship between watershed characteristics and runoff. The interaction between extreme rainfall and severe storm surges have a comprehensive impact on flooding (Bilskie and Hagen, 2018; Dawson *et al.*, 2008), exacerbating the flooding risk (Castrucci and Tahvildari, 2018; Shen *et al.*, 2019; K. Xu *et al.*, 2014). Modeling the rainfall-runoff relationship is fundamental in the fields of hydrology and water resource management. Such a relationship depends on several factors, such as geological settings, land cover and land use, soil properties, and human activities. Given its sophistication and site-specific features, modeling the rainfall-runoff relationship in a coastal watershed is still incomplete. The watersheds with a long-term record of rainfall and runoff observations and numerous wetlands and ponds can provide an excellent opportunity to examine the rainfall-runoff relationship for flood forecasting.

1.3 Dissertation Goal and Objectives

The ultimate goal was to advance existing knowledge in rainfall-runoff relationships and flood mitigation strategies in coastal watersheds with numerous wetlands and ponds. The specific objectives were to:

- Quantify the rainfall-runoff relationship as influenced the dynamic or sensitivity to climate change
- Setup a hydrologic model for a coastal watershed
- Use the model to predict impacts of land use, wetlands, and climate on streamflow
- Formulate a set of hypothetical scenarios for mitigating peak runoff
- Use the model to evaluate the scenarios
- Prioritize possible measures to flood reduction

In this regard, advanced statistical techniques and a Soil and Water Assessment Tool (SWAT) model were used. SWAT is a physically based, continuous time-step hydrologic model. A baseflow filter computer program was used to separate total streamflows into base and direct flows.

Achieving these objectives will have two-fold benefits. First, the results can serve as direct solutions to flooding issues for the coastal watershed. Second, the modeling will be the first-of-its-kind effort of applying SWAT to tackle coastal hydrology in changing climate, which will add new knowledge to existing literature. This dissertation:

- Advanced understanding of the physical mechanisms of coastal flooding with numerous wetlands and ponds
- Detected trends of future climates in the mid-Atlantic region
- Predicted future floods as influenced by climate change and human activity
- Developed adaptive measures for coastal flooding
- Formulated a conceptual modeling framework for considering combined impacts of heavy storms and rising sea levels

1.4 Dissertation Structure

This dissertation is organized into seven chapters. Chapter 1 (this chapter) provides the background information, conducts a literature review, and establishes the research goal and objectives. Chapter 2 discusses data and materials on the study area's geography, physiography, and hydro-climatology. Chapter 3 examines the observed rainfall-runoff relationships, detects trends in precipitation and streamflow, and separates direct runoff and baseflow. Chapter 4 scrutinizes the statistical rainfall-runoff relationships by using a Transfer Function modeling approach and comparing this approach with two commonly used stochastic models, namely Autoregresive Moving

Average (ARMA) and Autoregresive Moving Average with Exogenous Variables (ARMAX). Chapter 5 calibrates and validates a SWAT model and uses the model to tackle the flooding mechanisms. Chapter 6 assesses possible flood mitigation conceptual non-structural and structural measures. Chapter 7 draws general conclusions and makes recommendations for flood mitigation and future research.

CHAPTER 2

DATA AND MATERIALS

2.1 Blackwater River Watershed

The 1587.66 km^2 Blackwater River Watershed, located in southeast Virginia, has numerous swamps and forested wetlands (Smith *et al.*, 2015). The elevation of the watershed varies from -20 to 160 m above mean sea level. The land use and land cover are classified into agriculture, forest, urbanization, water bodies, and pasture. The watershed receives heavy storms, resulting in frequent flooding. It drains a large portion of southeastern Virginia in the east of the fall line. During high tidal periods, the Backwater River flows can be severely slowed down or even reversed upstream, causing localized flooding. For this reason, the watershed is sensitive to rising sea level. Once heavy storms swirl throughout the area, severe flooding occasionally occurs at several points along the river as a large volume of water flows downstream (Smith *et al.*, 2015). The watershed has experienced substantial changes over the last 140 years. The logging and burning of forests from late 1800s to early 1900s (Bergschneider, 2005) increased the stream flow temperature and caused more siltation, making the stream channels broader but shallower as well as lowering the watershed storage capacity and acid-base buffering capacity (Zurbuch, 1963).

The typical flood-prone zones are the areas near the cities of Zuni and Franklin, which border Southampton County and Isle of Wight County. These vulnerable points share a common geomorphological feature that the channel cross-sections are shallow and poorly defined and that the flood stages can be reached and/or exceeded very quickly. The storm and flooding are likely to become severer due to changing climate and rising sea level (Huntington, 2010; Oki and Kanae, 2006). As a coastal watershed, the Blackwater River Watershed can incur large-scale storm events, generating much runoff leading to flooding. For instance, Hurricane Floyd in 1999 followed by an unnamed Nor'Easter storm dumped 10 in rainfall in October 2006. Such flooding damages are relatively more significant for coastal watersheds, including the study watershed drained by the 105-mi-long Blackwater River meandering through southeast Virginia. The river originates in Prince George County (37°10'49"N 77°22'54"W), flows through Isle of Wight County, and then turns south into South Hampton. The Blackwater River is a tributary of the Nottoway River to form the Chowan River (Figure 2.1).

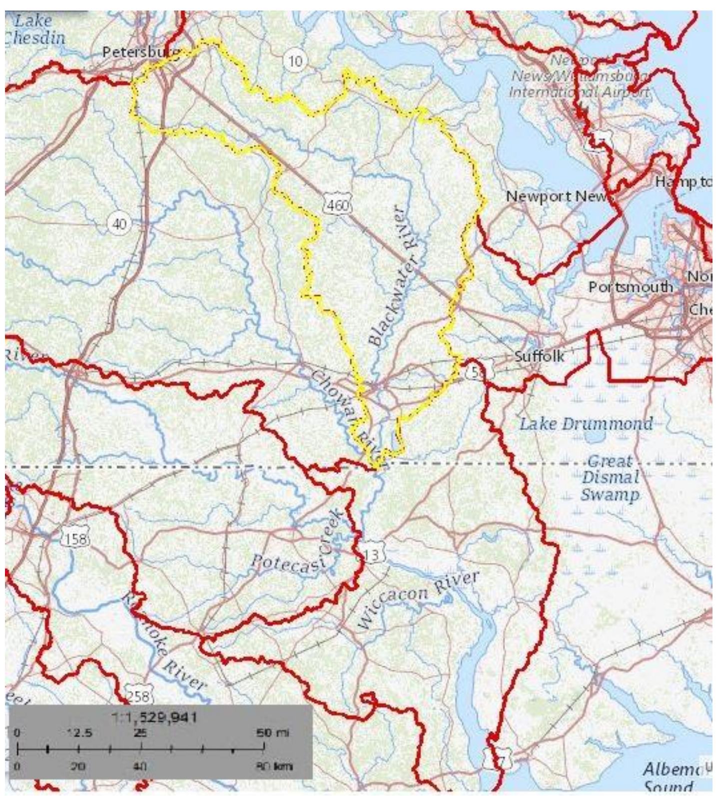

Figure 2.1. Map showing the location and flow path of the Blackwater River.

The Blackwater River is mostly a calm waterway, but it has a history of flooding during hurricanes, and tropical storms. Its name is self-explained by that its water is bright, dark, acidic, and low in nutrients and tannin stained. The river drains the area with a variety of farmlands. Because the Blackwater River watershed drains a large area of the fall line, when heavy rainfall occurs, severe flooding occasionally occurs in the population areas adjacent to the river, such as Zuni and Franklin bordering Southampton County and Isle of Wight County. The channels of these river segments are poorly defined and generally shallow with a limited conveyance capacity. Although the numerous swamps and forested wetlands in the watershed may provide some storages for floodwater, their capacities and attenuation effects have been degrading in the last 140 years (Michael, 2002). The flooding is likely to be exacerbated by climate change as well as the rising sea level. In the recent decades, the watershed incurred several severe floods, including the largest floods in September 1999 from Hurricane Floyd and October 2006 from an unnamed nor'-easter storm that dumped 10 inches of rain on the region.

Driven by tourism and residential, the land development along the river valley increased dramatically in 1970s. Such an increasing trend slowed down in 1980s and then was reversed since early 1990s, particularly during the economic recession of 1989 to 1993. The land development and past land-use practices were reasonably thought to have negatively impacted the watershed hydrology. The impacts should be reflected in the 1980 to 1993 streamflow data, which were used in this study (Smith *et al.*, 2015). Franklin (37°02′32″ N, 79°35′39″ W), which is located in Franklin County of the lower portion of the watershed, is a major population center (Figure 2.2). The Blackwater River runs along the eastern boundary of Franklin and plays a vital role on the industrialization of the city but has not been protected to notably flooding. In 1999, because of Hurricane Floyd, the Franklin's downtown was submerged under as much as 4-m-deep water when the river level raised to its historic peak value of 8.5 m, inundating 182 business and 150 homes. This flood resulted from a storm that generated a large amount of rainfall throughout the watershed most of which is located upstream of Franklin. In October 2006, Franklin incurred a similar flood from the unnamed nor'-easter storm mentioned above.

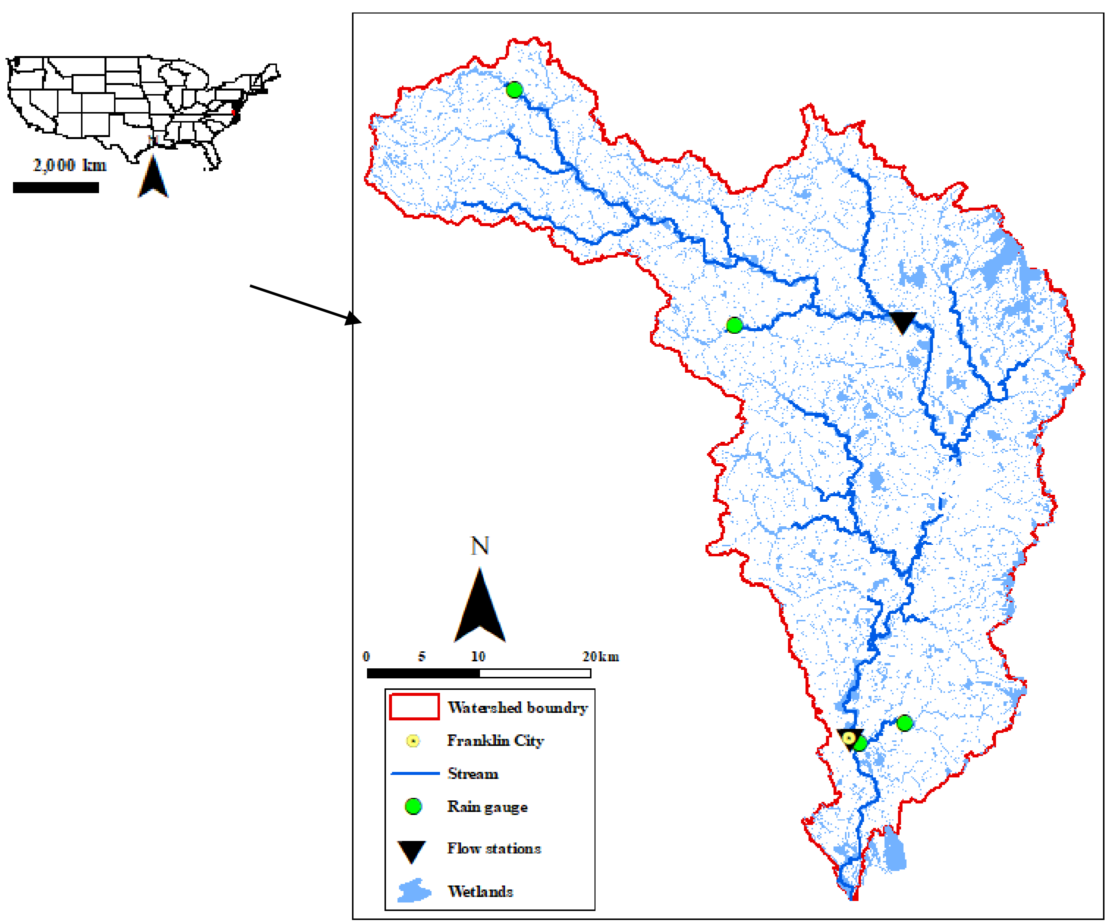

Figure 2.2. Map showing the location, rain gauges, flow stations, and wetlands of the Blackwater River Watershed.

On an average annual basis, the watershed receives 750 to 1750 mm precipitation, generating 350 to 1800 mm runoff. Although most portion of the precipitation occurs during summer, more runoff is generated during spring and winter.

2.2 Physiographic Data and Processing

Physiographic data describe the land's physical characteristics such as soil properties, land uses, topography, and drainage networks. For analysis purposes, a watershed usually needs to be divided into subbasins, each of which can include one or more hydrologic response units (HRUs). A HRU is a unique combination of homogenous soil type, land use, and topographic gradient (Winchell *et al.*, 2013). Its area and hydrologic parameters are determined in terms of the land use and soil distributions. Subdividing the watershed into small subbasins reveals various evapotranspiration and hydrologic conditions for diverse lands and soils (Kalcic *et al.*, 2015). This study used SWAT because it was developed to predict the impacts of land management practices on the water. SWAT can be used in large, complex watersheds taking into varying soils, land use land cover (LULC), and management practices over a long time period. Using ArcSWAT, the Blackwater River Watershed was subdivided into 6 subbasins and 35 HRUs (Figure 2.3).

2.2.1 Soils

Runoff depends on soil texture and structure because they determine the soil permeability

(Legret *et al.*, 1996). Water can flow through either saturated or unsaturated soils. In a saturated soil column, water moves downward and/or horizontally by its gravity, whereas in an unsaturated soil column, water can move downward by its gravity or upward by capillary suction. SWAT simulates water movements in both types of soils (S. L. Neitsch *et al.*, 2011) and calculates the volumetric water contents (i.e., soil moistures) of the soil layers (Easton *et al.*, 2008).

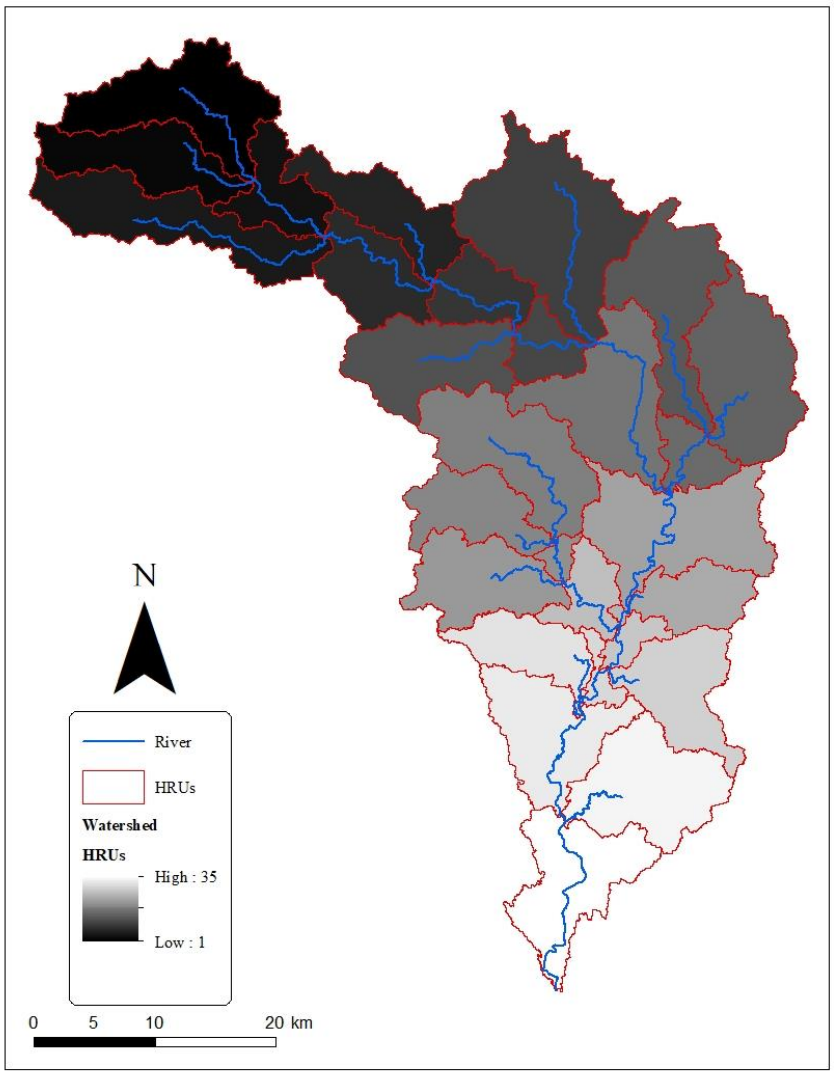

Figure 2.3. Map showing the HRUs of the Blackwater River Watershed.

The soil data were downloaded from the USDA-NRCS Soil Survey Geographic Database (SSURGO) website. SSURGO contains information on digital soil surveys and the most detailed level of soil geographic data as collected by the National Cooperative Soil Survey (Winchell *et al.*, 2013). SSURGO has a spatial resolution that is high enough for accurately predicting discharge (X. Wang and Melesse, 2006). The database, which was created by the U.S. Department of Agriculture (USDA) and Natural Resources Conservation Service (NRCS), is one of the most magnificent natural resource information systems and management in the world and provides spatial resolution for farm and ranch, land use, and land cover, and water bodies. SSURGO presents the soil spatial and attributes properties in a Geographic Information System (GIS) format (Easton *et al.*, 2008).

The SSURGO data for the eight counties in the Blackwater River watershed were downloaded and merged into a single file (X. Wang and Melesse, 2006). It maps soils in polygons with the boundaries of major land resource areas (MLRAs). MLRAs have geographically associated land resource units with common characteristics related to physiography, geology, climate, water resources, soils, biological resources, and land uses (NRCS, 2006; USDA, 2006). A soil survey area consists of parts of one or more MLRAs. Soil color, texture, size and shape of soil aggregates, kind and amount of rock fragments, distribution of plant roots, reaction, and other features identify various soils. Predictions about soil behavior are based not only on soil properties but also on such variables as climate and biological activity. Soil conditions are predictable over long periods, but they are not predictable from year to year (McAvoy and McAvoy, 1997). In Virginia, soils are enriched by the complex rivers running from mountains to the east. On the eastern coastal areas, the soils are densest and sandiest. According to USDA, the 50% area of this region has soils inappropriate for agriculture because they are acidic with a pH value of below 5.

2.2.2 Land Use and Land Cover (LULC)

Land use can have a substantial impact on flood risk (Wheater and Evans, 2009). The main changes in land use that impact hydrology are afforestation and deforestation, intensification of agriculture, drainage of wetlands, road construction, and urbanization (De Roo *et al.*, 2001). The most obvious outcome of land use is evapotranspiration (Calder, 1993). Deforestation reduces infiltration and enhances stormflow from rainfall (Peña-Arancibia *et al.*, 2019). Both the agricultural growth and over-increasing urbanization have resulted in significant changes in runoff amount and peak due to lessened interception and infiltration. While climate change has gradually affected the hydrological cycle spanning a long time period, land cover changes (Alex Bronstert *et al.*, 2002) by human activities can have imminent influences on runoff (Wheater and Evans, 2009). Runoff is generated when the infiltration capacity through land surface is exceeded and/or when infiltrating rainfall convinces a quick subsurface flow response or inundated conditions in the coastal zone (Alex Bronstert *et al.*, 2002). The typical land use drivers are infrastructure, residential doweling, urbanization, and transportation (Wheater and Evans, 2009). Urban areas have asphaltic and paved surfaces, reducing infiltration (Alex Bronstert *et al.*, 2002), whereas rural land covers primarily include woodlands, grasslands, and agricultural lands (O'Connell *et al.*, 2007). In Virginia, farming takes place in more than 69 counties and 18 cities. A considerable portion of the

Blackwater River Watershed has been used for agriculture and wood culture, where runoff is a function of the antecedent soil moisture condition and rainfall intensity (Alex Bronstert *et al.*, 2002; Winchell *et al.*, 2013). The results of previous studies revealed that changes in land use escalated the amount of runoff generated from rainfall with a decreased production threshold (Zhou *et al.*, 2019). The LULC data for the Blackwater River Watershed were downloaded from National Land Cover Database (NLCD), which provides nationwide land cover data. The land cover data were derived using 10-m Landsat imageries in 2016 which is coincide with collecting hydrology data. NLCD provides spatial reference and descriptive data for characteristics of the land surface such as thematic class (e.g., urban, agriculture, and forest), percent imperviousness, and percent tree canopy (Homer *et al.*, 2012).

2.2.3 Topography

Elevation data describe the topographic variation of land surface and delineate the stream channel and drainage network of the watershed (Band, 1986). The overland runoff depth, velocity, and direction depend on the topographic gradient (National Research Council, 2007). In the Blackwater River Watershed, many low-lying sites, adjacent to the coastal shorelines, riverine floodplains, and lake shorelines, can incur frequent flooding. Franklin is flood-prone with relatively low elevations: the highest elevation of 1746 m in Grayson County and the lowest elevation of 290 m in the area near the Atlantic Ocean. This study used the National Elevation Dataset (NED) in the Hydrology Extension of ArcMap^{TM} 10 to delineate the watershed and its subbasins as well as the drainage network (Li, 2018). The NED was downloaded from the U.S. Geological Survey (USGS) website https://www.usgs.gov/centers/eros/science/usgs-eros-archive-products-overview.

2.2.4 Drainage Network

The drainage network is elementary for water resources (Rosim *et al.*, 2015). It consists of dendritic streams, each of which drains a subbasin. Two or more higher-order (i.e., upstream) streams converge to form a lower-order (i.e., downstream) stream. It is essential to delineate the drainage network to simulate the rainfall-runoff processes (Rosim *et al.*, 2015). To characterize the drainage network, high-resolution elevation datasets are needed to trace the movement of runoff to the watershed outlet (Vieux, 2001). The Blackwater River originates from several swamps in City of Petersburg and flows southeast through Prince George County. It borders between Surry County and Sussex County and conveys the effluents out of several swamps, namely Warwick, Rotterdam, Coppahaunk, and Cypress. The river turns south and forms the border between Isle of Wight County and Southampton County, and conveys the effluents out of the other several swamps, namely Terrapin, Antioch, Seacock, Corrowaugh, and Kingsale. The Blackwater River Watershed covers portion of three cities (i.e., Franklin, Petersburg, and Suffolk) and five counties (i.e., Isle of Wight, Prince George, Southampton, Surry, and Sussex). The drainage network properties were extracted directly from the digital elevation model (DEM) using SWAT to help in the quick parameterization of hydrologic runoff models (Martz and Garbrecht, 1993). The sub-basin counts, reach length and total length, slope, and upstream and downstream coordinates of each channel link generated under different threshold values were computed in ArcGIS-based SWAT model (Martz and Garbrecht, 1993; M. Wu *et al.*, 2017).

2.3 Precipitation Data and Preprocessing

Precipitation can fall in the forms of drizzle, rain, sleet, snow, graupel, and/or hail. On average, Virginia receives 43 to 44 in precipitation annually. The data on daily precipitation at four gauges within the Blackwater River Watershed, namely Hopewell, Stony Creek, Suffolk Lake Kilby, and Holland (Figure 2.4), were downloaded from the National Oceanic and Atmospheric Administration website (NOAA) National Climate Data Center (NCDC) website https://www.ncdc.noaa.gov. The areal precipitation for a subbasin was assumed to be the same as that at its nearest gauge (Marquínez *et al.*, 2003).

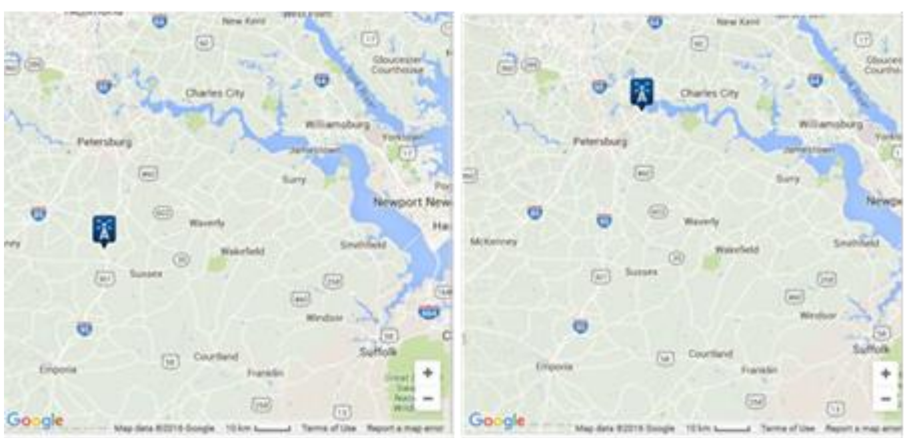

(a) (b)

[Figure 2.4.]

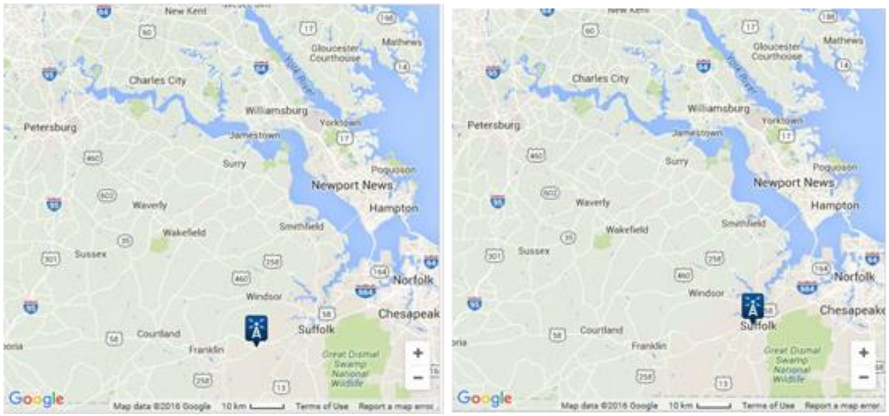

(c) (d)

Figure 2.4. Rain gauge: (a) Stony Creek; (b) Hopewell; (c) Suffolk ; and (d) Holland.

Although several other gauges also measure daily precipitation, these four gauges were chosen because the other gauges' record periods were not sufficiently long for the analysis. The selected four gauges had a record period of 1945 to 2015 and their characteristics are shown in Table 2.1.

Table 2.1. Characteristics of the four rain gauges used in this study.

Name	Suffolk Lake	Holland 1E	Stony Creek	Hopewell
Network: ID	USC00448192	USC0044404	USC00448129	USC00444101
Latitude (°)	36.7297	36.683	36.9742	37.2992
Longitude (°)	-76.6015	-76.7684	-77.4041	-77.2775
Elevation	6.7	24.4	32	12.2

Accurate precipitation data only exist at point locations, where the gauging stations are located. Hence, precipitation data measured at one climatic station in the watershed may not represent the precipitation falling on the entire watershed because the distributions of depth and duration of precipitation vary with space across the watershed area (Marquínez *et al.*, 2003). One of the important aspects of hydrology modeling is to estimate the total precipitation and its distribution within a watershed. The results show 35 subbasins, each of which has its drainage area and precipitation on a daily basis. All 35 subbasins' values were included in the analyses of amount of the precipitation throughout the record. More than 21 stations did exist in the Blackwater River Watershed; four of them just have been used. The Theissen polygon area-weighted average method was applied to calculate the average precipitation for each subbasin.

The Theissen polygon method (Bouhia *et al.*, 2001) was used to subdivide the Blackwater River Watershed into four polygons, each of which is represented by one of the four rain gauges. It was implemented by: 1) connecting the four rain gauges to form a triangular network; 2) perpendicularly bisecting each of the triangular edges and extending the bisection line either to intersect the watershed boundary or another bisection line; and 3) measuring the areas of the polygons.

The areal precipitation of the watershed was computed as (Teegavarapu and Chandramouli, 2005; Vicente-Serrano *et al.*, 2003):

$$\bar{P} = \frac{\sum_{i=1}^{4}(P_i A_i)}{\sum_{i=1}^{4} A_i} \tag{2.1}$$

Where P-bar is the areal precipitation of the watershed; P_i is the precipitation at gauge i;

and A_i is the area of the Thiessen polygon that includes gauge i (Teegavarapu and Chandramouli, 2005). Subsequently, visualization plots were generated to identify any daily, monthly, and annual precipitation trends from January 1951 to December 2015.

The area-weighted average is a reliable and flexible method for the estimation of average areal precipitation. The subbasins depend on the proportions of recorded precipitation amounts at stations and the division of the total watershed area into polygons is achieved using a triangular coordinate system (Şen, 1998). The weighted average is an average in which each observation in the data set is assigned or multiplied by a weight before summing to a single average value. In this process, each quantity to be averaged is assigned a weight that determines the relative importance of each quantity. Weightings are the equivalence of having that many like items with the same value involved in the average. These 35 subbasins have a summation area of 1588 km^2 (613 mi^2). In this case, the daily area-weighted average method was computed for precipitation for Franklin station with 1588 km^2 area, whereas for Dendron station the daily area-weighted average was computed for just 12 subbasins with 751.097 km^2 (290 mi^2). This analysis was conducted for both Franklin and Dendron stations for a consistent period from December 1950 to November 2015.

Furthermore, the daily precipitations were aggregated to obtain the corresponding monthly, seasonally, and annual values, which in turn were graphed to understand the relationships between precipitation and runoff. This dissertation examined the long-term annual, seasonal, and monthly precipitations versus the corresponding runoffs from 1951 to 2015.

2.4 Temperature Data and Preprocessing

Temperature is considered since its increasing will be notable in the future. Precipitation and temperature during summer have a negative correlation, indicating that warm weather tends to be dryer. In contrast, during winter, the precipitation rate increases and causes more runoff because of a low temperature (Zhao and Khalil, 1993).

The daily temperature data were also downloaded from the NOAA-NCDC website for the same four climate stations adjacent to the Blackwater River watershed, namely Hopewell, Stony Creek, Suffolk Lake Kilby, and Holland. Data on monthly mean temperature and the raw daily data were subjected to the quality control procedures that adjusted missing data and included the observation time.

2.5 Streamflow Data and Preprocessing

Streamflow is a complex function of precipitation and landscape characteristics such as LULC, topography, soil properties, and hydrologic conditions (N. R. C. S. NRCS, 2017). This dissertation predicted streamflow separately for each HRU and routed and aggregated it to obtain the total runoff for the study watershed. This increases the accuracy of load predictions and provides a much better physical description of the water balance (Winchell *et al.*, 2013). There are four streamflow gauges along the Blackwater River to collect discharge data. This dissertation used the data at two gauges (Figure 2.5), namely Dendron (37°01'30" N, 76°52'30" W) and Franklin (36°45′45″ N, 76°53′55″ W), which have a record since 1945.

Figure 2.5. The streamflow gauges of Dendron and Franklin.

Severe flooding occasionally occurred in the population areas (e.g., Zuni and Franklin) that are adjacent to the river. The channels of these river segments are poorly defined and generally shallow with a limited conveyance capacity. Although numerous swamps and forested wetlands may provide some number of storages for floodwater, their capacities and attenuation effects have been degrading. The flooding is likely to be exacerbated by changing climate and rising sea level. For instance, in the recent decades, the watershed incurred several large floods, including the largest one in September 1999 from Hurricane Floyd. Table 2.2 summarizes the historical floods incurred by City of Franklin.

Table 2.2. The floods occurred in City of Franklin, Virginia.

Flood Date	Flood Stage (m)	Flood Category[1]
Aug. 19, 1940	6.7	Major
Sep. 14, 1960	5.2	Moderate
Jun. 06, 1963	4.5	Flood
Mar. 22, 1975	4.3	Flood
Feb. 07, 1998	4.6	Flood
Sep. 20, 1999	8	Major
Apr. 13, 2003	4.4	Flood
Sep. 22, 2003	5.1	Moderate
Sep. 04, 2006	4.7	Flood
Oct. 10, 2006	6.9	Major

[1] Action: stage ≥ 2.4 m; Flood: stage = [3.7 m, 4.9 m); Moderate: stage = [4.9 m, 6.1 m); Major: stage ≥ 6.1 m.

The portion of precipitation seeps into the ground, while the remaining portion is converted into overland runoff flowing downhill. The runoff is extremely important because not only it supplies water to the streams and lakes but also changes the landscape by the action of erosion (Smith *et al.*, 2015). The drainage area above Dendron is 571.1 km^2, while the drainage area above Franklin is 1587.66 km^2. The daily discharge data at these two streamflow gauges were downloaded from the USGS website (Figure 2.6) for a record period of January 1951 to December 2015.

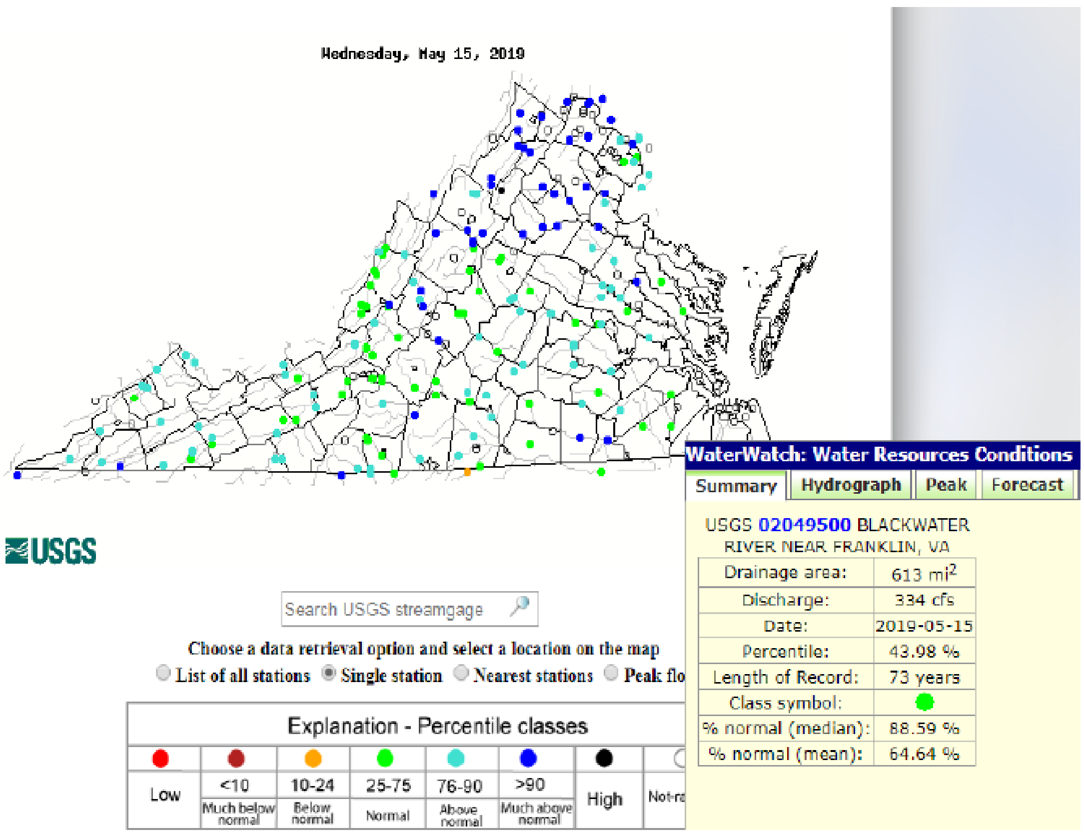

(a)

[Figure 2.6]

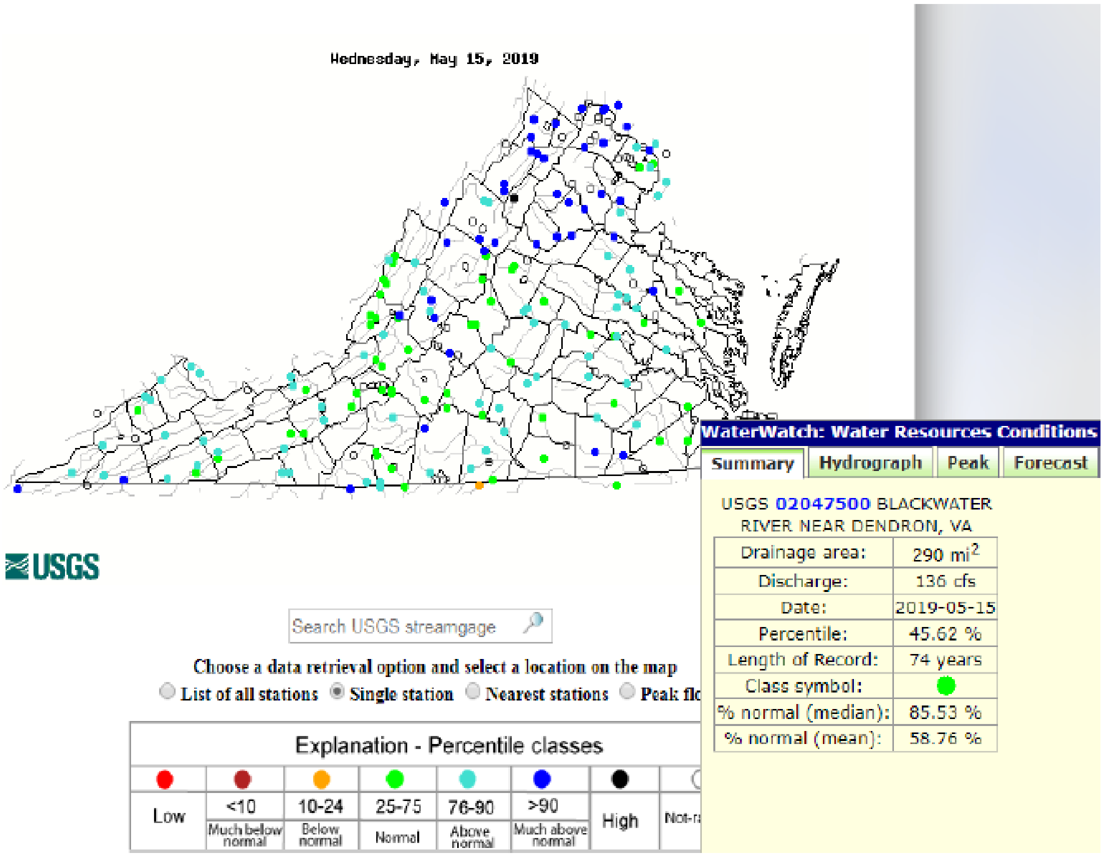

(b)

Figure 2.6. The website to download discharge data at: (a) Dendron; and (b) Franklin.

The missing and suspicious values were validated by using data from another station. Variabilities in annual and peak discharges are generally higher in areas where rainfall intensity is higher. For each HRU, the runoff was predicted separately and led to obtaining the total runoff for the watershed. Using the HRUs increased the accuracy and gave a much better physical description of the water balance in the prediction of the loadings (i.e., mass rates of sediment and nutrients transported by the runoff) from the subbasin.

2.6 Sub-conclusions

This dissertation used a variety of data for setting up and running the SWAT model, namely temperature, precipitation, streamflow, soil data, land use and land cover, topography, and drainage network. The hydrological cycle is a dynamic process which has been affected by global climate change and human activities. Stream flow changes are affected by both the amount of precipitation as a significant role and temperature fluctuation. Although the effect of precipitation and sea level rise on streamflow is more significant to increase flood stage in coastal watershed.

As a significant component of hydrologic cycle, runoff is affected by meteorological and geological factors in conjunction with land use. For simulation purposes, the Blackwater River Watershed was subdivided into six subbasins in terms of topography and 35 HRUs in terms of unique combinations of topography, soil properties, and LULC. Such a long-term record of rainfall and runoff time series can provide a good opportunity to examine the rainfall-runoff relationships in coastal watersheds.

CHAPTER 3

OBSERVED RAINFALL-RUNOFF RELATIONSHIPS

Runoff, as a vital component process of hydrologic cycle, is generated by rainfall. Its occurrence and quantity are dependent on the storm characteristics, namely rain intensity, duration, and temporal distribution. Runoff is sensitive to climate change because of its direct impacts on the storm characteristics (Molnar and Ramírez, 2001).

3.1 Detection of Trends in Precipitation and Streamflow

At the annual scale, both the precipitation and runoff fluctuated from year to year and had a very weak increasing trend (Figure 3.1). The mean annual precipitation in Virginia have increased about 2.4 cm over the last 70 years (Allen and Allen, 2019). The precipitation was increasing at 2.37 mm a^{-1}, while the runoff was increasing at 0.75 mm a^{-1}. The runoff varied synchronically with the precipitation (Figure 3.2). That is, the runoff in a year with a larger precipitation tended to be greater than that in a year with a smaller precipitation, and vice versa. At the monthly scale, on average, the precipitation in a summer month (June to August) was larger than that in a spring month (March to May), which in turn was larger than that in a winter month (December to February) followed by that in a fall month (September to November). The precipitation was smallest in September (110 mm) and largest in June (365 mm). Such an interannual distribution of monthly runoff was also generally true for most of the years (Figure 3.3); however, the interannual distribution of the monthly runoffs in one year could be different from that in another year (Figure 3.4), depending on the corresponding interannual distribution of the monthly precipitations and the fluctuation of the air temperatures.

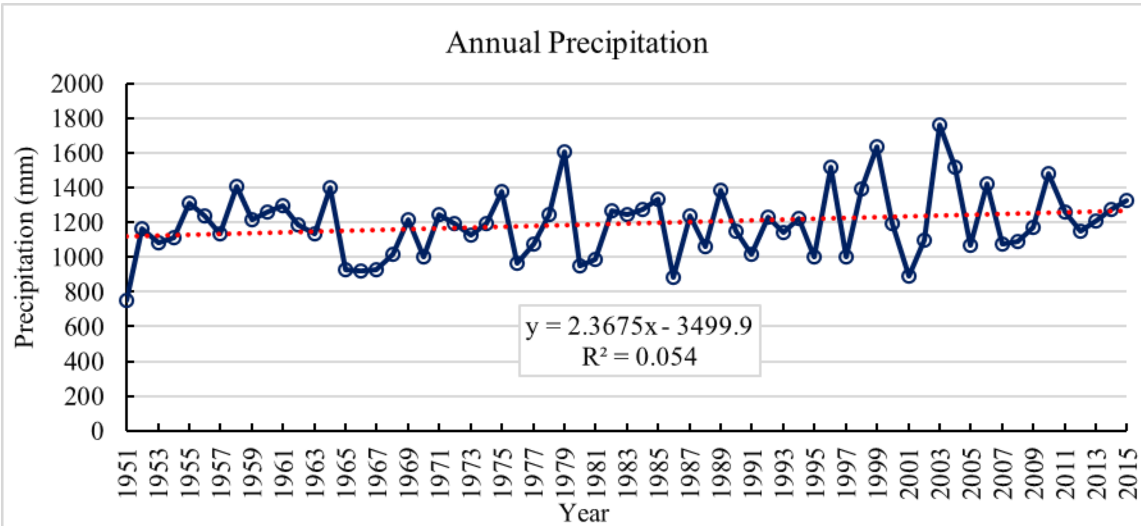

(a)

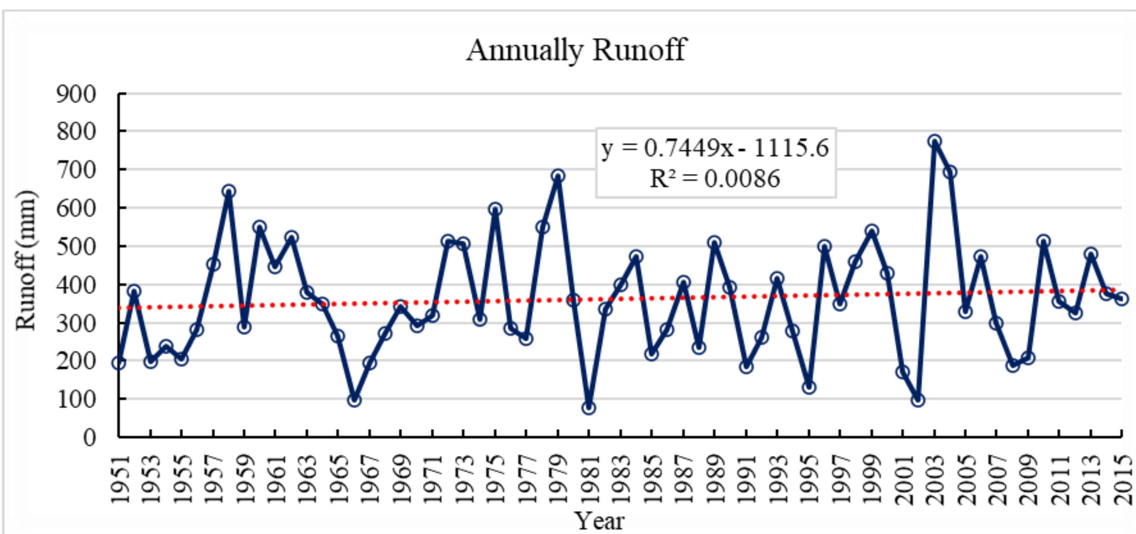

(b)

Figure 3.1. Plot showing the annual: (a) precipitation; and (b) runoff, of the Blackwater River Watershed.

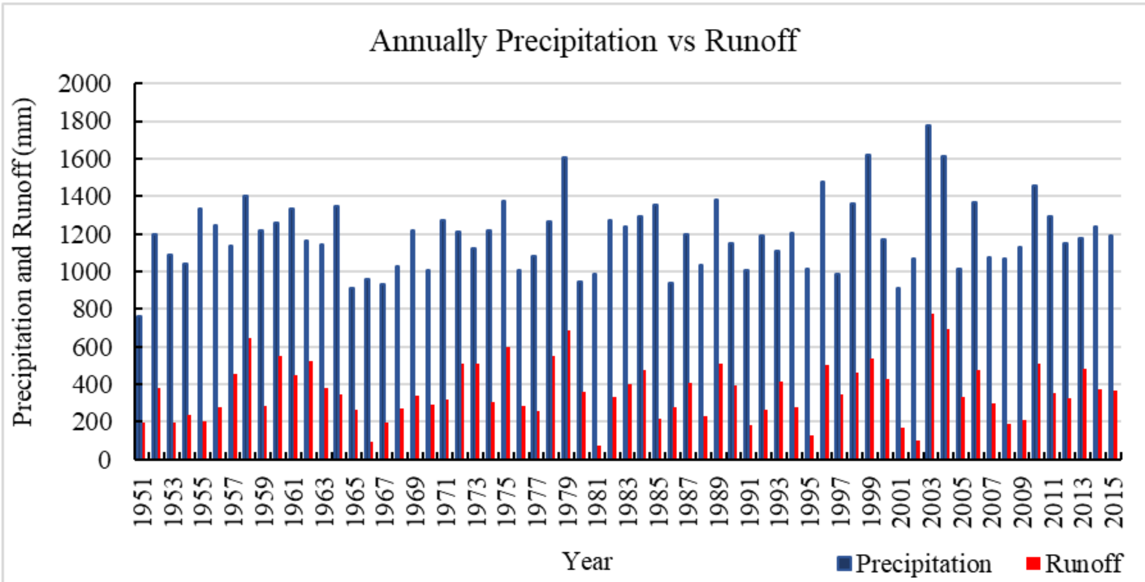

Figure 3.2. The annual precipitation versus the annual runoff, of the Blackwater River Watershed.

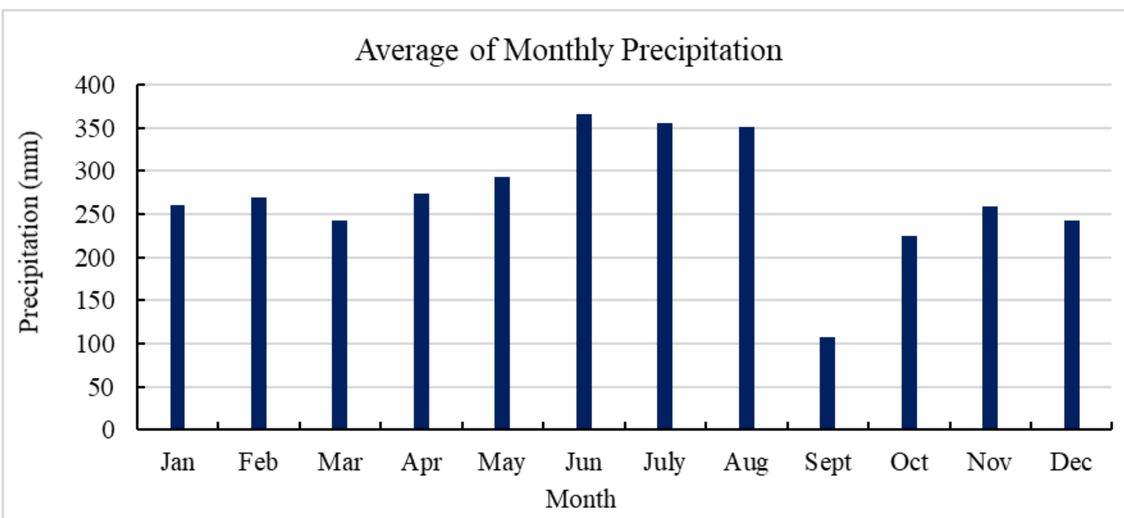

(a)

[Figure 3.3]

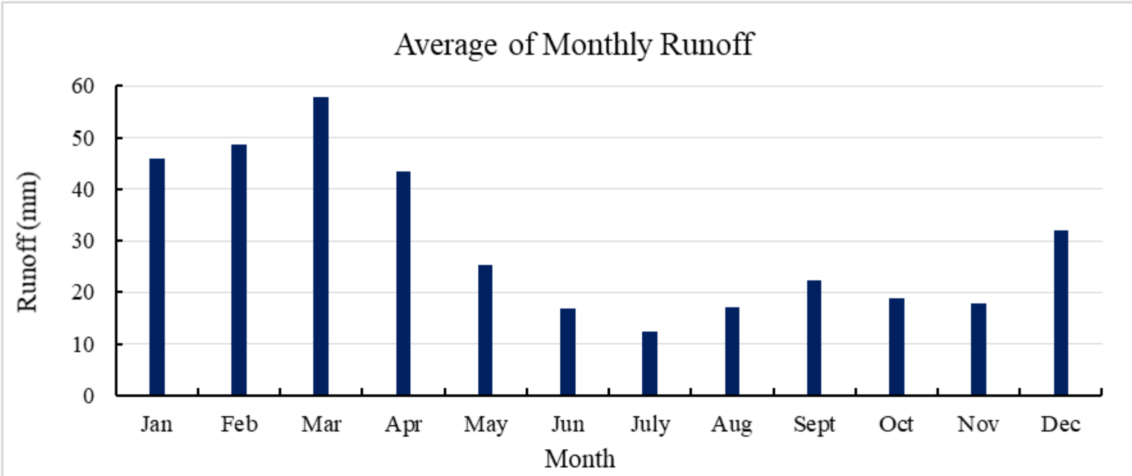

(b)

Figure 3.3. The 1951 to 2015 annual mean monthly: (a) precipitation; and (b) runoff.

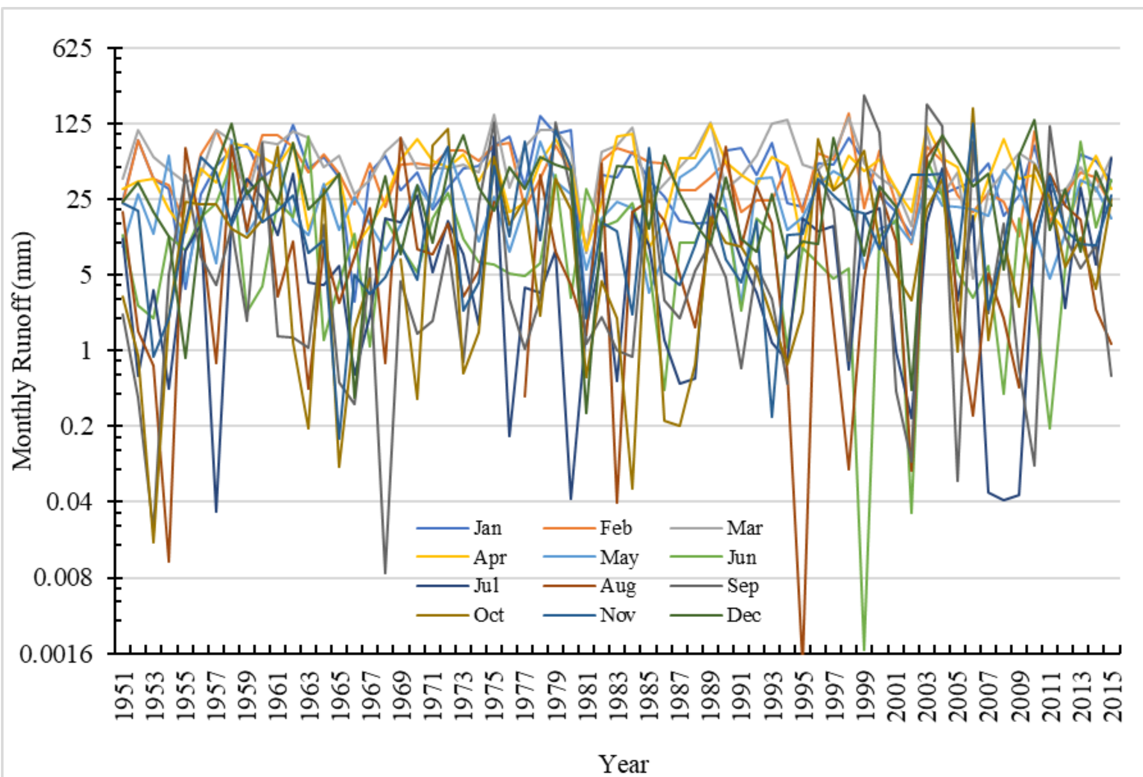

Figure 3.4. The monthly runoff of the Blackwater River Watershed.

Regardless of the time scales, the peak runoff did not exhibit any temporal trend. The annual peak runoff, computed as the ratio of the multiplication of the peak discharge and 365 days to the total drainage area of the Blackwater River Watershed, randomly fluctuated from year to year (Figure 3.5a), whereas the monthly peak runoff, computed as the ratio of the multiplication of the peak discharge of a month and the days of this month to the total drainage area, randomly fluctuated from month to month (Figure 3.5b). The two largest peaks were caused by the hurricane in 1999 and the Nor'-Easter storm in 2006, respectively. Those two extreme events dumped large amounts of precipitations in a short time (Figures 3.1a and 3.2). The annual peak runoff varied from 35 to 300 mm, with a coefficient of variation of $C_v = 0.67$, while the monthly peak runoff varied from 0.1 to 15 mm, with a $C_v = 0.75$; indicating a similar variability.

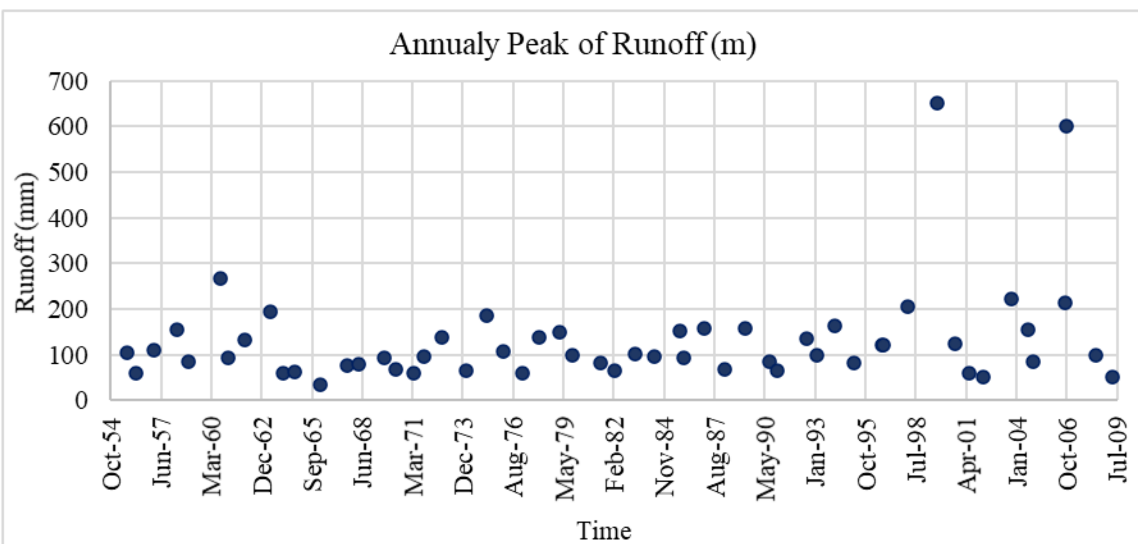

(a)

[Figure 3.5]

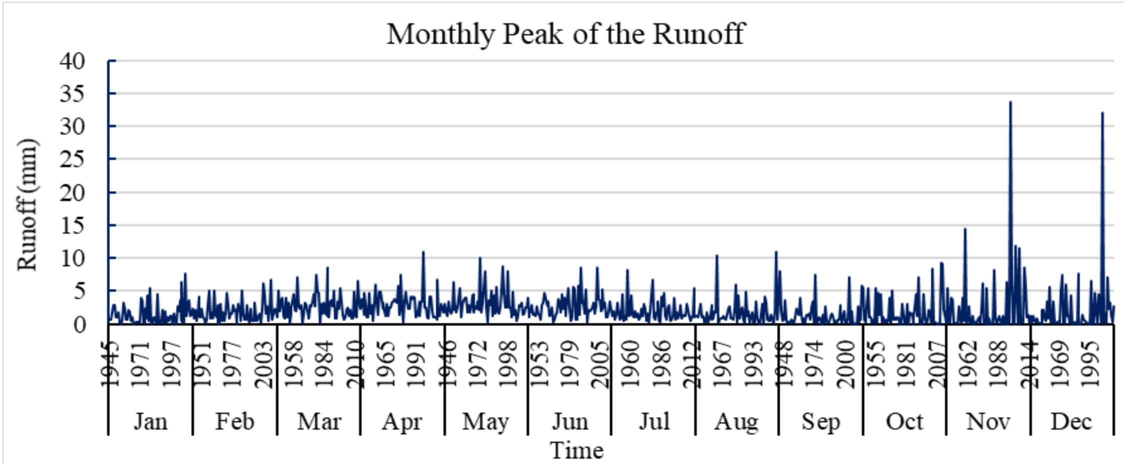

(b)

Figure 3.5. Plots showing the: (a) annual; and (b) monthly, peak runoff of the Blackwater River Watershed.

3.2 Separation of Direct Runoff and Baseflow

Surface runoff is the portion of the runoff that flows through the overland and ultimately reaches streams and/or other waterbodies (e.g., lakes). It happens when the rainfall intensity is larger than the soil infiltration capacity (Joel *et al.*, 2002) and the whole capacity of rainfall surpasses the interception, infiltration, and surface detention capacity of the watershed. The runoff flows on the land surface gathering in the river. Subsurface flow occurs once permeated rainfall meets an underground zone of low transmission and moves above the zone to the soil surface to appear as a seep or spring (Burton Jr and Pitt, 2001). Baseflow occurs once there is a properly steady flow into a river from shallow aquifer. The flow comes from ponds, wetlands, or an aquifer that are fed by infiltrated water and/or surface runoff (Conversation and Recreation, 1999). The first step in the river management and maintaining sustainability is to figure out the main components of streamflow, namely direct runoff and baseflow, whose effects on streamflow are so essential to the ecosystems and communities in the watershed (Jung *et* *al.*, 2016). In this regard, a filter program (J. Arnold *et al.*, 1995) can be used to split the baseflow and direct runoff using the observed streamflow data in gauged watersheds (Lee *et al.*, 2018). The program assesses the contributions of baseflow and direct runoff to streamflow. Both baseflow and direct runoff provides a seasonally altered contribution to streamflow. Given that a decrease in groundwater storage and rise in direct runoff increase the chance of the flood (Jung *et al.*, 2016), the purpose of separating baseflow and direct runoff was to better quantify the rainfall-runoff relationships and to provide a better estimate of the SWAT model's alpha parameter. The baseflow filter program can offer multiple passes through the filter, namely first pass, second pass, and third pass, allowing for users to select and use the desired number of passes to calculate the baseflow for the streamflow (Lyne and Hollick, 1979). In principle, the more passes are used, the more accurate the result.

Baseflow can be defined as groundwater exfiltration from shallow aquifers (Wittenberg, 2003). It occurs once there is a properly steady flow into a river from aquifers. Baseflow can be estimated as the ratio of the streamflow that is constant between precipitation events. In addition, baseflow is deriving from the riparian area where water moves to groundwater and then recharge to stream flows (Larocque et al., 2010). The flow comes from ponds, wetlands, or an aquifer fed by infiltrated water and/or surface runoff (Conversation and Recreation, 1999). Separation of baseflow is usually used to define what percentage of a streamflow hydrograph takes place from baseflow and what percentage takes place from the surface flow. The effect of the direct runoff and baseflow on streamflow are so essential to the ecosystems and communities in the watershed (Jung *et al.*, 2016). Although baseflow increases by infiltration to recharge subsurface storage, evapotranspiration decreases baseflow through evaporation of water from surfaces and transpiration of water within a plant (Singh, 1968). Likewise, river incision can critically decline the baseflow by dropping the water table and aquifer. Baseflow response to fall precipitation is larger due to quick drainage from the area of great transmissivity close to the stream. (Cooper *et al.*, 1995). During fall, baseflow can rise without any precipitation because plants do not use as much water as in summer, when baseflow from the aquifer is decreased by high evaporation.

For the Dendron gauge, at the annual scale, almost 50% of the total streamflow was baseflow (Figure 3.6a), at the seasonal scale, on the other hand, the percentage varied. In spring (Figure 3.6b), the baseflow contributed more than half of the total streamflow for some years, whereas in the other three seasons (Figures 3.6c, d, e), the direct runoff had more contributions. As expected, the percentage of baseflow was lowest in summer. Similarly, for the Franklin gauge, the baseflow accounted for a large percentage of the total streamflow at the annual scale and in spring and winter. In summer and fall, the streamflow was primarily from the direct runoff generated by rainfall. For the study watershed, baseflow and direct runoff were basically equal.

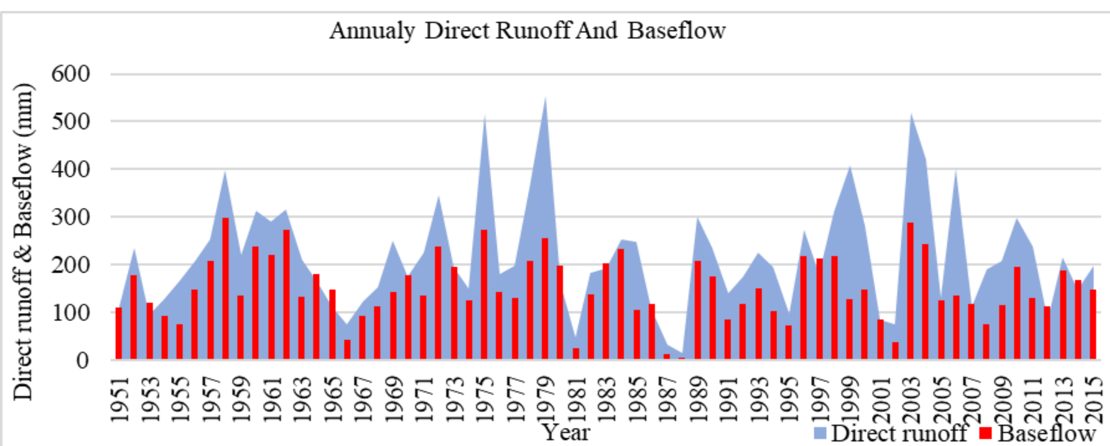

(a)

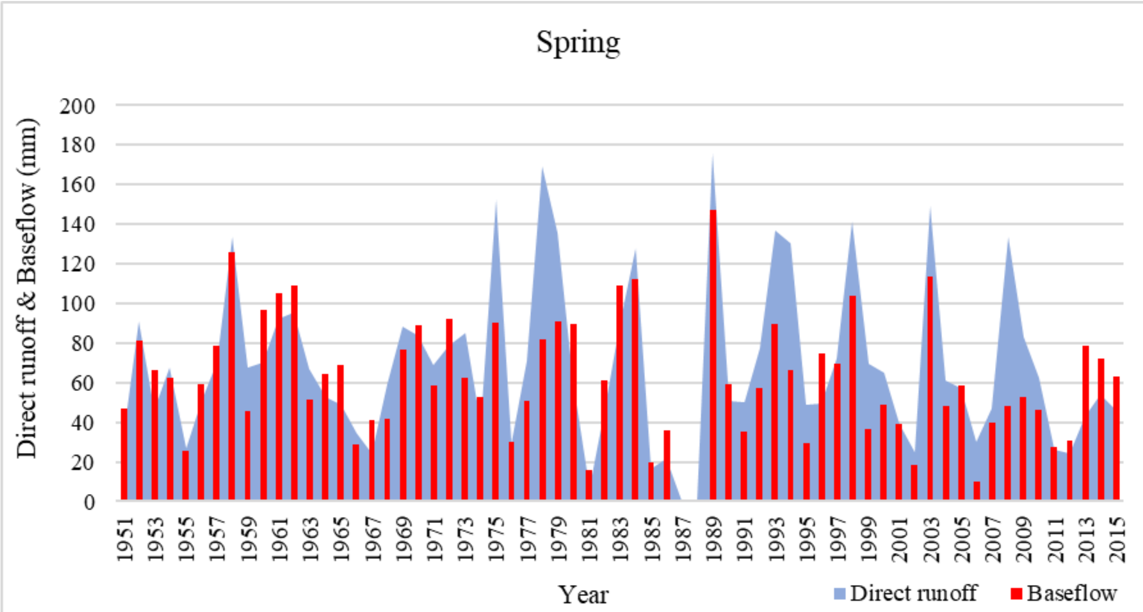
Spring
Direct runoff & Baseflow (mm)
Year
Direct runoff
Baseflow

(b)

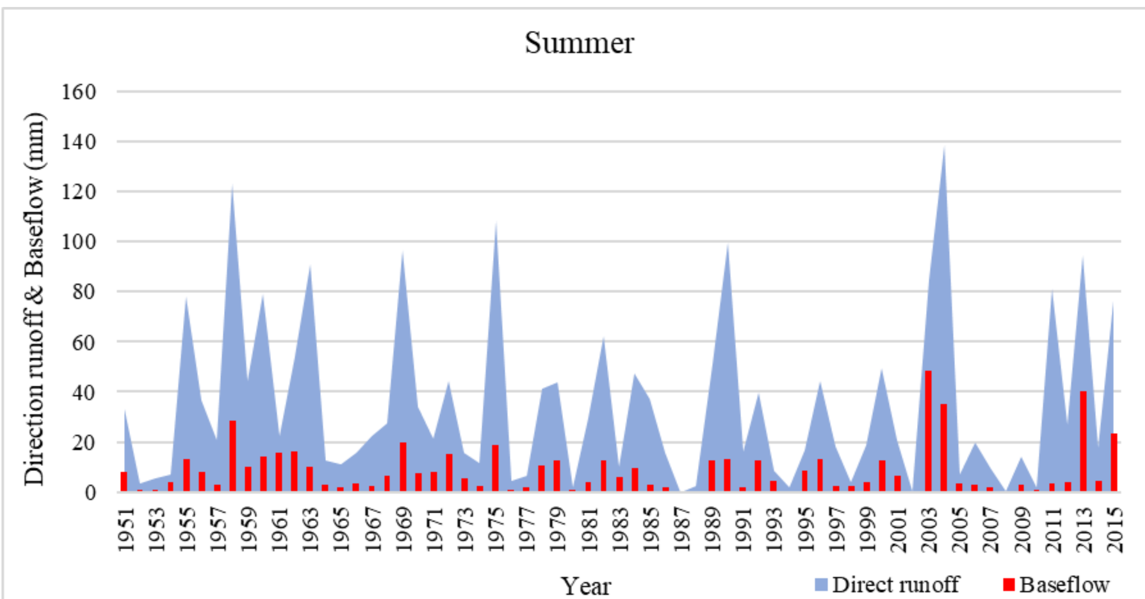
Summer
Direction runoff & Baseflow (mm)
Year
Direct runoff
Baseflow

(c)

[Figure 3.6]

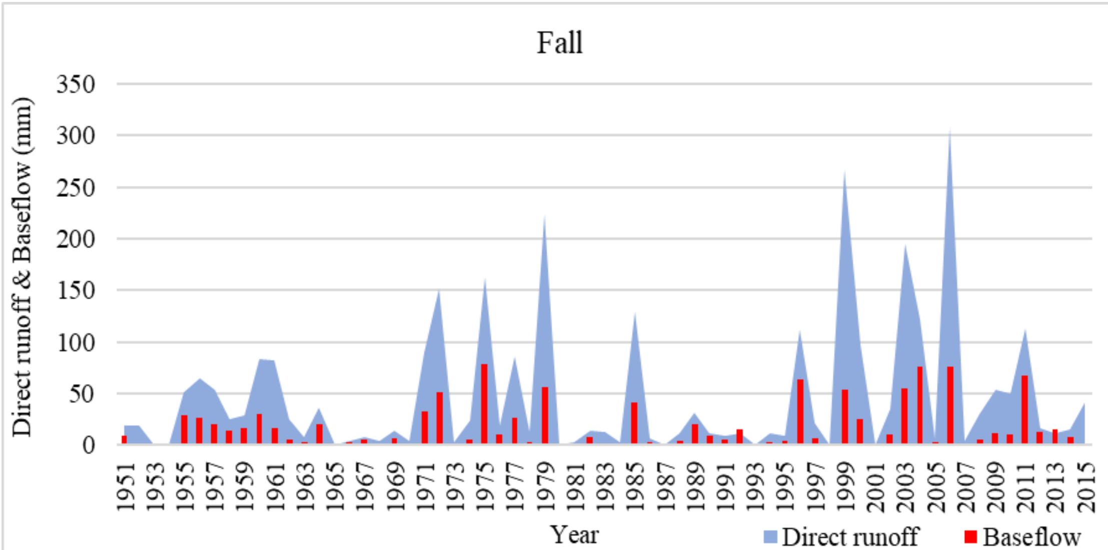

(d)

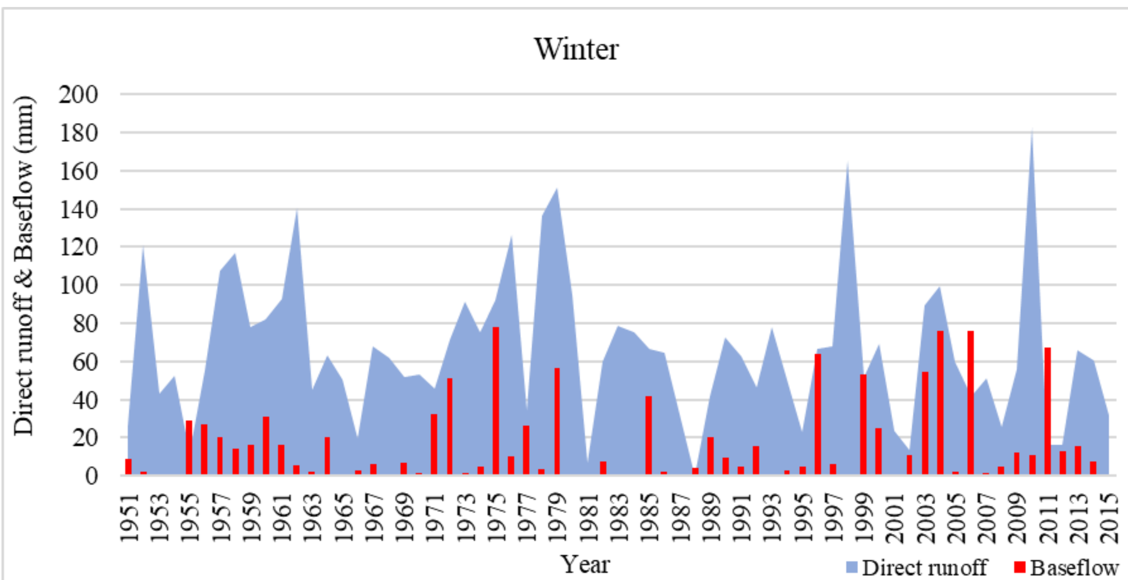

(e)

Figure 3.6. For the Dendron streamflow gauge. The direct runoff versus baseflow at the: (a) annual; (b) spring; (c) summer; (d) fall; and (e) winter, time scale.

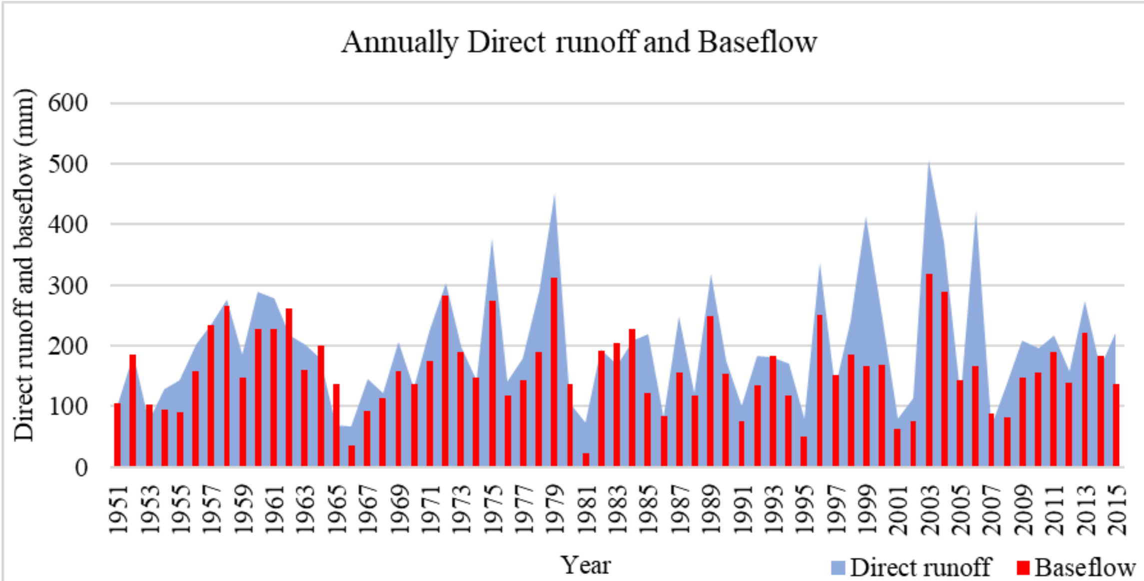
Annually Direct runoff and Baseflow
Direct runoff and baseflow (mm)
600
500
400
300
200
100
0
1951 1953 1955 1957 1959 1961 1963 1965 1967 1969 1971 1973 1975 1977 1979 1981 1983 1985 1987 1989 1991 1993 1995 1997 1999 2001 2003 2005 2007 2009 2011 2013 2015
Year
Direct runoff
Baseflow

(a)

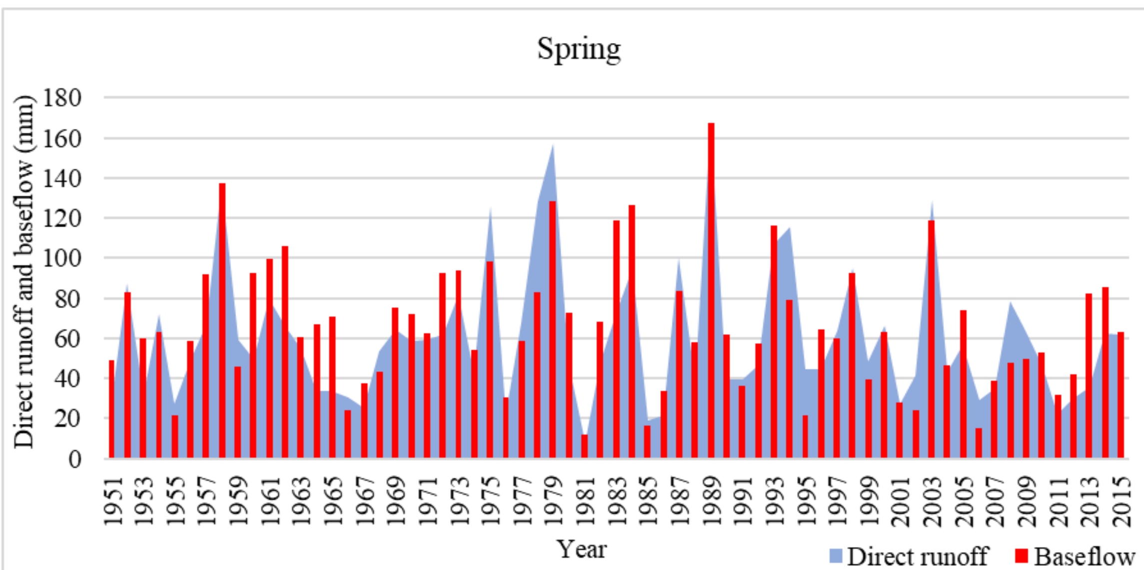
Spring
Direct runoff and baseflow (mm)
180
160
140
120
100
80
60
40
20
0
1951 1953 1955 1957 1959 1961 1963 1965 1967 1969 1971 1973 1975 1977 1979 1981 1983 1985 1987 1989 1991 1993 1995 1997 1999 2001 2003 2005 2007 2009 2011 2013 2015
Year
Direct runoff
Baseflow

(b)

[Figure 3.7]

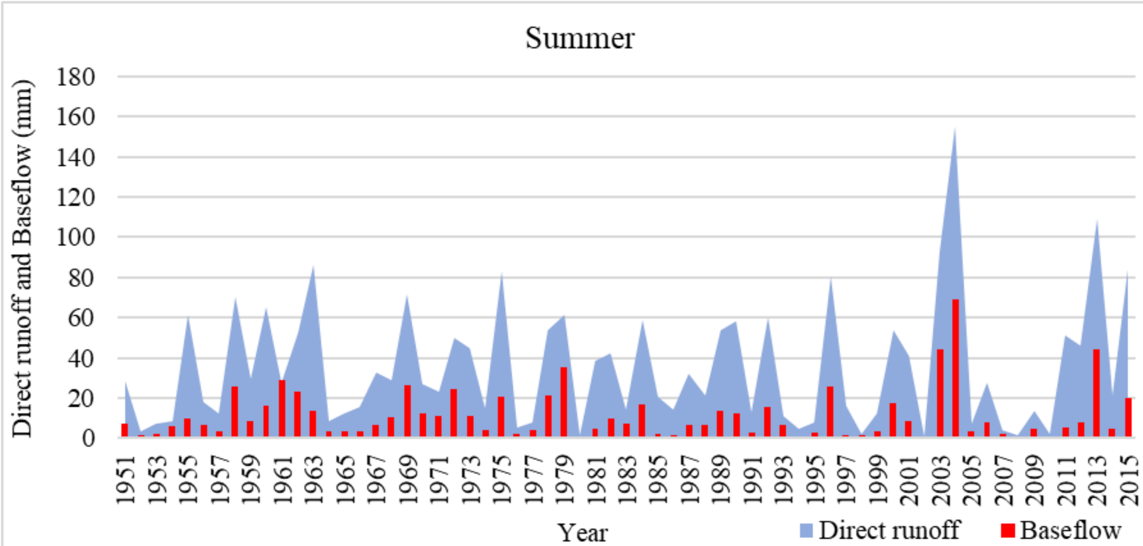
Summer
Direct runoff and Baseflow (mm)
Year
Direct runoff
Baseflow

(c)

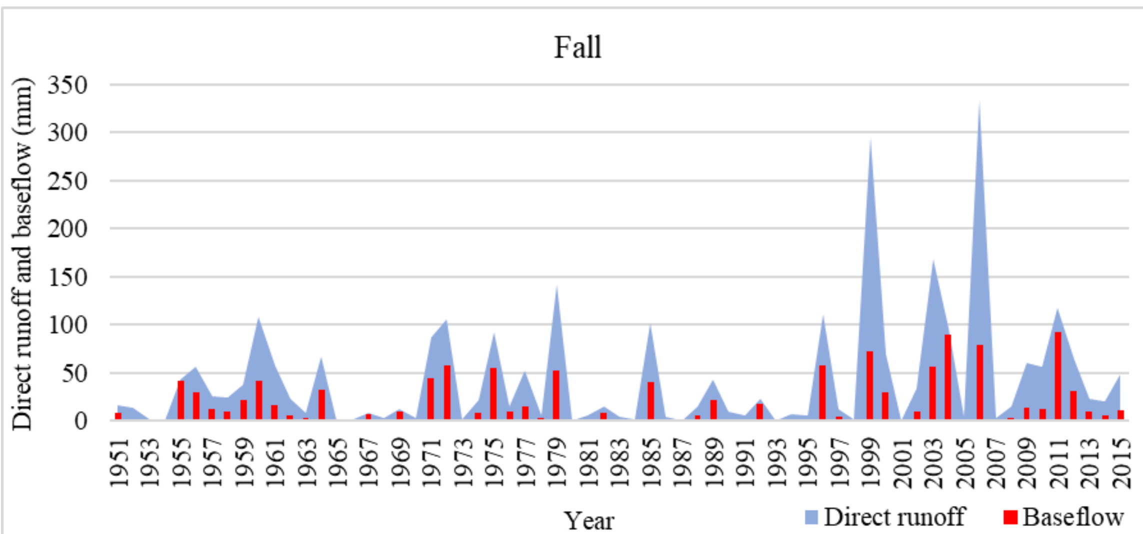
Fall
Direct runoff and baseflow (mm)
Year
Direct runoff
Baseflow

(d)

[Figure 3.7]

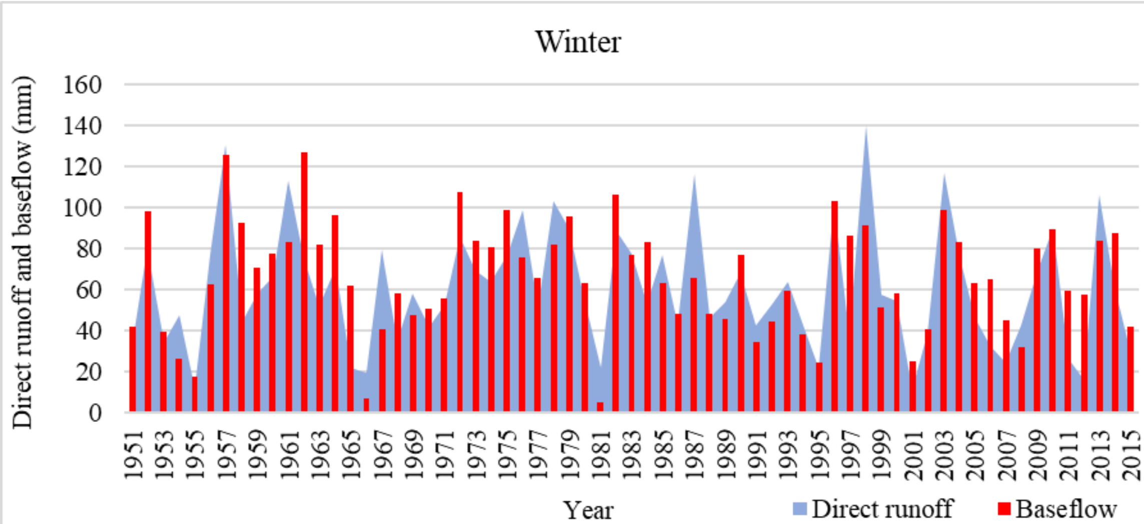

(e)

Figure 3.7. For the Franklin streamflow gauge. The direct runoff versus baseflow at the: (a) annual; (b) spring; (c) summer; (d) fall; and (e) winter, time scale.

3.3 Rainfall-Runoff Relationship

The rainfall-runoff relationships in the Blackwater River Watershed were analyzed. As expected, the precipitation duration, distribution, and intensity are important factors for the relationships (Desta, 2006). Hydrologists commonly assume that there is an empirical relationship between watershed area and runoff. However, there is a physical relationship between rainfall and runoff since runoff tends to increase with rainfall and vice versa (Rafter, 1903). When rainfall occurs at a time, a portion of the rainfall can be intercepted by canopy while the rest reaches the land surface to be infiltrated and/or converted into overland runoff. The time interval and drainage area (Marchi *et al.*, 2019) of interest can affect such a relationship. Besides, there are also other physiographical factors that have direct influences on the percentage of rainfall that can be converted into overland runoff.

In this dissertation, the analysis of rainfall-runoff relationships was conducted by storm events. It uses hydrographs to discover the correlation of the rainfall and the contribution to runoff during a storm and then set a threshold to find the contribution of rainfall to runoff (Kasei *et al.*, 2013). The analysis was implemented in Microsoft® Excel. The values of direct runoff were the outputs of the filter program discussed in section 3.1.

3.3.1 Percolation and Baseflow

The high percolation capacities of the upper soil layer and the relatively large hydraulic conductivity of the fractured aquifer should contribute to the quick increase and decrease of the groundwater table levels. The baseflow hydrograph directly follows the streamflow hydrograph and baseflow is an important component of streamflow during its peaking period (R. Zhang *et al.*, 2013).

The baseflow hydrographs (Figure 3.8) show that there is an annually surface runoff component during the entire (65 years) record period. This observed response may also be related to the frequent rainfall events. Although the annual baseflows at both Dendron and Franklin stations are compatible, there is the lowest rates of baseflow in 1987 and 1988 at Dendron (Figure 3.8a) due to the highest average temperature during the summer and lowest average annual precipitation (N. R. C. S. NRCS, USDA (United States Department of Agriculture), 2000). At the seasonal scales, the baseflow rates are high during spring and winter and are low during summer and fall for both Dendron and Franklin gauges (Figure 3.9).

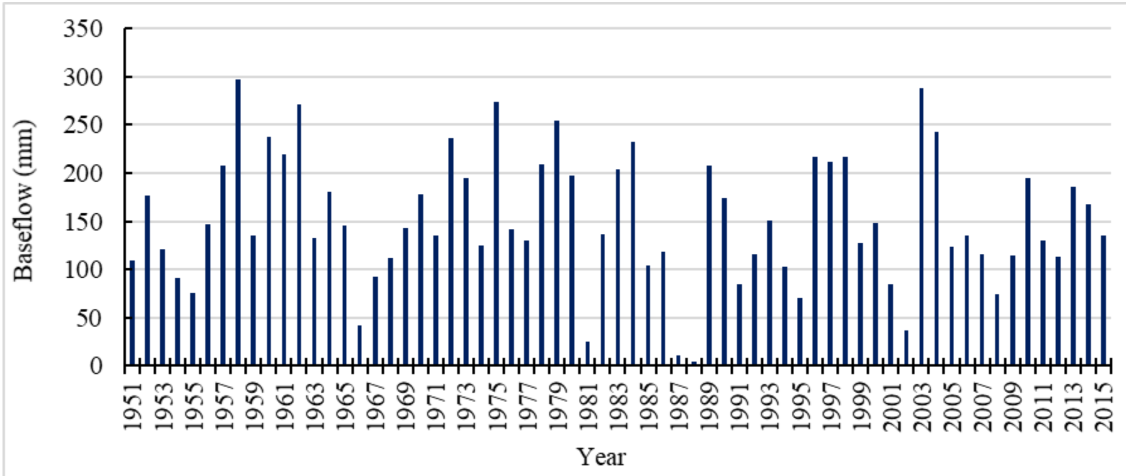

(a)

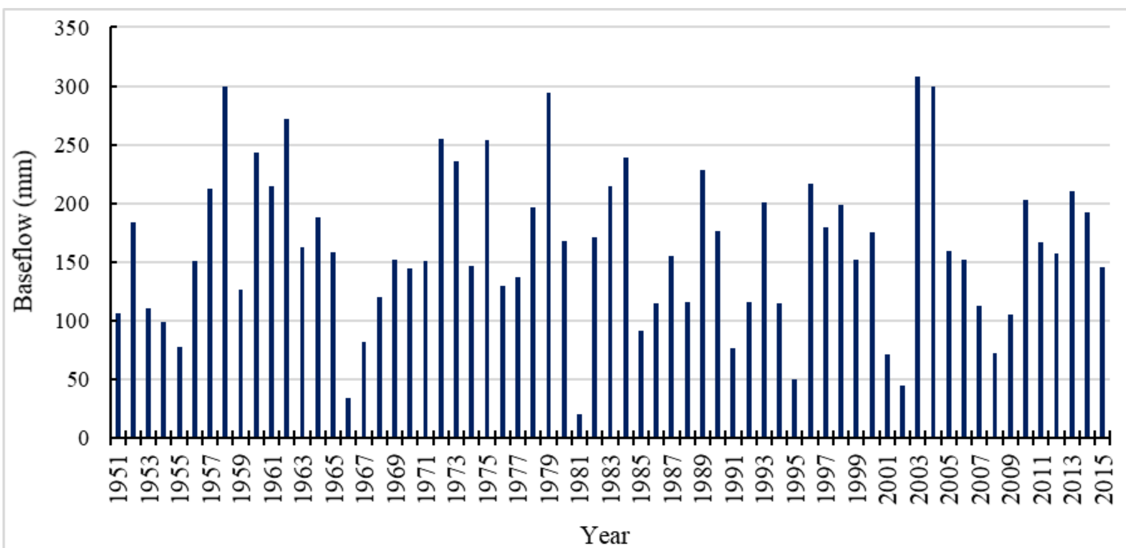

(b)

Figure 3.8. The annual baseflows at: (a) Dendron; and (b) Franklin.

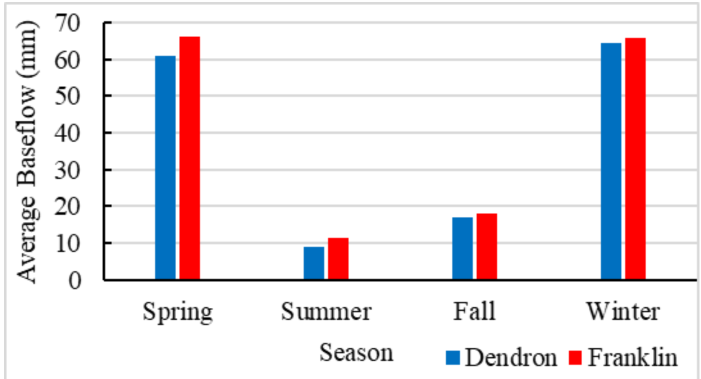

Figure 3.9. The annual average seasonal baseflows at Dendron and Franklin.

3.3.2 Depression Storage

Depressions are the low-lying patches and account for most of the retention capacity on watershed surfaces (Ullah and Dickinson, 1979). They can store precipitation that otherwise would become runoff. The precipitation collected in depressions is then diminished either by infiltration or evaporation. Depressions survive on permeable and impermeable surfaces similarly; however, depressions are usually much larger on least disturbed and permeable surfaces. Topography plays an important role on surface flow generation (Frei and Fleckenstein, 2014), surface runoff, soil erosion, and other hydrologic processes (X. Chu *et al.*, 2010). In this dissertation, wetland mapper was downloaded from National Wetlands Inventory website https://www.fws.gov/wetlands/data/Mapper.html and used to determine the depressions in Blackwater River watershed. Table 3.1 presents the water surface areas of different types of wetlands that function as depressions.

Table 3.1 Water surface areas of the depressions in Blackwater River Watershed.

Wetland type	mi^2
lake	2.69
Fresh Water Pond	4.03
Freshwater Emergent Wetland	4.88
Other	0.09
Freshwater Forested/Shrub Wetland	103.29
Riverine	3.64
Sum	118.62

3.3.3 Surrogate Statistics

The double-mass curve at either Dendron (Figure 3.10a) or Franklin (Figure 3.10b), showing the cumulative total runoff versus the cumulative precipitation, is basically linear, indicating that the impacts of human activities in the past 65 years on the watershed hydrology were minimal. For the drainage area above Dendron, an amount of 82 mm rainfall, while for the drainage area above Franklin, an amount of 6540 mm rainfall, might be lost to canopy interceptions, depression storages (e.g., wetlands, ponds, and channels), soil storages, percolations, and evapotranspiration prior to the inception of runoff. This indicates that the drainage area between Dendron and Franklin had abundant storages with natural effects in reducing runoff volume and peak. The overall ratios of total runoff to precipitation for the drainage areas above the two streamflow gauges were found to be 0.3, implying that the relationship between total runoff and precipitation might be independent of the spatial locations across Backwater River Watershed, which is further verified by plotting the annual total runoff versus precipitation (Figure 3.11).

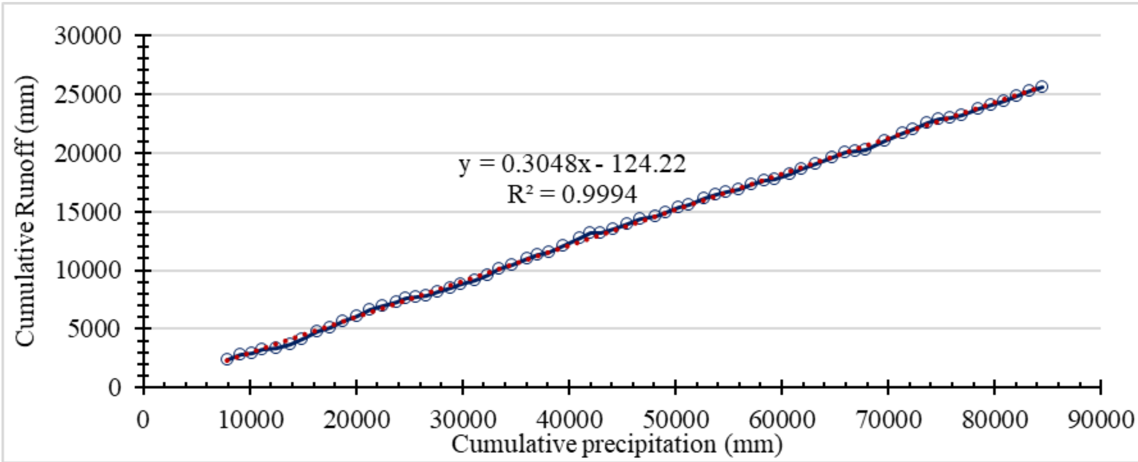

(a)

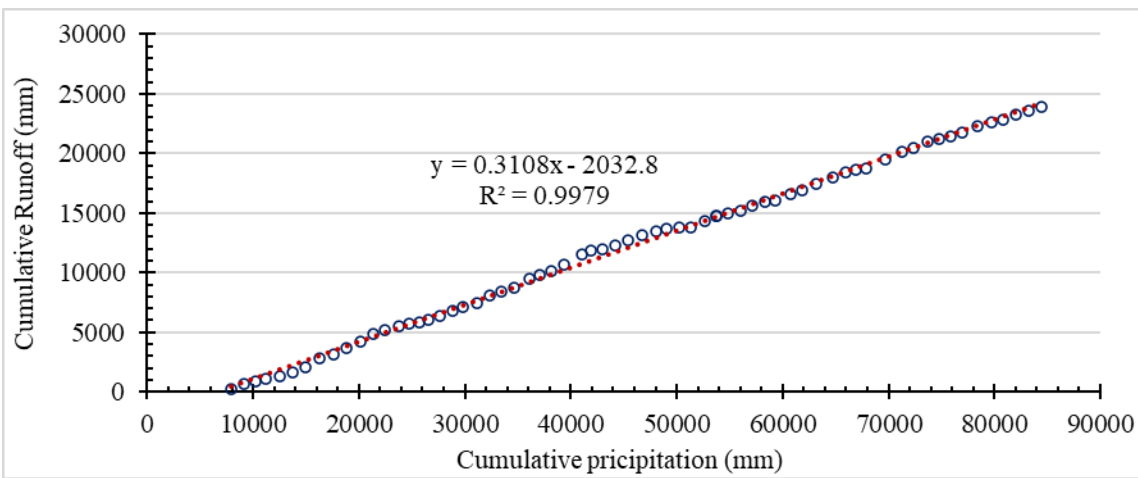

(b)

Figure 3.10. The double-mass curve at: (a) Dendron; and (b) Franklin.

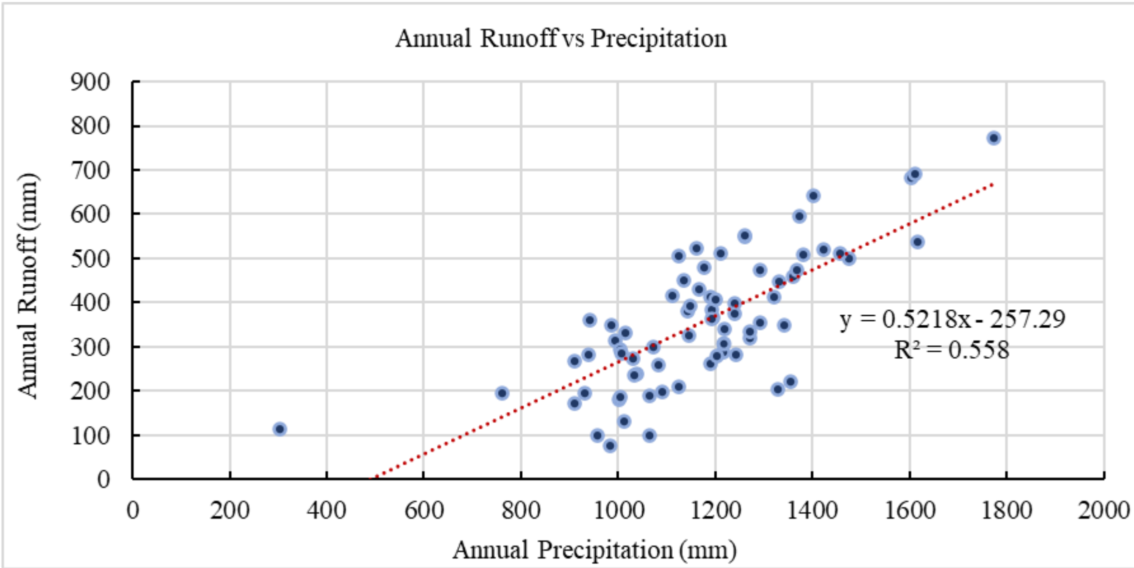

(a)

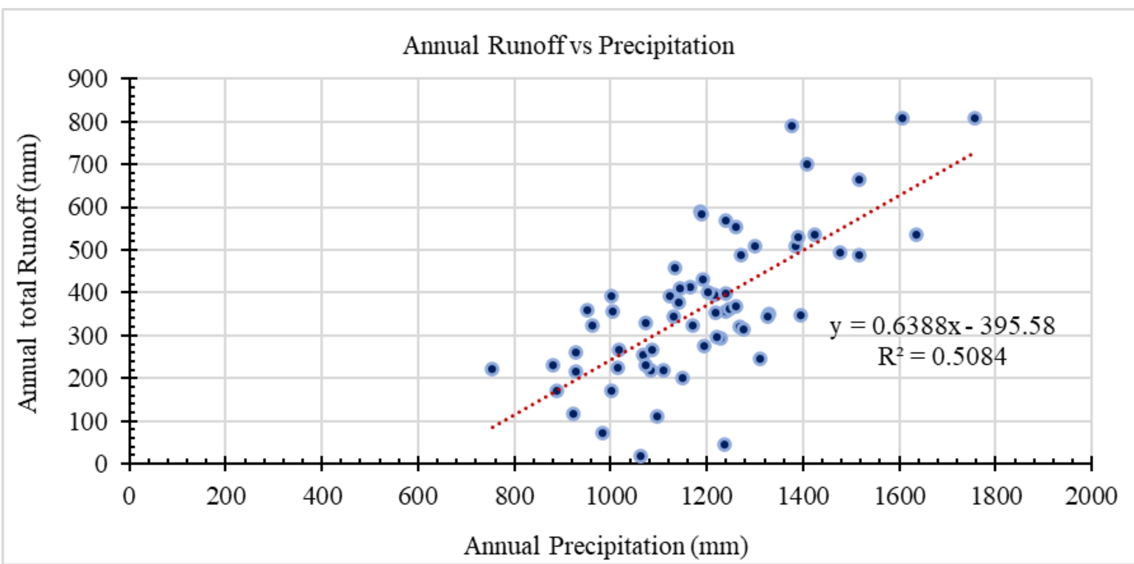

(b)

Figure 3.11. The annual runoff versus precipitation at: (a) Dendron; and (b) Franklin.

3.3.4 Exploration Analysis

The runoff coefficients (Table 3.2) are examined in terms of their means, standard deviations, and medians. At the drainage areas upstream of Franklin and Dendron, the monthly coefficients were higher in December to April than those in other months. During this time period, the values of means and medians are comparable, indicating that the runoff coefficients are normally distributed.

Table 3.2 The runoff coefficients of the drainage areas upstream of Dendron and Franklin.

Descriptive Statistics	Winter Months and Season				Spring Months and Season				Summer Months and Season				Fall Months and Season			
	Dec	Jan	Feb	Winter	Mar	Apr	May	Spring	June	July	Aug	Summer	Sept	Oct	Nov	Fall
Dendron Station																
Mean	0.18	0.26	0.25	0.22	0.37	0.25	0.16	0.24	0.10	0.10	0.15	0.10	0.19	0.14	0.14	0.16
Standard deviation	0.15	0.24	0.20	0.11	0.29	0.19	0.14	0.12	0.14	0.17	0.29	0.10	0.40	0.26	0.19	0.20
Median	0.14	0.18	0.21	0.21	0.30	0.22	0.11	0.23	0.07	0.04	0.04	0.07	0.02	0.03	0.07	0.08
Franklin Station																
Mean	0.17	0.24	0.24	0.21	0.29	0.23	0.16	0.21	0.12	0.09	0.13	0.10	0.11	0.12	0.12	0.13
Standard deviation	0.14	0.18	0.17	0.09	0.20	0.16	0.14	0.10	0.15	0.16	0.18	0.08	0.20	0.20	0.15	0.16
Median	0.13	0.19	0.21	0.19	0.25	0.20	0.11	0.20	0.08	0.05	0.06	0.08	0.02	0.02	0.06	0.07

3.3.5 Statistical Measures for the Relationship

The correlation coefficient was calculated and used to measure the relationship goodness. In addition, visualization plots showing predicted versus observed values were generated to examine the goodness. Further, the coefficient of determination (R^2), Nash-Sutcliffe efficiency (NSE), and percent error (PE) was also calculated as measuring statistics. To calibrate and validate the model, some numerical information is needed to assess the model performance. In this dissertation, the measured daily discharges at Franklin and Dendron were used to assess the model performance.

R^2 indicates the predicting power of the model. It represents the proportion of the variance in the dependent variable that is predicted from the independent variable. R^2 varies between zero and one, with a greater value indicating a better performance (Santhi *et al.*, 2001; Van Liew *et al.*, 2003). It can be calculated as:

$$R^2 = \frac{\sum_{i=1}^{n}(O_i - \bar{O})(P_i - \bar{P})}{\sqrt{\sum_{i=1}^{n}(O_i - \bar{O})^2}\sqrt{\sum_{i=1}^{n}(P_i - \bar{P})^2}} \tag{3.1}$$

where n is the number of observations; O_i is the i^{th} observation; Pi is the i^{th} prediction; $\bar{O}$ is the mean of observations; and $\bar{P}$ is the mean of predictions.

The runoff coefficient is a parameter widely used in hydrology to describe basin response to storm and predict direct runoff or infiltration (Blume *et al.*, 2007). Although its values depend on rainfall, soil properties and land uses can play significant roles as well.

NSE is used to evaluate the projecting power of hydrological models. It ranges from – ∞ to one. An efficiency of one (NSE = 1) corresponds to a perfect match between simulated and observed values, whereas an efficiency of zero (NSE = 0) indicates that the model predictions are as accurate as the mean of the observed data. An efficiency less than zero (NSE < 0) indicates that the mean observed value is a better predictor than the simulated value (Golmohammadi *et al.*, 2014; Ibarra-Zavaleta *et al.*, 2017). NSE is computed as:

$$\mathrm{NSE} = 1 - \frac{\sum_{i=1}^{n}(O_i - P_i)^2}{\sum_{i=1}^{n}(\bar{O} - \bar{P})^2} \tag{3.2}$$

3.3.6 Analysis of the Relationships

The analysis was conducted by storm events. It uses hydrographs to discover the correlation of the rainfall and the contribution to runoff during the storm and then set a threshold to find the contribution of rainfall to runoff (Kasei *et al.*, 2013). The analysis was implemented in Microsoft® Excel. The values of direct runoff were the outputs of the filter program discussed in section 3.2.

The relationship between the direct runoff of a watershed and the impressive rainfall over the watershed causing the runoff are considered in this subsection. The watershed shape, size, and slope the are the significant characteristics. Rainfall intensity and duration have effects on the relationship. For example, if the rainfall intensity is constant, the duration of the rainfall controls the peak and the time base of the surface runoff. Another aspect that could influence the relationship between rainfall and runoff is the spatial distribution of rainfall. Moreover, the direction of storm movement and the direction of the watershed drainage networks can affect both the dignity of peak flow and time base.

3.3.6.1 Direct Runoff versus Precipitation

The overall ratios of direct runoff to precipitation for the drainage areas above the two streamflow stations were found to be compatible, implying that the relationship between direct runoff and precipitation might be independent of the spatial locations across the Backwater River Watershed. This can be further verified by plotting the monthly and seasonal direct runoffs versus the corresponding precipitations. The direct runoffs varied concurrently with the precipitations (Figure 3.12). For both drainage areas, about 10 to 20% of the total precipitation was converted into direct runoff. This is further verified by examining the 23 largest storm events (Figure 3.13). In summer, while precipitation increased, the direct runoff decreased; in winter, on the other hand, while precipitation decreased, the direct runoff increased. Such opposite changes of precipitation and runoff can be attributed to seasonal variations of air temperatures and embodied by the runoff coefficients (Figure 3.14). Figure 3.15 shows there is a significant correlation between precipitation and runoff such that by increasing precipitation the direct runoff increased. The maximum annual precipitations occurred in 1979, 1999, 2003, and 2006, which resulted in largest direct runoffs in those years.

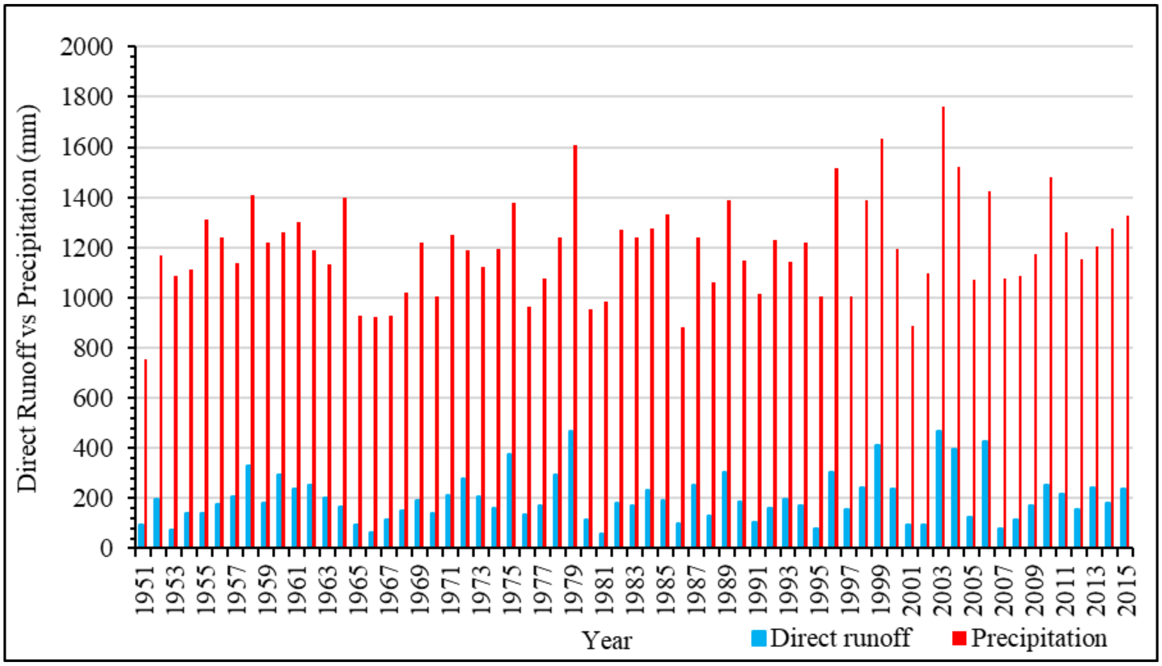

(a)

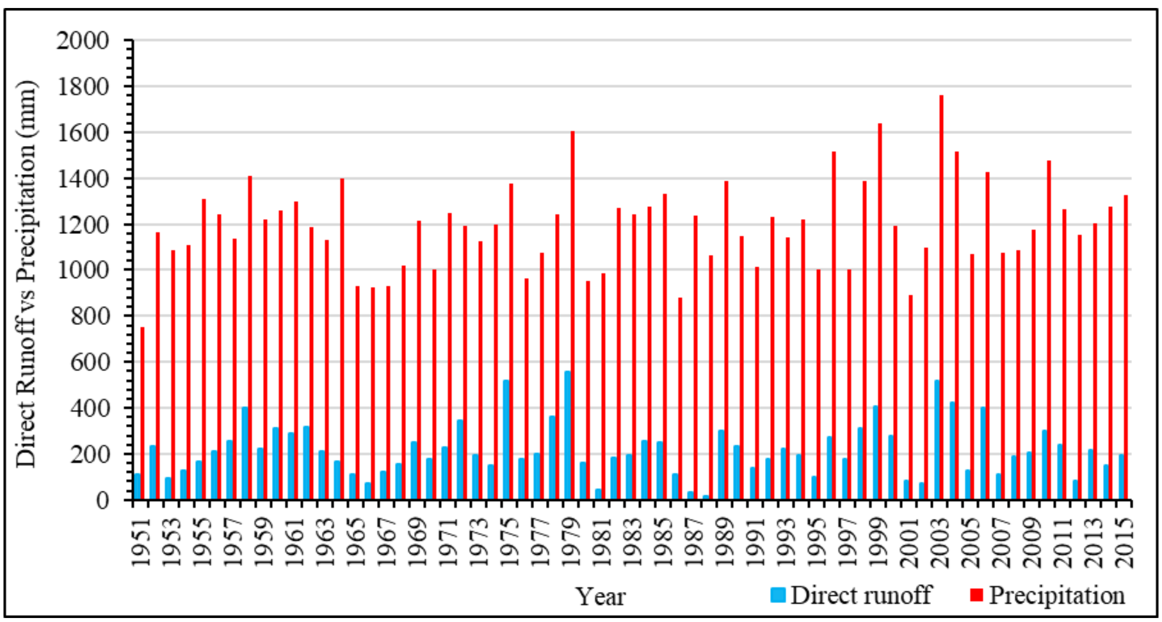

(b)

Figure 3.12. Annual direct runoff vs. precipitation at: (a) Dendron; and (b) Franklin.

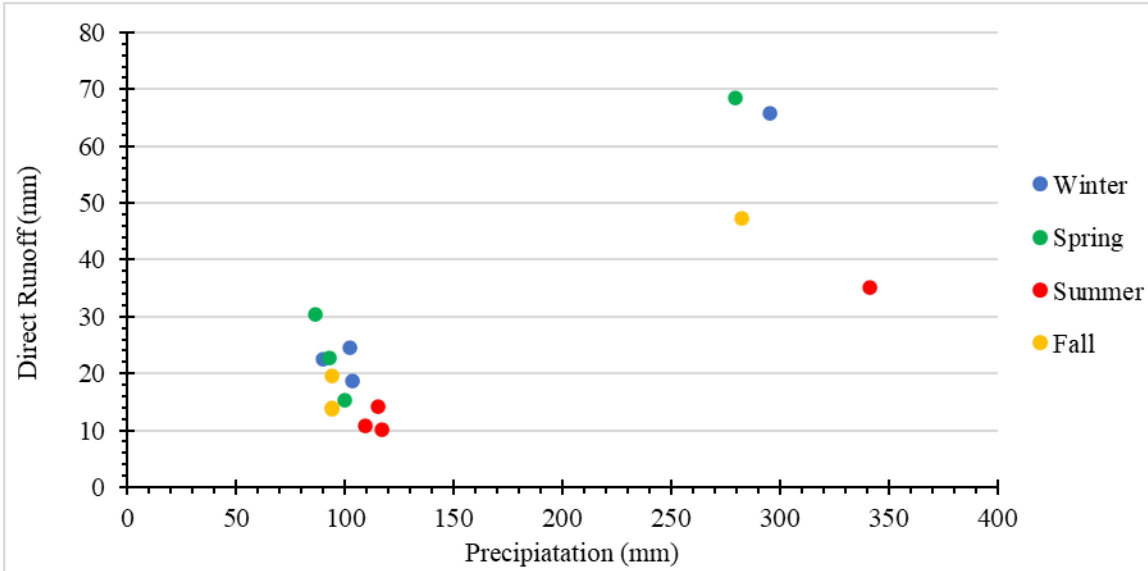

(a)

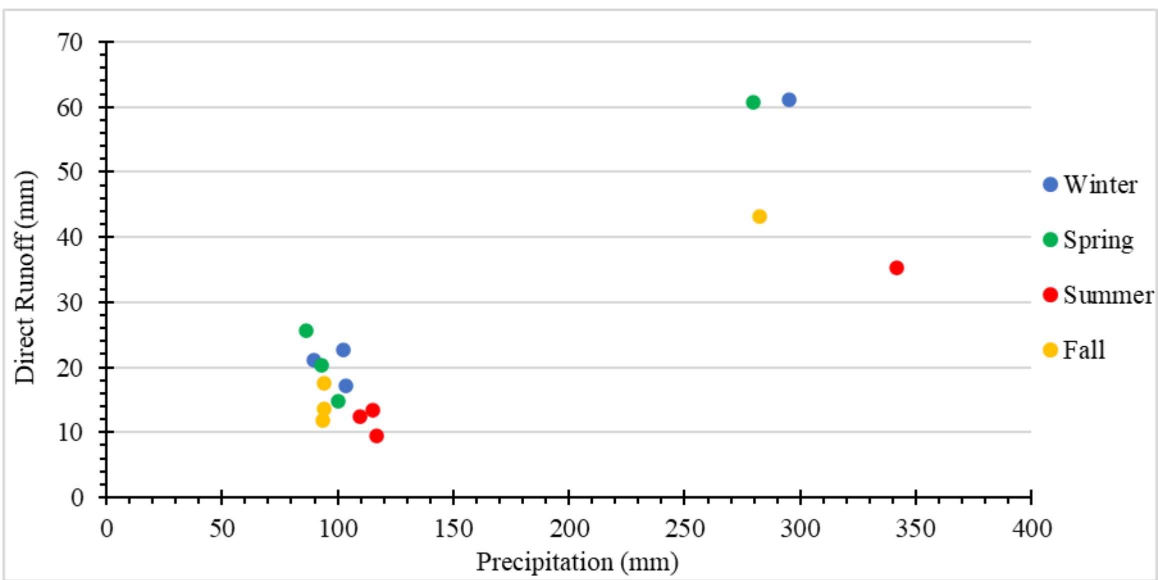

(b)

Figure 3.13. Seasonal direct runoff vs. precipitation at: (a) Dendron; and (b) Franklin.

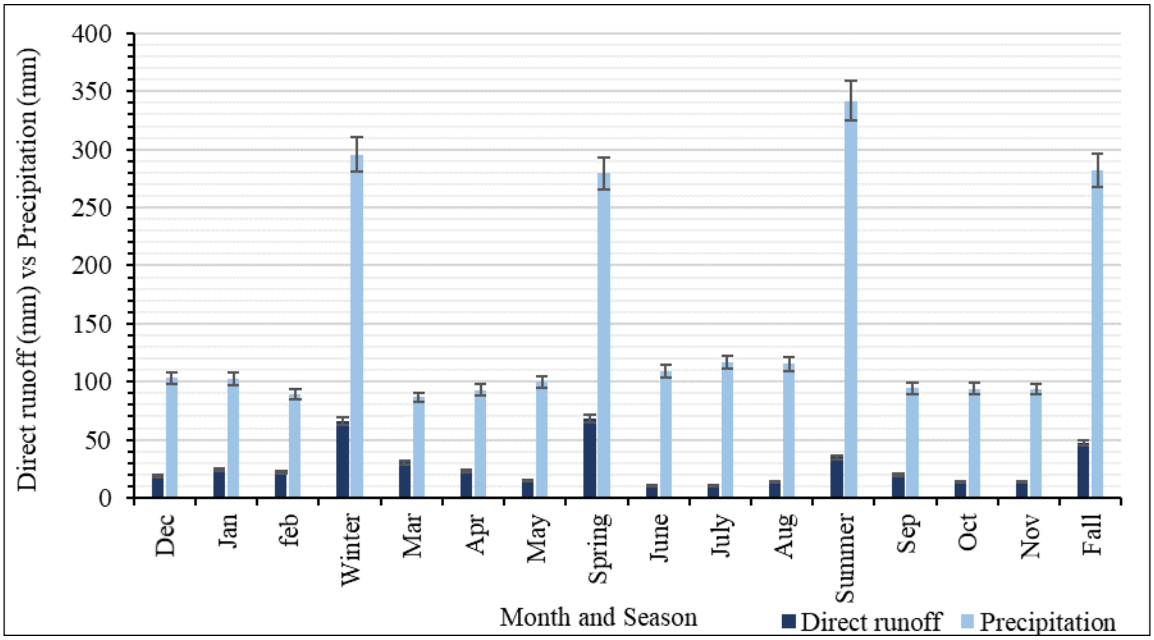

Figure 3.14. Runoff coefficients from 1951 to 2015 for Blackwater River Watershed.

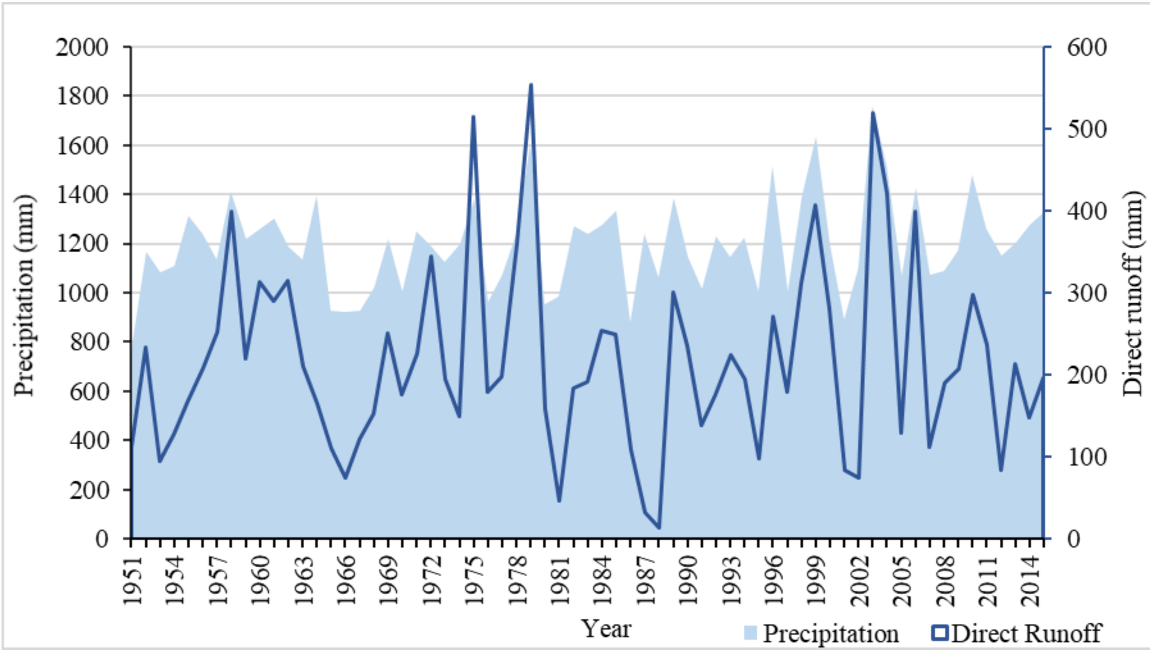

(a)

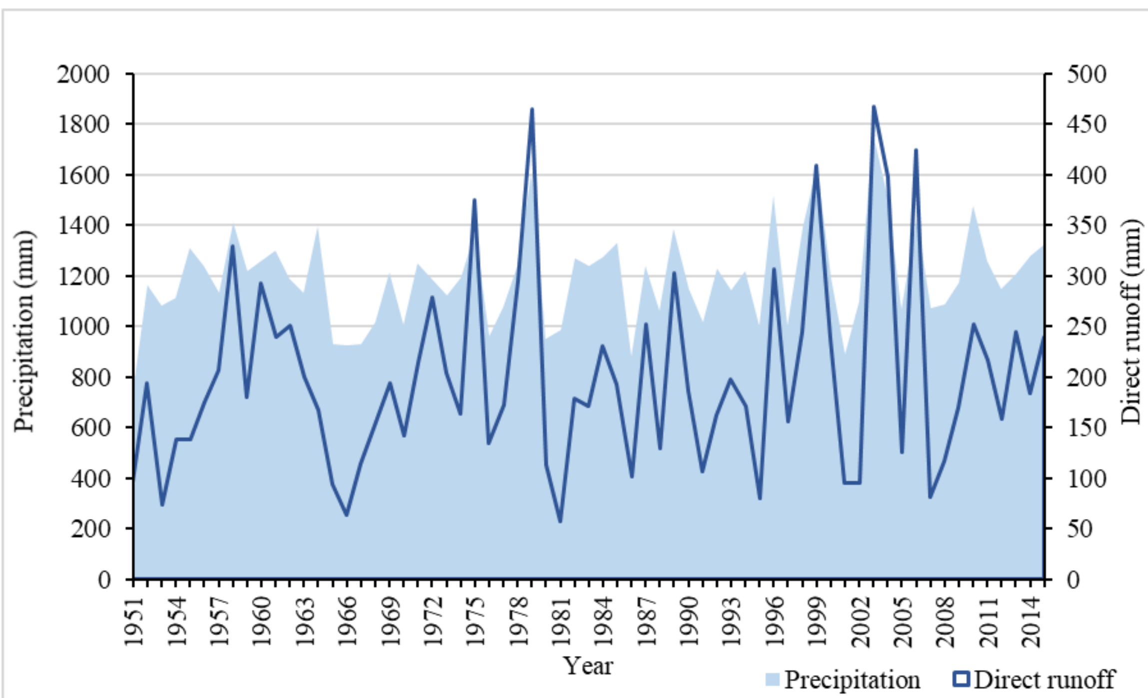

(b)

Figure 3.15. Annual precipitation and direct runoff at: (a) Dendron; and (b) Franklin.

3.3.6.2 Direct Runoff versus Baseflow

Figure 3.16 shows the annual baseflow, direct runoff, precipitation, and percentage of direct runoff for the drainage areas above Franklin and Dendron. For the drainage area above Dendron, almost 50% of the total runoff was baseflow, whereas for the drainage area above Franklin, the baseflow accounted for a large percentage of the total runoff. For both drainage areas, the maximum annual precipitations occurred in 1979 (1607 mm), 1999 (1636 mm), and 2003 (1760 mm), which generated the largest direct runoffs and baseflows. At Dendron, the percentage of direct runoff reached its maximums in 1988 (3 %), 1999 (2.7%), and 2006 (2.9%). At Franklin, the maximum percentages of direct runoff were observed in 1981(3.6 %), 1999 (3.4%), and 2006 (3.5%). The relatively large percentages of direct runoff in 1999 and 2006 can be attributed to the Nor'easter and hurricane Floyd, respectively.

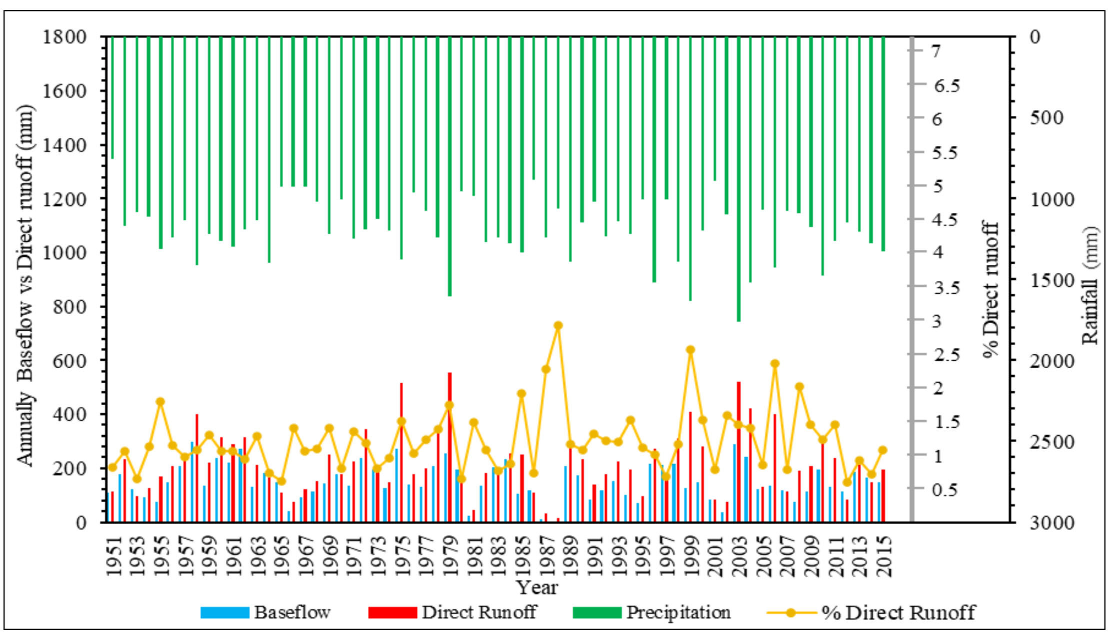

(a)

[Figure 3.16]

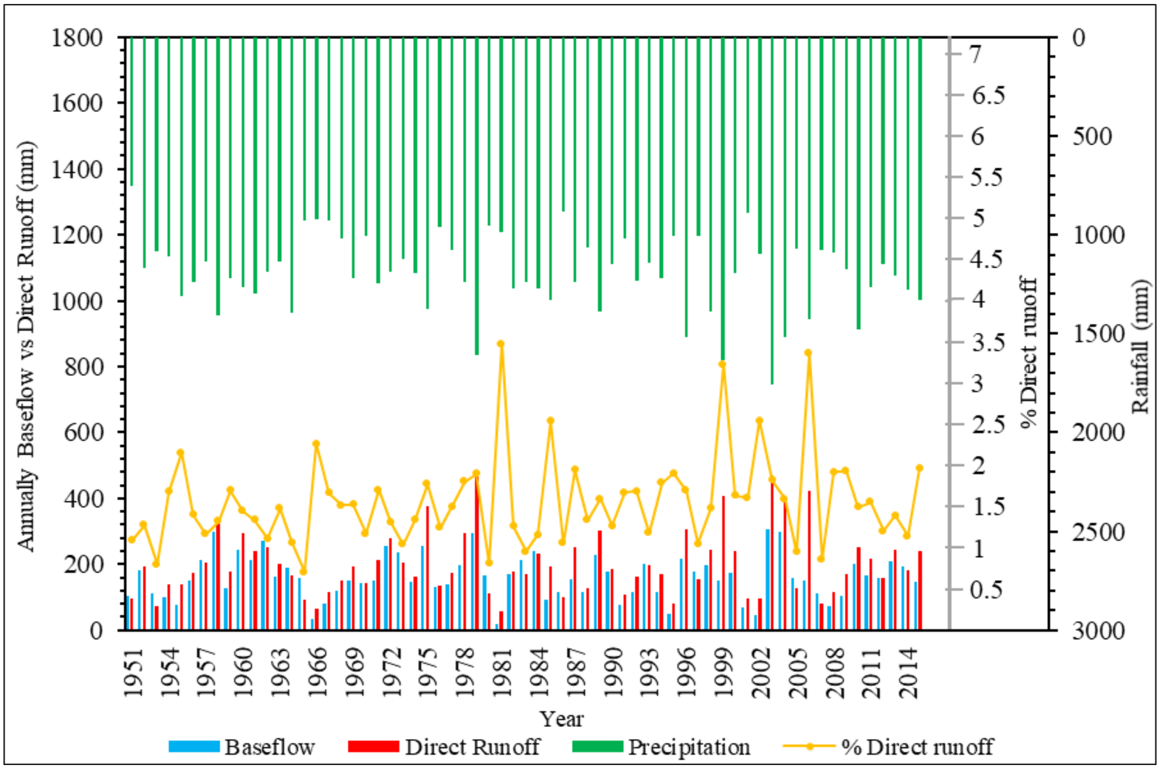

(b)

Figure 3.16. Participations of annual precipitation at: (a) Dendron; and (b) Franklin.

3.4 Sub-conclusions

For Blackwater River Watershed, while both precipitation and runoff fluctuated annually and from season to season within a year, the data in the past 65 years did not indicate either a significant increasing or decreasing trend in precipitation. The weak increasing trends (i.e., positive slopes of the regression trendlines in Figure 3.1) were probably caused by the two outlier storms occurred in 1999 and 2006; so, climate change can be downplayed for the study watershed. In addition, the rainfall-runoff relationship was not changed by human activities, as indicated by the linear double-mass curves

(Figure 3.10). This means that for a given storm, the resulting streamflow hydrograph at a point of interest along the Blackwater River was expected to be same regardless of times (e.g., 1950s versus 1990s). The floods occurred in the watershed might primarily be caused by storms with an above-normal rainfall intensity and/or duration rather than by human activities. Also, the storage capacities provided by depressions, wetlands, channels, and soils might have a large spatial variability (Figure 3.11). Along the Blackwater River, the total streamflow consisted of a large fraction of baseflow. At the annual scale, baseflow accounted for more than 50% of streamflow (Figures 3.6a and 3.7a). Such a percentage was larger in spring (Figures 3.6b and 3.7b) and winter (Figures 3.6e and 3.7e), whereas it was smaller in summer (Figures 3.6c and 3.7c) and fall (Figures 3.6d and 3.7d). At both Franklin and Dendron, although precipitation increased in summer, the corresponding runoff decreased; and vice versa (Figures 3.13 and 3.14). Higher temperatures with steady precipitation tended to produce less runoff, whereas lower temperatures were favorite for producing more runoff. Streamflow can typically be divided into two components: direct runoff and baseflow. The portion of direct runoff is generally greater than that of baseflow.

CHAPTER 4

STATISTICAL RAINFALL-RUNOFF RELATIONSHIPS

This chapter discusses the statistical analyses of rainfall-runoff relationships using the long-term data on precipitation and streamflow in Blackwater River Watershed. The major results are several statistical models that extrapolate the observational relationships presented in Chapter 3 and can be used for forecasting runoff of future climate.

4.1 Background

Several methods have been used to study relationships among runoff, precipitation, and temperature. Among them, time series analysis is most popular. It is realized by several processes for modeling and forecasting hydrological time series (Tankersley *et al.*, 1993). Many studies used autoregressive moving average (ARMA) process for predicting runoff sequences (Hipel and McLeod, 1994). The ARMA forecasts future values of a time series using lagged observations as well as lagged values of residual errors. However, this approach is not able to count for the effect of covariates. Currently, the ARMA does not include an exogenous variable (ARMAX) for assessing hydrologic data. This issue was resolved in this dissertation to address the relationship between time series data and some other explanatory variables by considering the impact of autocorrelation between observations. On the other hand, the transfer function model is another approach to assess a series of serially correlated observations (dependent variable) dependent on some interventions (independent variable). This model accounts for the association between two time series when one has a considerable impact on the other. In existing literature, both the ARMAX and transfer function models have been widely used.

A Markov switching time series was applied on a daily runoff series from Lake Taupo, New Zealand by combining three ARMA models for rising, falling, and normal states in the runoff data (Legates and McCabe Jr, 1999). The trend analysis on the hydrological cycle in the Yellow River basin, China, suggested that the decreasing trend in rainfall was followed by the downward trend in runoff (C. Liu and Zheng, 2004). The multivariate autoregressive (MAR) and autoregressive (AR) models were applied and evaluated for modeling rainfall-runoff data in Odra River, Poland (Niedzielski, 2007). The artificial intelligence (AI) and artificial neural network (ANN) approaches have been implemented for modeling hydrological data. The performance of the AI and ARMA models in forecasting monthly flow data in the Lancangjiang River were compared by Qi *et al.* (2009). A combination of seasonal ARMAX and ANN processes was proposed for modeling and capturing the periodicity features of runoff-rainfall series from two watersheds in northwest Iran (Nourani *et al.*, 2011). A multivariate generalized autoregressive conditional heteroscedasticity (MGARCH) model was conducted to remove heteroscedasticity from the residuals of the ARMAX model of the rainfall-runoff process of Saint-Laurent watershed, Quebec, Canada (Modarres and Ouarda, 2013).

Nigam *et al.* (2014) applied several time series models including SARIMA and PARIMA for assessing the most accurate approach for modeling and forecasting rainfall-runoff data. Moravej and Khalili (2015) assessed the conditions when the ARMA model is adequate for analyzing stream flow data. The ANN hybrid approach was developed to overcome the deficiency of ARIMAX and ANN for modeling spikes of runoff coefficients (Pektaş and Cigizoglu, 2013). Ghorbani *et al.* (2016) suggested that data-based models such as ANN have a better performance in modeling rainfall-runoff data than hydrologic simulation models. The ensemble empirical model decomposition (EEMD) approach was coupled with the ARIMA model to improve forecasting of annual runoff time series in Biliuhe River, China (W.-c. Wang *et al.*, 2015).

However, the association between runoff and rainfall-temperature sequences has rarely been examined. The objective of this dissertation was to assess the relationship between runoff and rainfall time series in Blackwater River Watershed located in east coastal Virginia using the transfer function model, with air temperature as a covariate. The adequacy of the final transfer function was evaluated using Dickey-Fuller, KPSS, Ljung-Box, and Box-Cox Transformation. Moreover, to justify the complexity of the final model, its modeling performance was compared with several simplest time series models.

4.2 Transfer Function Modeling

Hydrological time series are complex and dynamic through the existence of cross-correlation between response and explanatory variables along with the serial correlation between them. Thus, more advanced approaches are required to investigate this complication. Transfer function models have been introduced to study the relationship between two or more time series when the current and past values of one can predict the future values of the other (Box and Tiao, 1975). A transfer function model of two ARMA processes, i.e., response $\{Y_t\}$ and predictor $\{X_t\}$ time series, is defined as (Brockwell *et al.*, 2016):

$$\mathrm{Y_t} = \sum_{j=0}^{\infty} \tau_j \mathrm{X}_{t-j} + \mathrm{N_t} \tag{4.1}$$

where the bivariate process $\{(Y_t, X_t)\}$ is stationary; $\{N_t\}$ is zero-mean stationary; and $\tau_j{}'s$ are coefficients of the explanatory variable $\{X_t\}$.

It has been proposed (Box and Jenkins, 1976; Brockwell *et al.*, 2016) that systematic pattern in the coefficients τ_j could be expressed as a polynomial including fewer parameters as $T(B) = \delta(B)B^d/\omega(B)$. By substituting and simplifying, Eq. (4.1) can be rewritten as:

$$\mathrm{Y_t} = \frac{\delta(\mathrm{B})\mathrm{B^d}}{\omega(\mathrm{B})}\mathrm{X_t} + \mathrm{N_t} \tag{4.2}$$

where $\omega(B)$ is the autoregressive operator with the order p'; $\delta(B)$ is the moving average operator with the order q' ; having the same form as $\phi(B)$ and $\theta(B)$; and $d \geq 0$ is called delay parameter which is the smallest value of j such that τ_j is not zero and indicates that the influence of the input on output is delayed by d lags.

The term N_t is the residual of the lagged regression model on the input and output series. From Eq. (4.2), the ARMA model of residuals can be expressed as $N_t = \phi^{-1}(B)\theta(B)N_t'$. Hence, the final transfer function model can be expressed as:

$$\phi(B)\omega(B)Y_t = \phi(B)\delta(B)B^d X_t + \omega(B)\theta(B)N_t' \qquad (4.3)$$

Eq. (4.3) decomposes response time series into three components, including: 1) previous values of response series and their deviation from the series mean; 2) previous values of predictor variable and their deviation from predictors' mean; and 3) innovations.

4.3 ARMA and ARMAX Modeling

The ARMA (Box and Jenkins, 1976) is one of the most frequently used stochastic methods for modeling and forecasting time series. The ARMA (p, q) model is defined as:

$$\mathbf{Y_t = \phi_1 Y_{t-1} + \cdots + \phi_p Y_{t-p} + Z_t + \theta_1 Z_1 + \cdots + \theta_q Z_{t-q}} \qquad (4.4)$$

where $\{Y_t\}$ is a stationary time series; $\{Z_t\}$ is a Gaussian white noise series with mean zero and variance σ^2; p and q show the orders of AR and MA terms, respectively.

The ARMA model studies the association between historical observations to measure autocorrelation between outcomes for predictive purpose. In this approach, the AR terms are the lagged values of outcome significantly correlated with recent observation, and the MA components are the lagged errors. By these two terms, Eq. (4.4) can be rewritten as:

$$\mathbf{\phi(B)Y_t = \theta(B)Z_t} \qquad (4.5)$$

where $\phi(B) = 1 - \phi_1 B - \phi_2 B^2 - \cdots - \phi_p B^p$ and

$\theta(B) = 1 + \theta_1 B + \theta_2 B^2 + \cdots + \theta_p B^q$ are autoregressive and moving average operators, respectively; and B is the backward shift operator such that $B^j Y_t = Y_{t-j}$.

The autocorrelation function (ACF) of an ARMA process is given as $\rho(h) = \gamma(h)/\gamma(0)$, where $\gamma(h) = cov(Y_{t+h}, Y_t)$. Several hydrological time series can be modeled by a seasonal pattern with a fixed period. A seasonal ARMA model can be expressed as:

$$\boldsymbol{\phi}(\mathbf{B})\boldsymbol{\Phi}(\mathbf{B}^s)\mathbf{Y}_t = \boldsymbol{\theta}(\mathbf{B})\boldsymbol{\Theta}(\mathbf{B}^s)\mathbf{Z}_t \tag{4.6}$$

where $\Phi(B^s) = 1 - \Phi_1 B^s - \Phi_2 B^{2s} \cdots - \Phi_P B^{Ps}$,

$\Theta(B) = 1 + \Theta_1 B^s + \Theta_2 B^{2s} \cdots + \Theta_Q B^{Qs}$, $\phi(B)$, and $\theta(B)$ are given by Eq. (4.5).

Such a model of Eq. (4.6) is expressed as $SARIMA(p, q) \times (P, Q)_s$ process with period s, where p and q show the orders of seasonal AR and seasonal MA process, respectively.

In the case of existing an exogenous covariate variable, X_t, Eq. (4.5) can be written as:

$$\boldsymbol{\phi}(\mathbf{B})\mathbf{Y}_t = \boldsymbol{\beta}\mathbf{X}_t + \boldsymbol{\theta}(\mathbf{B})\mathbf{Z}_t \tag{4.7}$$

Such a model of Eq. (4.7) has been introduced as ARMAX (autoregressive moving average with exogenous variable). It can address the impact of one or more additional explanatory variables on the independent (i.e., predicting) variable.

4.4 Parameter Estimation

Several methods have been introduced for estimating parameters of an ARMA process; and the maximum likelihood estimation (MLE) is the most popular one. The Gaussian likelihood of an ARMA model (Brockwell *et al.*, 2016; Q. Yao and Brockwell, 2006) has been used to exploit MLE of parameters (ϕ, θ), which are those values that minimize the following expression (Brockwell *et al.*, 2016):

$$l(\phi,\theta) = ln\left(\frac{1}{n}S(\phi,\theta)\right) + \frac{1}{n}\sum_{j=1}^{n} ln(r_{j-1}) \tag{4.8}$$

$$\hat{\sigma}^2 = \frac{1}{n}\, S(\hat{\phi},\hat{\theta}) \tag{4.9}$$

$$S(\hat{\phi},\hat{\theta}) = \sum_{j=1}^{n}\left(Y_j - \hat{Y}_j\right)^2 / r_{j-1} \tag{4.10}$$

$$r_j = E\left(Y_{j+1} - \hat{Y}_{j+1}\right)^2 / \sigma^2 \tag{4.11}$$

The delay parameter, d, can be determined using the cross-correlation function (CCF) expressed as:

$$\boldsymbol{\rho}_{\mathbf{ZZ'}}(\mathbf{h}) = \boldsymbol{\gamma}_{\mathbf{ZZ'}}(\mathbf{h})/(\boldsymbol{\gamma}_{\mathbf{ZZ}}(\mathbf{0})\boldsymbol{\gamma}_{\mathbf{Z'Z'}}(\mathbf{0}))^{-1/2} \tag{4.12}$$

where $Z_t = \omega(B)\theta^{-1}(B)Y_t, Z_t' = \omega(B)\theta^{-1}(B)X_t$, and $\gamma_{ZZ'}(h) = cov(Z_{t+h}, Z_t')$.

The boundaries for the CCF are computed as $\pm 1.96/\sqrt{n}$, where n is the number of observations. In addition, coefficients $\{\tau_j, j = 0,1,\cdots\}$ in Eq. (4.1) are estimated as:

$$\hat{\tau}_j = \hat{\rho}_{ZZ'}(h)\hat{\sigma}_Z/\hat{\sigma}_{Z'} \tag{4.13}$$

where $\hat{\sigma}_Z^2 = Var(Z_t)$, $\hat{\sigma}_{Z'}^2 = Var(Z_t')$, and $\hat{\rho}_{ZZ'}(h)$ is obtained by (4.8).

The orders (i.e., p and q) of an ARMA process are selected by minimizing three statistics, namely Akaike information criterion (AIC), Akaike information corrected criterion (AICC), and Bayesian information criterion (BIC). These statistics are computed as:

$$AIC = -2\ln\left[L\left(\phi_p, \theta_q, S\left(\phi_p, \theta_q\right)/n\right)\right] + 2(p+q+1) \tag{4.14}$$

$$AICC = -2\ln\left[L\left(\phi_p, \theta_q, S\left(\phi_p, \theta_q\right)/n\right)\right] + 2(p+q+1)n/(n-p-q-2) \tag{4.15}$$

$$\mathrm{BIC} = -2\ln\left[\mathrm{L}\left(\phi_p, \theta_q, S\left(\phi_p, \theta_q\right)/n\right)\right] + \log(n)(p + q + 1) \tag{4.16}$$

where $\mathrm{L}\left(\phi_p, \theta_q, S\left(\phi_p, \theta_q\right)/n\right)$ is the Gaussian likelihood of an ARMA process (Brockwell *et al.*, 2016; Q. Yao and Brockwell, 2006).

In addition, two other measures of forecast accuracy, namely root mean squared error (RMSE) and mean absolute scaled error (MASE) (Hyndman and Koehler, 2006) were computed and used to compare the models of interest. Further, four evaluation criteria were used to measure the adequacy of the model of interest; they are Dickey-Fuller test for stationary (Dickey and Fuller, 1979), Ljung-Box test for serial correlation (Ljung and Box, 1978), KPSS test for stationary residuals (Kwiatkowski *et al.*, 1992), and Box-Cox transformation for testing constant variance (Box and Cox, 1964).

4.5 Results

This section examines performances of the ARMA, ARMAX, and transfer function methods in modeling monthly runoff data in Blackwater River watershed, Virginia, between January 1950 and December 2015. Precipitation and air temperature were considered as the exogenous variables in the ARMAX model. In the transfer function model, temperature was considered as an exogenous variable and precipitation as an explanatory variable.

Time series plots of runoff and rainfall observations are illustrated in Figure 4.1. Rainfall and temperature reach their maximums during summer (June to August), during which runoff attains its minimum (Table 4.1 and Figure 4.2). The ACF and PACF plots of runoff-rainfall sequences (Figure 4.3) indicate that AR (1) with seasonal pattern and ARMA (1, 1) processes could be suitable for the runoff and rainfall observations, respectively. Hence, it is suggested that a transform function model including first-order AR process on runoff, second order AR, and second order MA on rainfall could be an appropriate model for describing the observed runoff-rainfall time series. The CCF between runoff and rainfall suggest no delayed effect of rainfall on runoff sequence (i.e., $d = 0$) (Figure 4.4). The negative lags indicate that rainfall is prior to runoff.

Table 4.1. Statistics of monthly runoff, rainfall, and temperature from 1950 to 2015.[1]

Month	Runoff (mm)	Rainfall (mm)	Temperature(c)
Jan	45.56 (25.24)	365.91 (150.58)	3.57 (2.59)
Feb	48.41 (26.48)	328.92 (134.88)	4.98 (2.14)
Mar	57.54 (31.63)	390.66 (151.53)	9.21 (1.91)
Apr	43.10 (26.49)	338.51 (147.13)	14.64 (1.51)
May	25.29 (20.36)	390.82 (145.07)	18.99 (1.46)
Jun	16.85 (19.40)	407.25 (179.37)	23.24 (1.26)
Jul	12.77 (17.15)	516.43 (189.48)	25.20 (1.02)
Aug	17.05 (23.78)	518.25 (246.56)	24.26 (1.18)
Sep	22.47 (46.11)	459.68 (324.62)	20.89 (1..30)
Oct	18.81 (32.50)	360.00 (201.27)	14.81 (1.89)
Nov	19.61 (23.19)	327.79 (186.23)	9.86 (1.72)
Dec	31.83 (25.64)	349.82 (154.58)	5.38 (2.51)

[1] The number outside bracket is mean and the number in bracket is standard deviation.

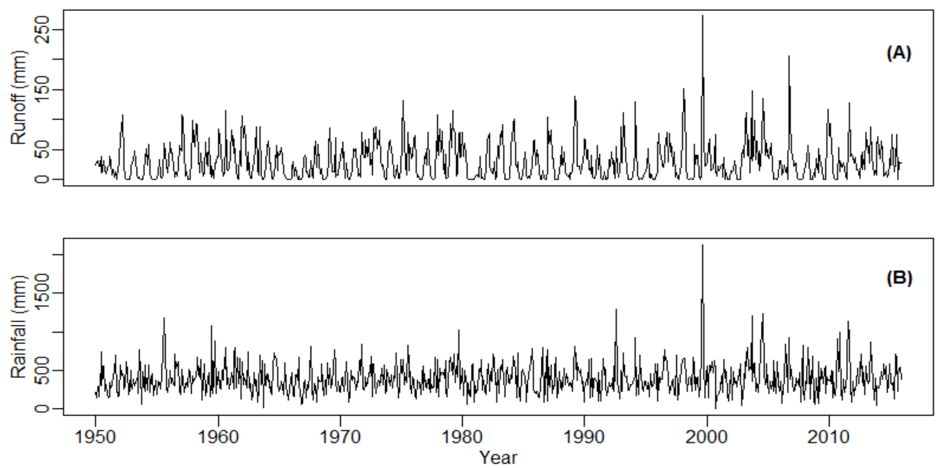

Figure 4.1. Plot of: (a) runoff; and (b) rainfall. The observed time series for Blackwater River Watershed from January 1950 to December 2015.

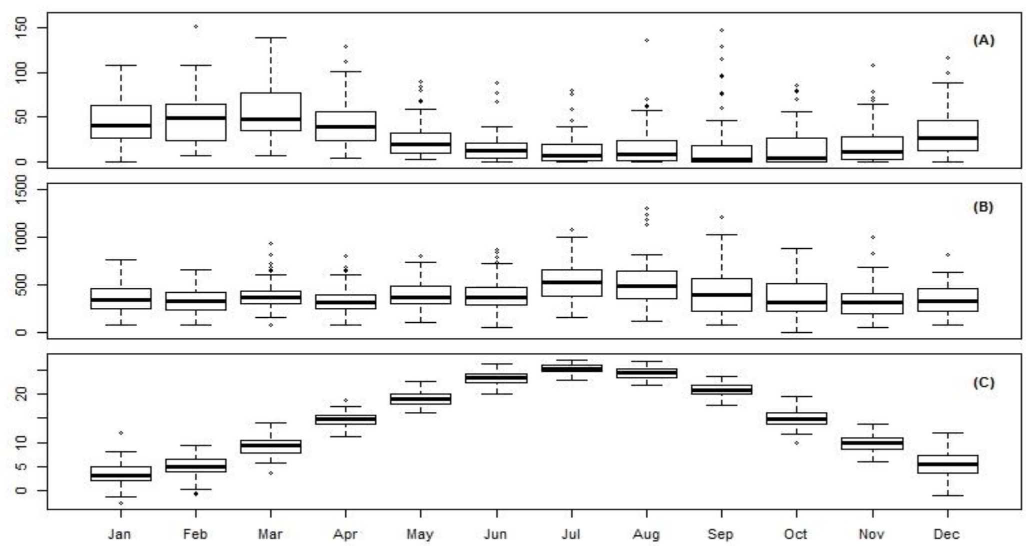

Figure 4.2. Plot of monthly: (a) runoff (mm); (b) rainfall (mm); and (c) temperature (˚C). The record period is from January 1950 to December 2015.

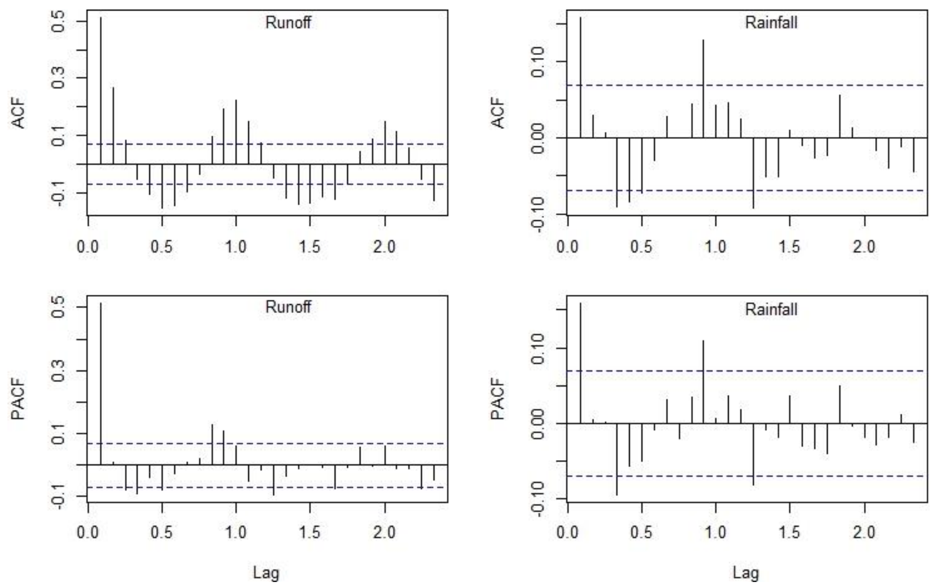

Figure 4.3. ACF and PACF plots for runoff and rainfall time series.

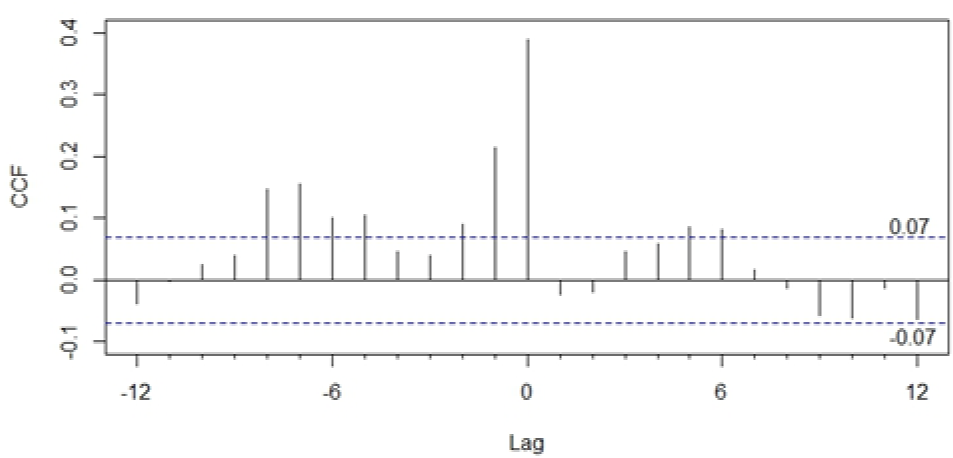

Figure 4.4. CCF plot for runoff-rainfall time series.

To find the best model, a set of transfer function models with $p = 1, 2$; $q = 0,1,2$;

$p' = 0,1,2,3$; and $q' = 0,1,2,3$, including seasonal factor $s = 0,1$ and temperature, were tried. Then the performance of all 192 models were compared using the AIC, AICC, and BIC criteria. The five best-fitted models are presented in Table 4.2. According to the results, Model 1 ($p = 2, s = 1, q = 0, p' = 0, q' = 2$) has the lowest AIC and AICC values, however, Model 2 ($p = 1, s = 1, q = 0, p' = 0, q' = 2$) has the lowest BIC value.

Table 4.2. Performance comparison of suggested transfer function models.

Model	Runoff	Rainfall	AIC	AICC	BIC
1	$\text{ARMA}(2,0)(1,0)_{12}$	$\text{ARMA}(0,2)$	**7110.713**	**7110.820**	7138.760
2	$\text{ARMA}(1,0)(1,0)_{12}$	$\text{ARMA}(0,2)$	7110.935	7111.011	**7134.308**
3	$\text{ARMA}(1,1)(1,0)_{12}$	$\text{ARMA}(0,2)$	7111.347	7111.454	7139.394
4	$\text{ARMA}(2,1)(1,0)_{12}$	$\text{ARMA}(1,2)$	7111.722	7111.865	7144.444
5	$\text{ARMA}(2,0)(1,0)_{12}$	$\text{ARMA}(1,2)$	7112.701	7112.843	7145.422

Moreover, both models were compared with two simpler models, namely AR (1) and ARMAX (1, 0), with rainfall-temperature as exogenous variables. Table 4.3 reveals that the transfer function models have lower AIC, AICC, BIC, RMSE, and MASE values; therefore, they are more suitable than two other models. Table 4.4 provides the MLE estimators for the parameters of Model 2. Although Model 1 has lower AIC and AICC than Model 2, the coefficient of second order autoregressive component is insignificantly different from zero, 95% confidence interval $(-0.02, 0.12), p = 0.14$, which suggests that Model 1 may be over-fitted. Therefore, Model 2 seems more adequate and preferred over Model 1 for modeling the runoff-rainfall time series.

Table 4.3. Evaluation criteria for the AR, ARMAX, and transfer function models.

Model	RMSE	MASE	AIC	AICC	BIC
AR	26.15	0.94	7425.97	7426.07	7451.019
ARMAX	22.45	0.83	7188.15	7188.25	7216.197
Model.1	21.54	0.796	**7110.713**	**7110.820**	7138.760
Model.2	21.57	0.796	7110.935	7111.011	**7134.308**

The final model is Model 2. It shows that runoff amount at time t is significantly correlated with runoff from time $t-1$ with a seasonal pattern of 12 months. In addition, the current runoff is significantly influenced by recent rainfall as well as rainfall error from the last two time points. The term of rainfall error or deviation of rainfall from mean refers to the amount of rainfall which is unusually more or less than expected value in the last two time points. Further, it is a significant negative correlation between runoff and temperature at time t. The scatter plots of runoff by rainfall, temperature, and previous runoff are illustrated in Figure 4.5.

Table 4.4. Parameter estimations for Model 1 and Model 2.[1]

Model		Coefficient	Estimate (S.E)	p-value
Model 1	Runoff	ϕ_1	0.38 (0.04)	<0.001***
		ϕ_2	0.05 (0.04)	0.14
		Φ_1	0.12 (0.04)	0.001**
	Rainfall	β_1	0.07 (0.003)	<0.001***
		θ_1'	0.03 (0.003)	<0.001***
		θ_2'	0.01 (0.003)	<0.001***
	Temperature	β_2	-1.74 (0.16)	<0.001***
Model 2	Runoff	ϕ_1	0.39 (0.03)	<0.001***
		Φ_1	0.12 (0.04)	0.001**
	Rainfall	β_1	0.07 (0.003)	<0.001***
		θ_1'	0.03 (0.003)	<0.001***
		θ_2'	0.01 (0.003)	<0.001***
	Temperature	β_2	-1.74 (0.16)	<0.001***

[1] *: significant at a significance level of $\alpha = 0.1$; **: significant at $\alpha = 0.05$; ***: significant at $\alpha = 0.01$.

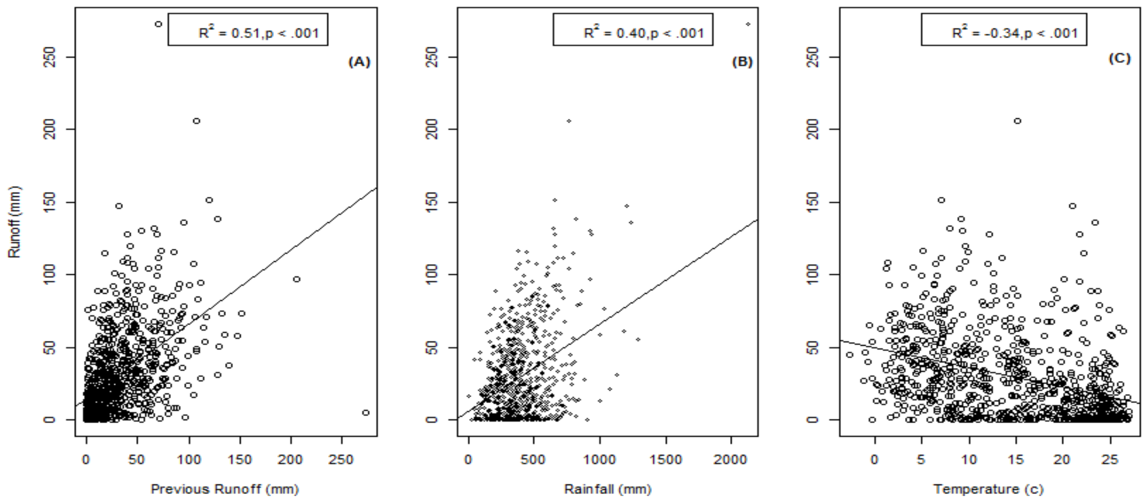

Figure 4.5. Runoff versus: (a) previous runoff; (b) rainfall; and (c) temperature.

Additionally, Dickey-Fuller and KPSS tests suggest that the fitted values and residuals obtained from the transfer function Mode l and Model 2 are stationary. The Ljung-Box test and Box-Cox transformation do not support the existence of any serial correlation and heteroscedasticity in the residuals (Table 4.5). Figure 4.6 specifies that standard residuals of Model 2 behave as an identically independent (i.i.d) sequence with mean zero and constant variance one. Hence, the adequacy of Model 2 can be concluded.

Table 4.5. Assumption check for transfer function model.

	Statistic	p	Null Hypothesis
Dickey-Fuller	-7.75	0.01	Fitted values are not stationary
KPSS	0.05	0.1	Residuals are stationary
Ljung-Box, $\mathbf{x^2(df)}$	0.34 (1)	0.56	No serial correlation in residuals
Box-Cox Transformation, $\boldsymbol{\lambda}$	0.85	-	Power transformation is not required for λ around 1

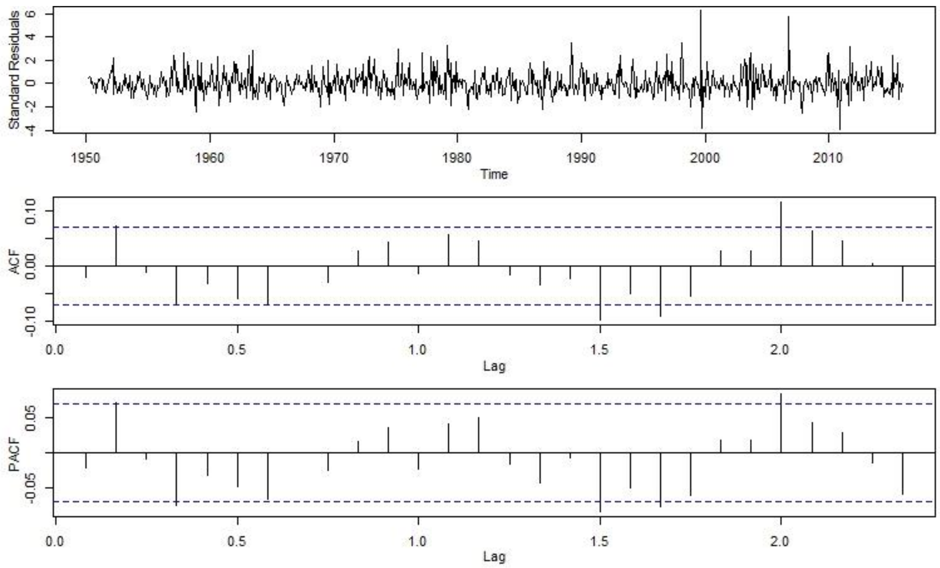

Figure 4.6. ACF and PACF and plot of standard residuals.

Moreover, Model 2 is conducted to predict the values of the runoff series. The fitted (January 2008 to December 2016) and predicted values (January to December 2017) of runoff series, including Lower Predicted Intervals (LPI) and Upper Predicted Intervals (UPI), are obtained from Model 2 (Figure 4.7). The predictors of h-step ahead of runoff values are computed in the following manner. First, an MA (1) process is used to predict the h-step ahead of rainfall values. Then, the mean values of monthly temperature are calculated. Finally, forecasted runoff values are computed by Model 2 using predicted rainfall values and monthly mean temperature. Note that negative LPI values were adjusted to zero.

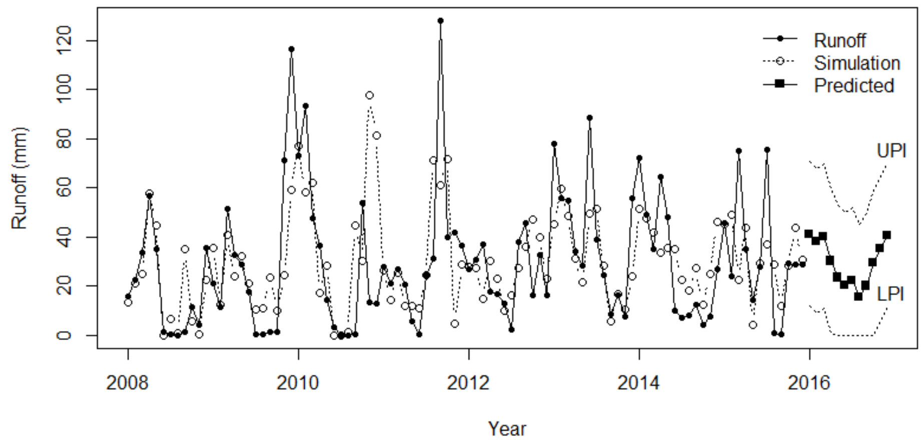

Figure 4.7. Observed and fitted runoffs by the transfer function model. The record is from January 2012 to December 2015.

4.6 Sub-conclusions and Discussion

There are several similarities and differences between findings of this study with those of prior studies, however, the model employed here is more comprehensive in terms of detecting autocorrelation between runoff and rainfall sequences along with temperature as an exogenous variable.

A Bayesian dynamic approach and Gibb's sampler are used to analyze daily runoff based on past runoff-rainfall sequence. In this model, a combination of three states of runoff is considered, namely rising, falling, and normal. It is shown that high runoff values are followed by considerable runoff even during the falling regime (S. Neitsch, 2005). Although this dissertation indicates the effect of rainfall on runoff, but this effect is limited to the rising regime. Another study (C. Liu and Zheng, 2004) found that the decreasing trend in rainfall was significantly associated with decreasing trend in runoff, but the effect of temperature was not included in the model.

Artificial Intelligence (AI) approaches have been employed on the runoff time series and been compared with the ARMA model (Qi *et al.*, 2009). Although it is suggested that AI fitted the data better, the proposed models are not adjusted for the influence of rainfall-temperature covariates.

Moreover, a water-balance model specified the positive correlation between runoff and rainfall time series; however, it did not support the impact of temperature on runoff (McCabe and Wolock, 2011). A combination of seasonal ARMA and Artificial Neural Network (ANN) approach on runoff-rainfall time series detected significant autocorrelation between runoff-rainfall observation as well as seasonality factor (Nourani *et al.*, 2011), though temperature was not taken into account. On the other hand, different hybrid methods have been introduced in the cases of nonlinearity and heteroscedasticity among residuals of the ARMAX model (Nourani *et al.*, 2011; Pektaş and Cigizoglu, 2013), while this dissertation did not indicate any evidence of the violation of the assumptions.

In this dissertation study, runoff values are so abundant at some time points due to some "shocks." However, it would not be rational to drop or correct them as outliers because they contain crucial information and are essential for modeling and interpreting the association between runoff and rainfall time series. The highest runoff value was recorded in September 1999 followed by October 2006. The former case was a consequence of hurricane Floyd when the Blackwater River rose quickly due to the tremendous amount of rainfall (approximately five times more than the monthly average). The same pattern was observed in the latter case (the amount of rainfall in September and October 2006 are approximately two times more than the monthly average) along with high runoff value in October 2006. As a result, the amount of runoff was much more than expected in November 2006. Contrarily, from June to September 2010, the amount of runoff was much lower than average due to lower rainfalls during this time period. Obviously, all these cases follow the pattern expressed by the recommended model of this dissertation. Further, the final model generates negative LPI values for low runoff observations, which are not a critical drawback since LPI is not a CI for coefficients and does not reduce the power of the model.

CHAPTER 5

RAINFALL-RUNOFF MODELING USING SWAT

Soil and Water Assessment Tool (SWAT) is a physically based, continuous time-step hydrologic model. As a powerful interdisciplinary watershed modeling tool (Gassman *et al.*, 2007), SWAT provides variable spatial delineation of connections and processes within a watershed to assess water resource problems and overland runoff over a long time period (Cheng *et al.*, 2016). ArcSWAT is used to analyze the effect of the spatial distribution of watershed features and other climatic factor affecting streamflow. To precisely modeling water quality and quantity, SWAT needs specific data on topography, weather (precipitation, temperature), hydrography (groundwater reserves, channel routing, ponds or reservoirs, sedimentation patterns), soil properties (composition, moisture and nutrient content, temperature, erosion potential), crops, vegetation and agronomic practices (S. Neitsch, 2005). Significant factors to define stream flow, such as rainfall, temperature, elevation, slope, aspect, land cover and soil, will not be averaged over a watershed as done in many previous studies (Desta, 2006).

5.1 Model Setup

This study used SWAT because it was developed to predict impacts of land management practices on water and because it can be used in large, complex watersheds taking into varying soils, land use land cover (LULC), and management conditions in a long run. SWAT was used to mimic the hydrologic processes at the watershed scale. It is one of the most widely used watershed-scale simulation tools with worldwide applications for watershed management. For simulation purposes, a watershed needs to be subdivided into several subbasins in terms of topography. A subbasin is further subdivided into several hydrologic response units or HRUs, each of which is a unique combination of homogenous soil type, land use, and topographic gradient (Kalcic *et al.*, 2015; Winchell *et al.*, 2013). The HRUs are the basic units for the generation of runoff, which in turn is routed through the overland and drainage systems of the inclusive subbasin. The primary hydrologic processes, namely rainfall, runoff, evapotranspiration, infiltration, percolation, and baseflow, are considered. SWAT requires a diversity of information to predict the effects of soil, land use, land cover, temperature, precipitation, slope, and runoff on water supplies, pollution, soil erosion, crop production, water quality, and flooding. It was developed to evaluate effects of alternative management decisions on water resources and nonpoint-source pollution in large river basins (J. G. Arnold *et al.*, 2012).

The inputs for a subbasin include weather, land cover, type of soil, and management within the subbasin, lakes and/or reservoirs, groundwater; and the main channel or reach, draining the subbasin. The runoff, sediment, nutrient, and pesticide loadings to the main channel from each subbasin are simulated in terms of the physical hydrologic processes.

The National Elevation Dataset (NED), LULC, and SSURGO were used to delineate the watershed and its subbasins, the drainage network, and HRUs. NED provides basic elevation information and mapping applications in the United States and most of North America. The accuracy of the NED differs because of the variable quality of the source data. Since topographic information is an important requirement for so many hydrologic studies, the NED has reached large usage by the geospatial data users. An essential role of the use of the NED is provision of thorough dataset documentation including data quality and accuracy metrics. The important geospatial data contained in the NED are assessed, verified, and can be applied with increased confidence in the resulting outcomes (Gesch *et al.*, 2014). The initial values of the model parameters were automatically estimated from the grids.

The SWAT Watershed Delineation interface carries out a set of advanced GIS functions to aid the user in segmenting the watershed into several hydrologically connected subbasins for modeling purposes. In this regard, the outlets of the subbasins are automatically defined as the confluences between the adjacent streams, while they can be redefined or deleted, and more additional outlets can be added manually. The initial values of the parameters (e.g., slope and slope length) for each subbasin are calculated from the NED and stored in the attribute table of the updated watershed and reach themes as an additional field in the streams and subbasin database files.

The Blackwater River Watershed was subdivided into 6 subbasins and 35 HRUs. For each HRU, runoff is predicted separately and led to obtaining the total runoff for the watershed. Using HRU increases the accuracy and gives a much better physical description of the water balance in the prediction of the loadings (runoff with sediment, nutrients, etc. transported by the runoff) from the subbasin. The areal precipitation for a subbasin was assumed to be same as that at its nearest gauge (Marquínez *et al.*, 2003).

The watershed boundary is defined by topographic gradients, resulting in delineated areas where surface-water runoff drains downstream into a common surface-water body, such as lake, creek, stream, or portion of a river to outlet points (e.g., bays, oceans or reservoirs). The input information for each subbasin is grouped into categories of weather, specific land cover, soil, and management. The loadings of runoff, sediment, nutrient, and pesticide to the main channel in each subbasin are simulated by considering the effects of several physical processes that influence the hydrology.

5.2 Calibration and Validation

Calibration and validation are typically performed by splitting the available observed data into two datasets: one for calibration and another for validation. Data are most frequently split by periods, carefully ensuring that the climate data used for both calibration and validation are not substantially different. That is, wet, moderate, and dry years should occur in both periods (Gan *et al.*, 1997).

To validate and calibrate the results, we used Baseflow Filter program for runoff to separate surface runoff and groundwater runoff. Based on annual results, runoff is diminished during dry season, which is attributed to increased temperature (Pugh and Westerman, 2014). The decline in runoff during summer is perceived across the country in all physiographic sections (Pugh and Westerman, 2014). In regions of higher altitudes where there is larger rainfall, the possibility for increased water yield is greater (Baker and Laflen, 1982). Soil depth and land use impact the potential of water yield (Desta, 2006). Furthermore, the intensity of the planted area has an influence on the surface flow from the watershed. Figure 5.1 shows the annual simulated rainfall and runoff. For a given rainfall event, it tended to generate more runoff per unit drainage area above than below Dendron, as indicated by a larger runoff coefficient for the drainage area above Dendron (Figure 5.2).

The runoff coefficient is defined as the ratio of direct runoff to precipitation and measures the fraction of precipitation that is converted into runoff, whereas the non-runoff coefficient, which is equal to one minus the runoff coefficient, measures the fraction of precipitation that is subject to the aforementioned interception, storage, percolation and evapotranspiration losses. The runoff coefficient for the drainage area above Dendron varied from zero to 0.6, while the runoff coefficient for the drainage area above Franklin ranged from 0.05 to 0.32. Regardless of the drainage areas, the relationship between non-runoff coefficient and precipitation was found to be much better than that between runoff coefficient and precipitation (Figure 5.3a versus Figure 5.2a and Figure 5.3b versus Figure 5.2b). The relationships between non-runoff coefficient and precipitation had a coefficient of determination $R^2 > 0.89$. The good relationships between non-runoff coefficient and precipitation were also true at seasonal scales (Figures 5.4 and 5.5).

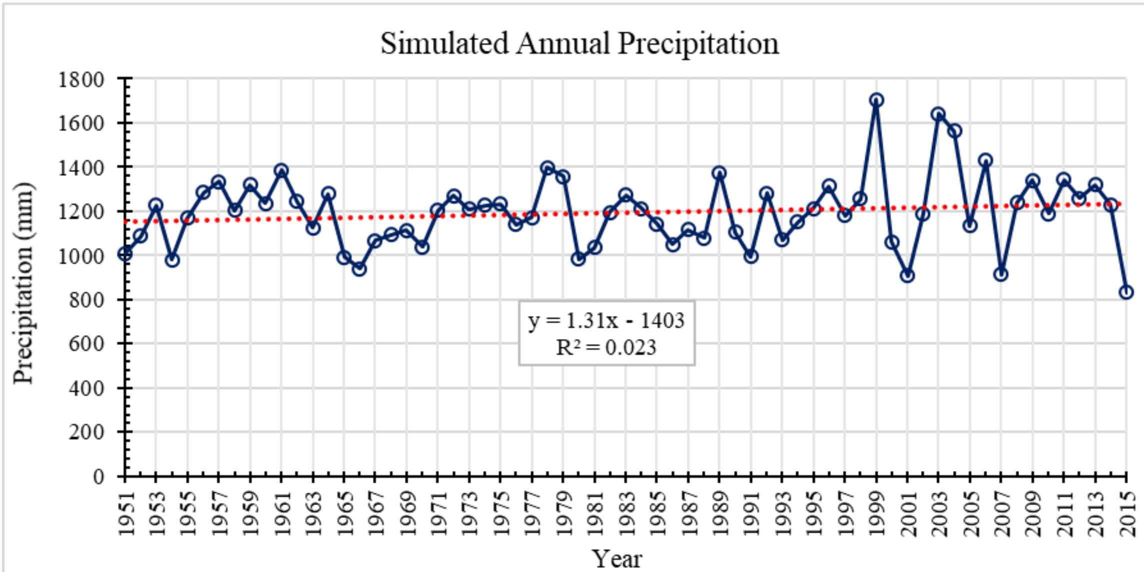

(a)

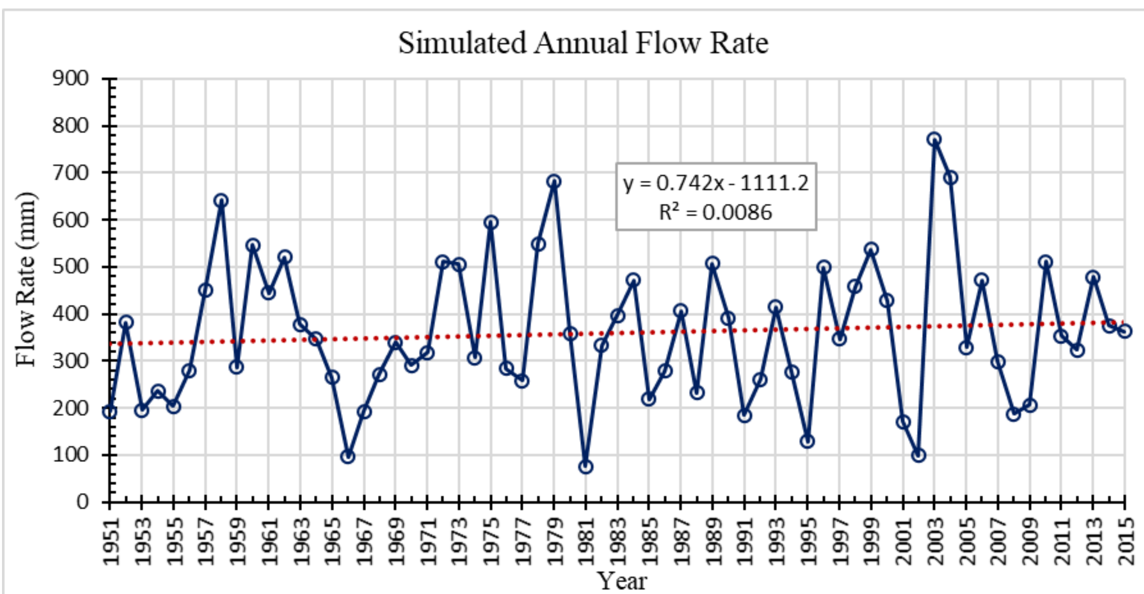

(b)

Figure 5.1. Plot showing the simulated annual: (a) precipitation; and (b) flow rate, of the Blackwater River Watershed.

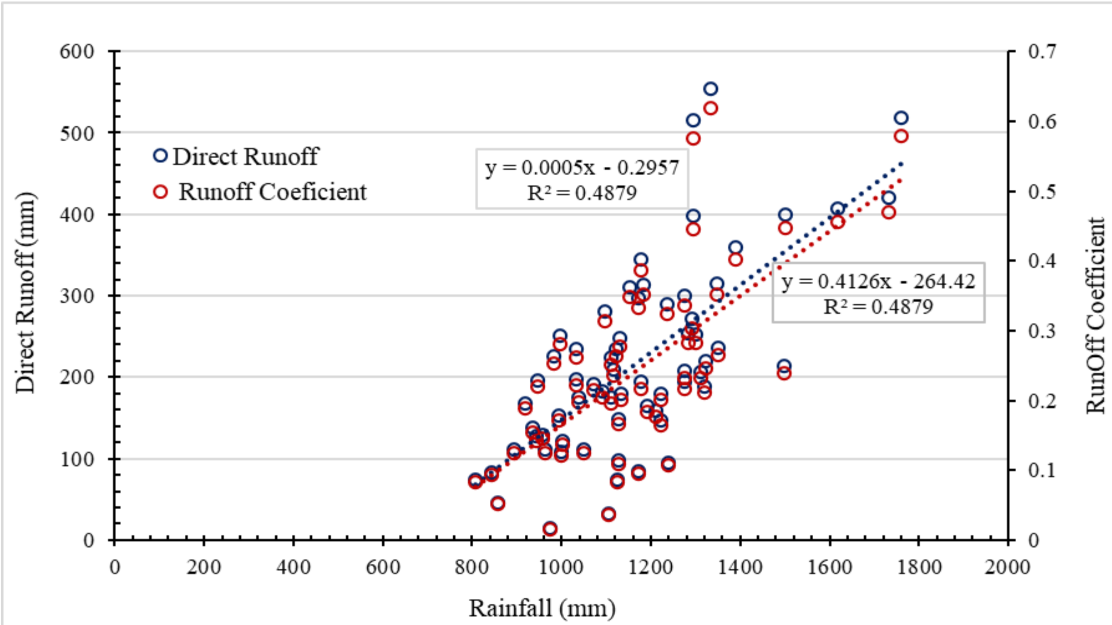

(a)

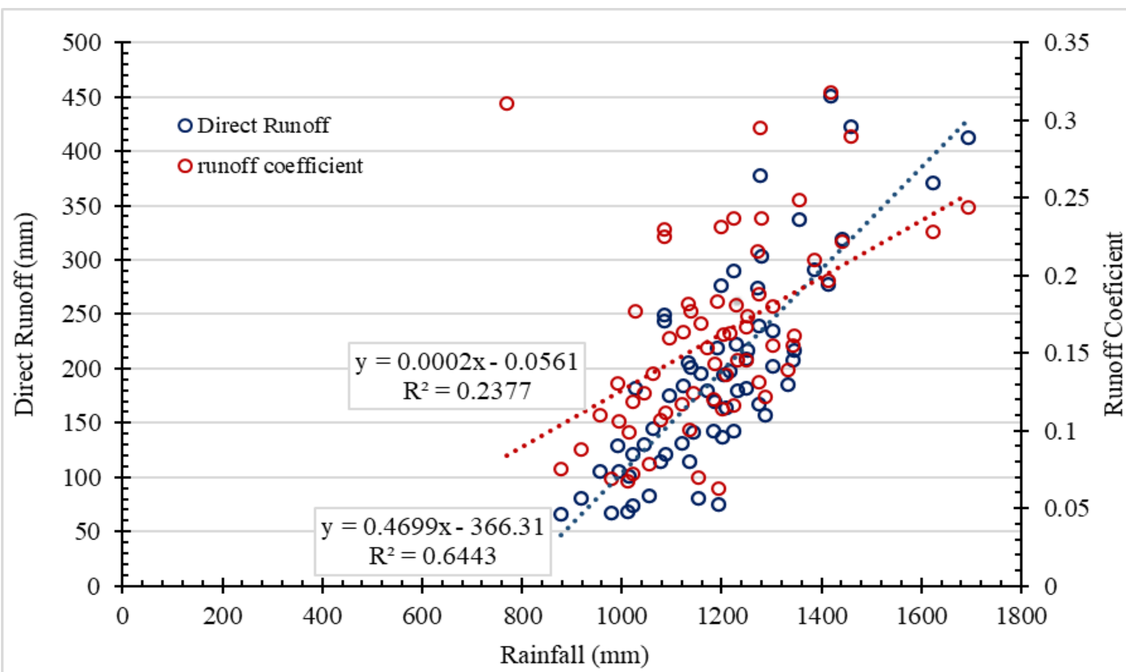

(b)

Figure 5.2. Plots showing the annual runoff and runoff coefficient versus annual rainfall for the drainage area above: (a) Dendron; and (b) Franklin. The blue hollow circle signifies direct runoff, while the red hollow circle signifies runoff coefficient.

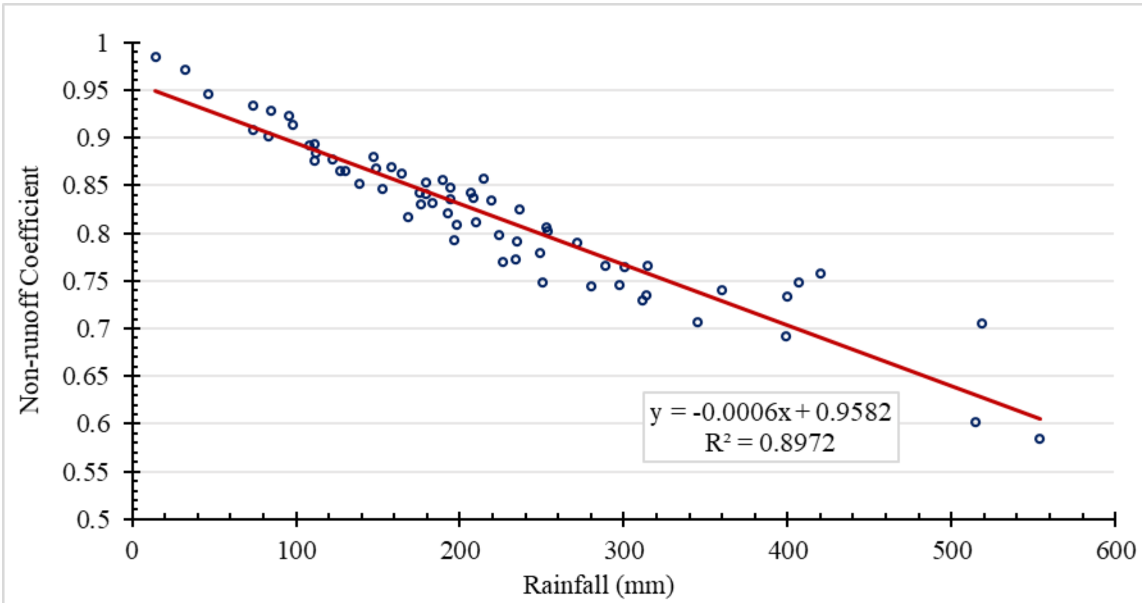

(a)

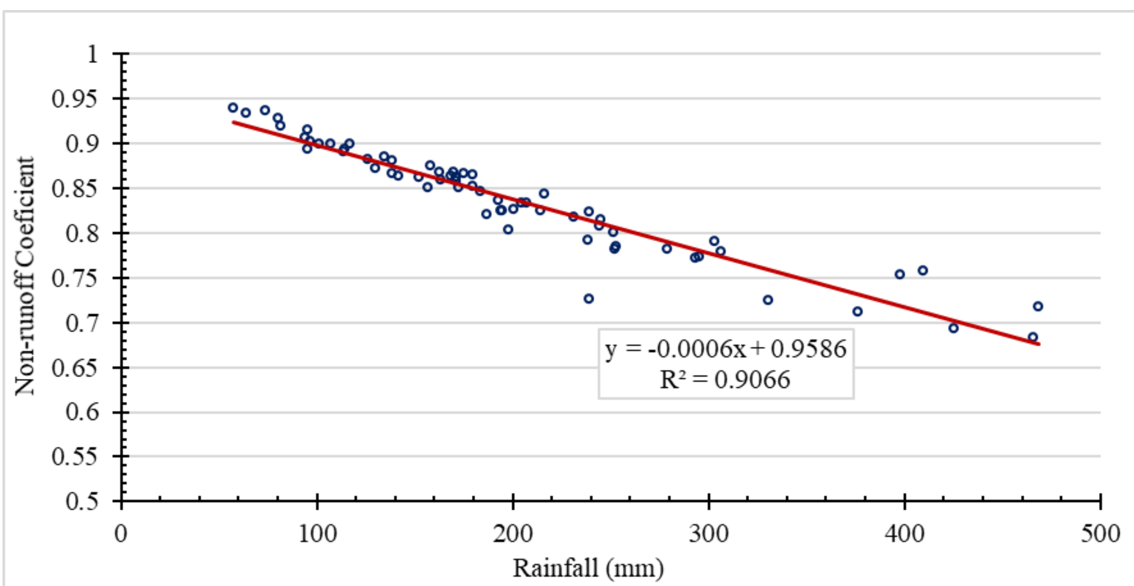

(b)

Figure 5.3. Plots showing the annual non-runoff coefficient versus annual precipitation for the drainage area above: (a) Dendron; and (b) Franklin. The non-runoff coefficient is defined as one minus the runoff coefficient, which in turn is defined as the ratio of the direct runoff to precipitation.

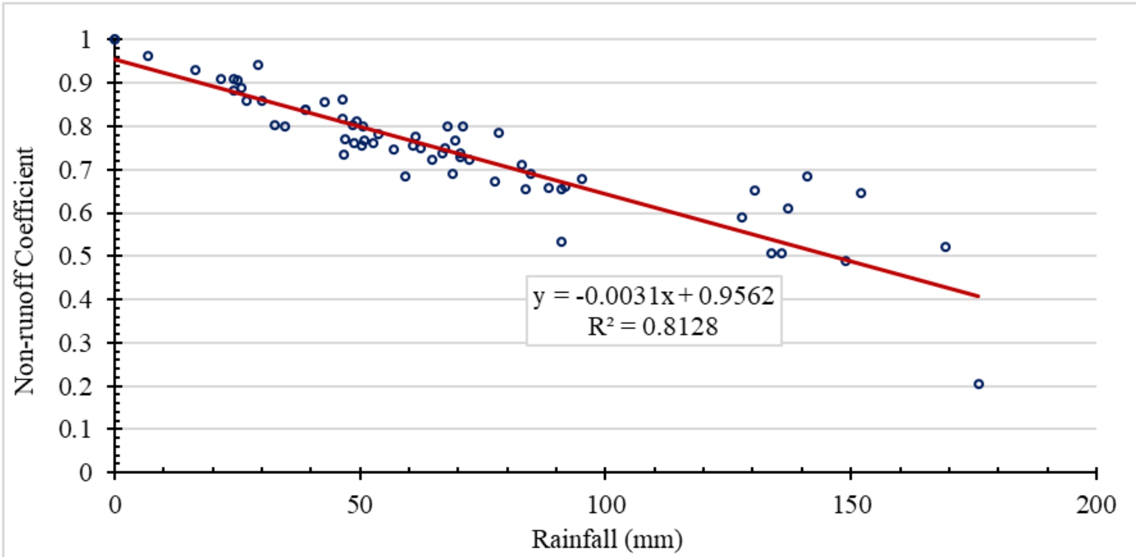

y = -0.0031x + 0.9562
R² = 0.8128
Non-runoff Coefficient
Rainfall (mm)
0
50
100
150
200
0
0.1
0.2
0.3
0.4
0.5
0.6
0.7
0.8
0.9
1

(a)

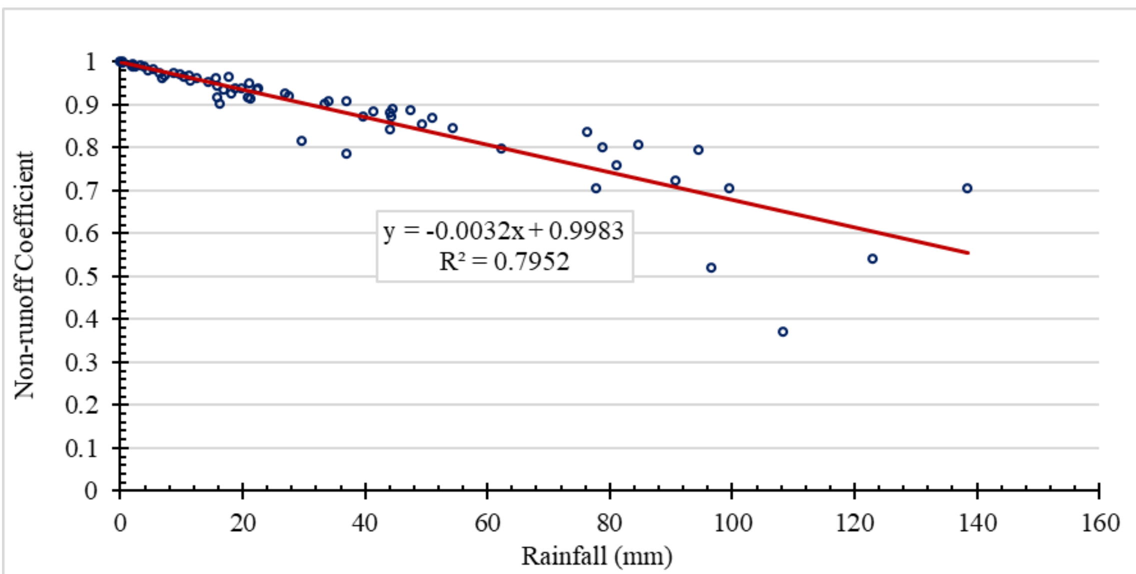

y = -0.0032x + 0.9983
R² = 0.7952
Non-runoff Coefficient
Rainfall (mm)
0
20
40
60
80
100
120
140
160
0
0.1
0.2
0.3
0.4
0.5
0.6
0.7
0.8
0.9
1

(b)

[Figure 5.4]

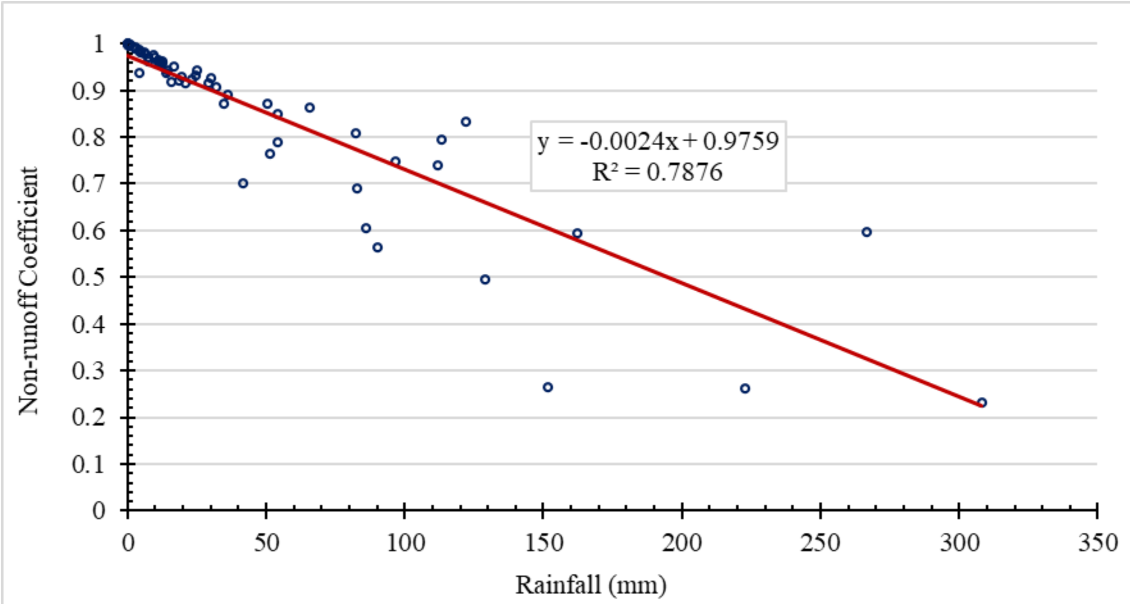

(c)

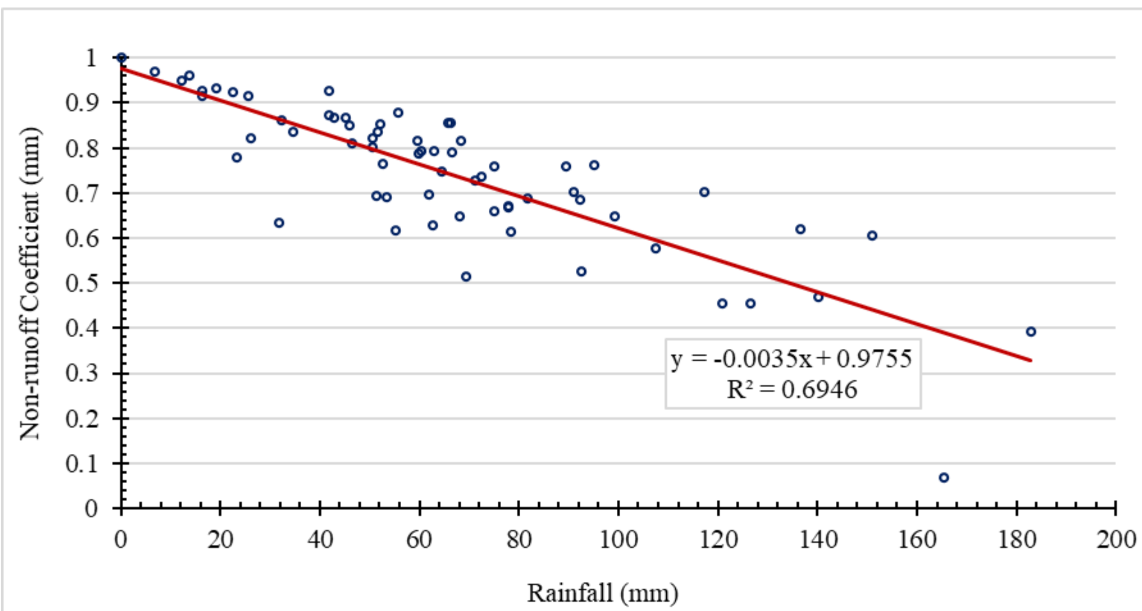

(d)

Figure 5.4. Plots showing the seasonal non-runoff coefficient (equal to one minus runoff coefficient) versus seasonal precipitation for the drainage area above Dendron in: (a) spring; (b) summer; (c) fall; and (d) winter.

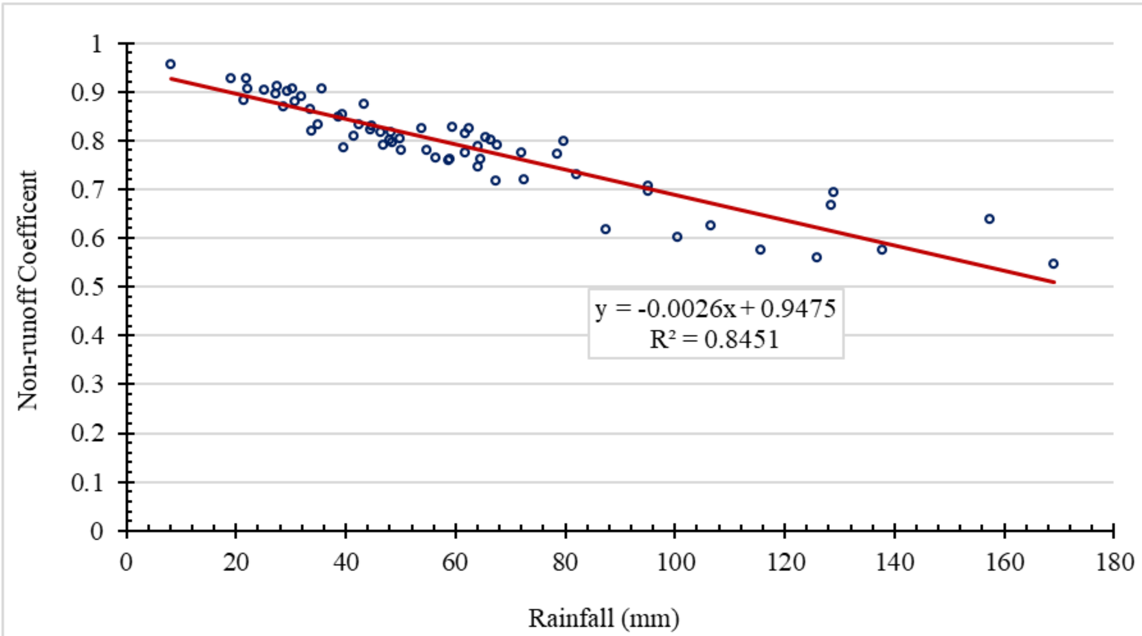
y = -0.0026x + 0.9475
R² = 0.8451
Non-runoff Coefficent
Rainfall (mm)
0
0.1
0.2
0.3
0.4
0.5
0.6
0.7
0.8
0.9
1
0
20
40
60
80
100
120
140
160
180

(a)

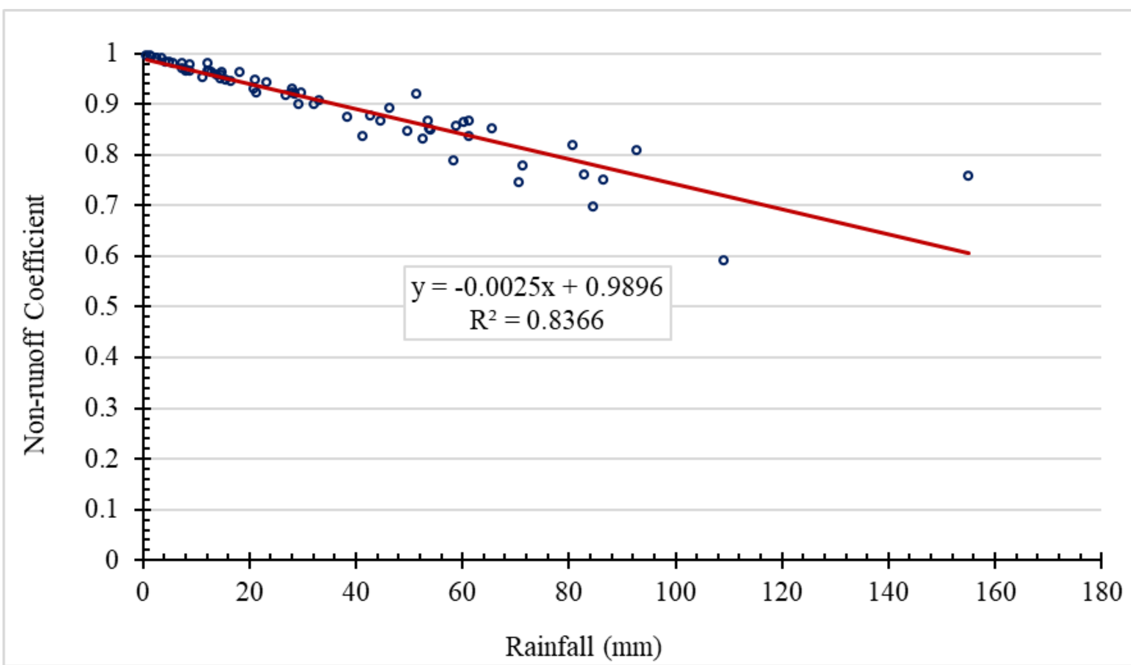
y = -0.0025x + 0.9896
R² = 0.8366
Non-runoff Coefficient
Rainfall (mm)
0
0.1
0.2
0.3
0.4
0.5
0.6
0.7
0.8
0.9
1
0
20
40
60
80
100
120
140
160
180

(b)

[Figure 5.5]

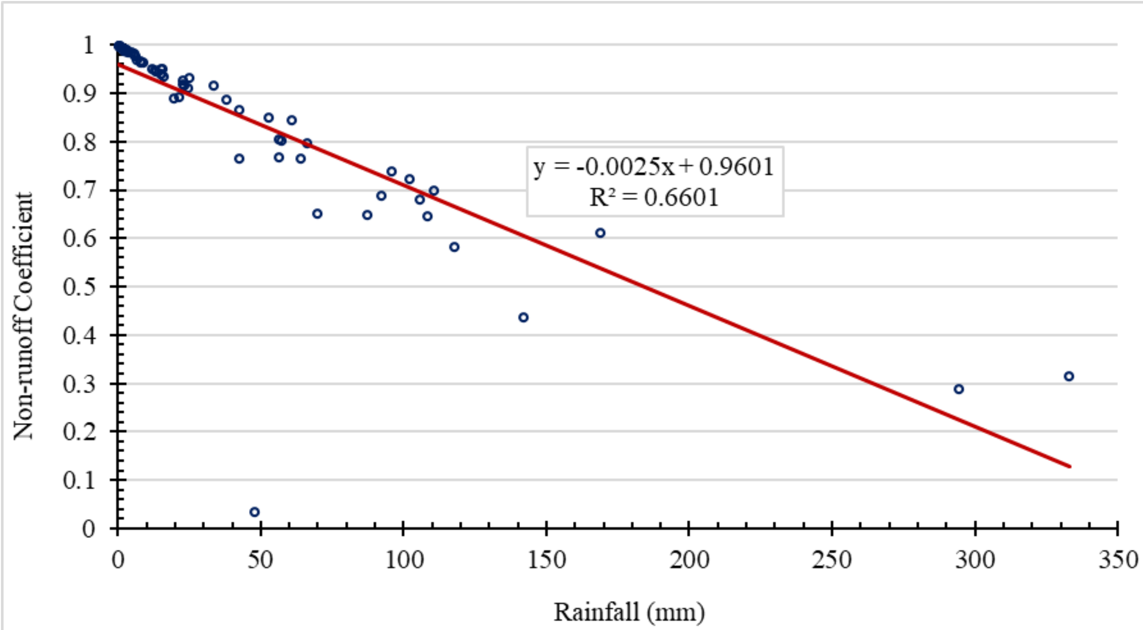

(c)

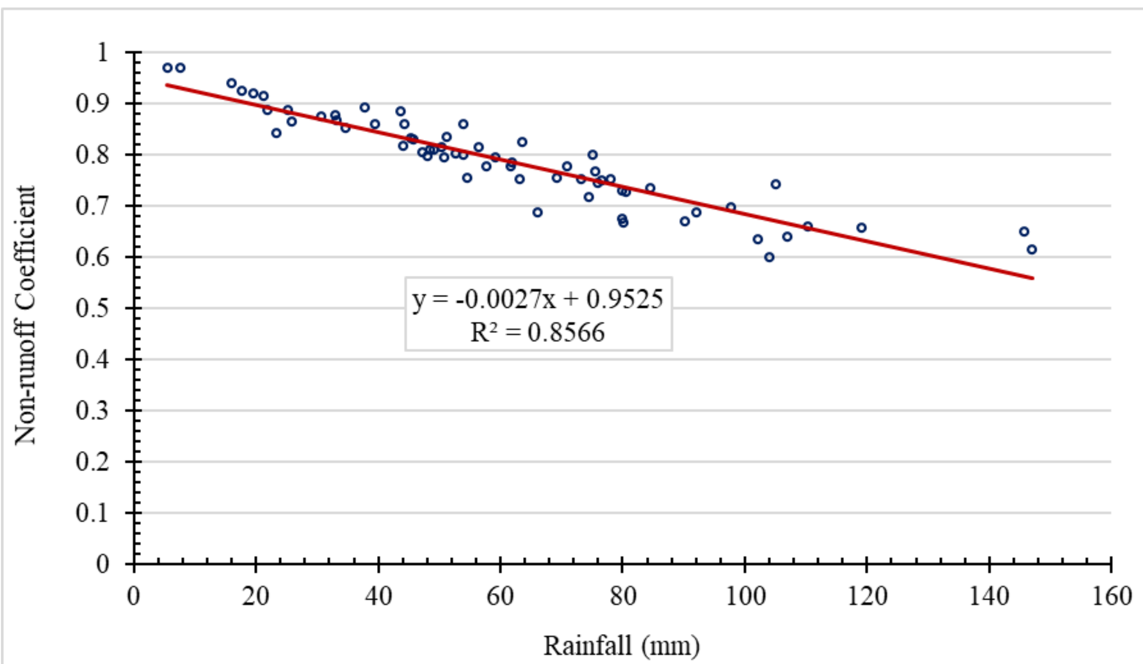

(d)

Figure 5.5. Plots showing the seasonal non-runoff coefficient (equal to one minus runoff coefficient) versus seasonal precipitation for the drainage area above Franklin in: (a) spring; (b) summer; (c) fall; and (d) winter.

The Nash-Sutcliffe model efficiency coefficient (NSE) is another statistics widely used to measure the performance of hydrologic models (Leavesley *et al.*, 1983). It can vary from negative infinity to 1.0, with higher values indicating a better agreement (Nash and Sutcliffe, 1970). Observing extreme values (outliers) in hydrology is not rare, which could critically influence the precision of the model. To overcome this issue, a modified NSE can be calculated as (Moriasi *et al.*, 2007):

$$d = 1 - \frac{\sum_{i=1}^{N}(O_i - P_i)^2}{\sum_{i=1}^{N}(|P_i - \bar{O}| + |O_i - \bar{O}|)^2} \quad (5.1)$$

where d is the modified NSE and can range from zero to one with values closer to one indicating a better model performance; N is the number of observations; Oi is the ith observation value; P_i is the i^{th} prediction value; $\bar{O}$ is the mean of the observation values; and $\bar{P}$ is the mean of the prediction values.

The d values for the drainage areas above Dendron and Franklin were determined as 0.69 and 0.63, respectively. This indicate that the SWAT model performed very well for the Blackwater River Watershed.

5.3 Scenario Simulations

At the annual scale, the SWAT model captured the overall variations of the observed direct flows at Dendron and Franklin (Figures 5.6 and 5.7), while it obviously under-predicted the annual runoff volumes. This can be attributed to that the model did not include the storages as discussed in section 3.3. At the seasonal scale, the SWAT model had a poorer performance in reproducing both the volumes and flows (Figures 5.8 and 5.9). To improve the prediction accuracy, additional data on wetlands, ponds, and forests will need to be collected so that they can be reflected in the model. Nevertheless, the current model was judged to be acceptable for screening and prioritizing alternative scenarios for mitigating floods in the Blackwater River Watershed.

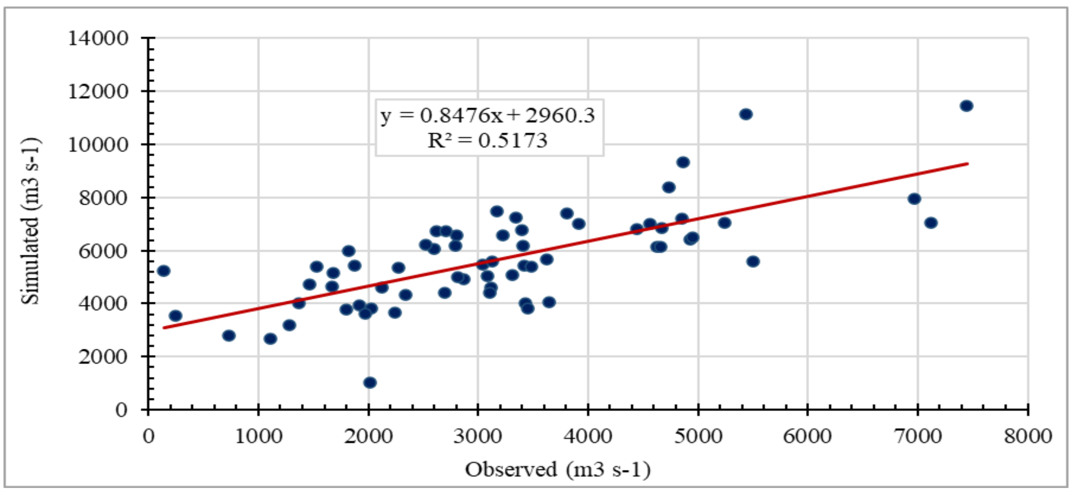

(a)

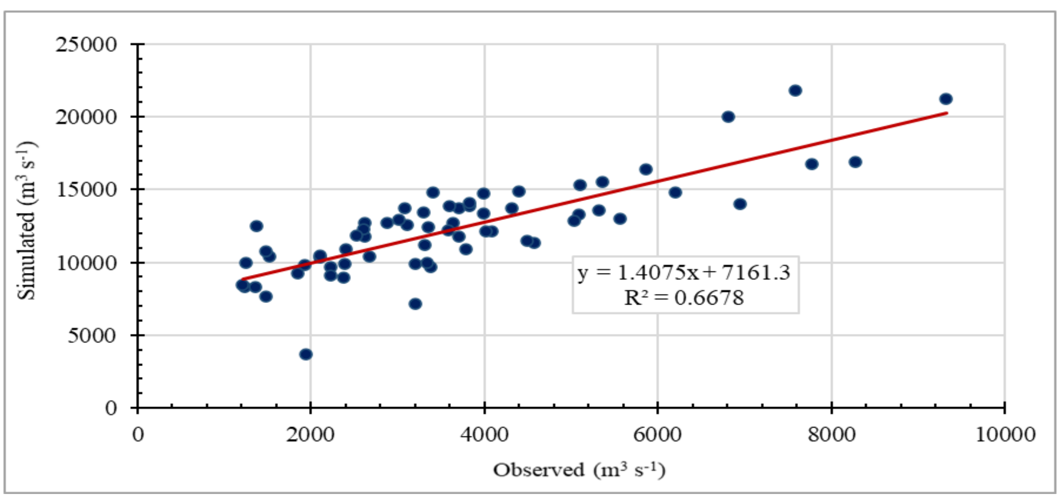

(b)

Figure 5.6. The simulated versus observed mean annual streamflow at: (a) Dendron; and (b) Franklin.

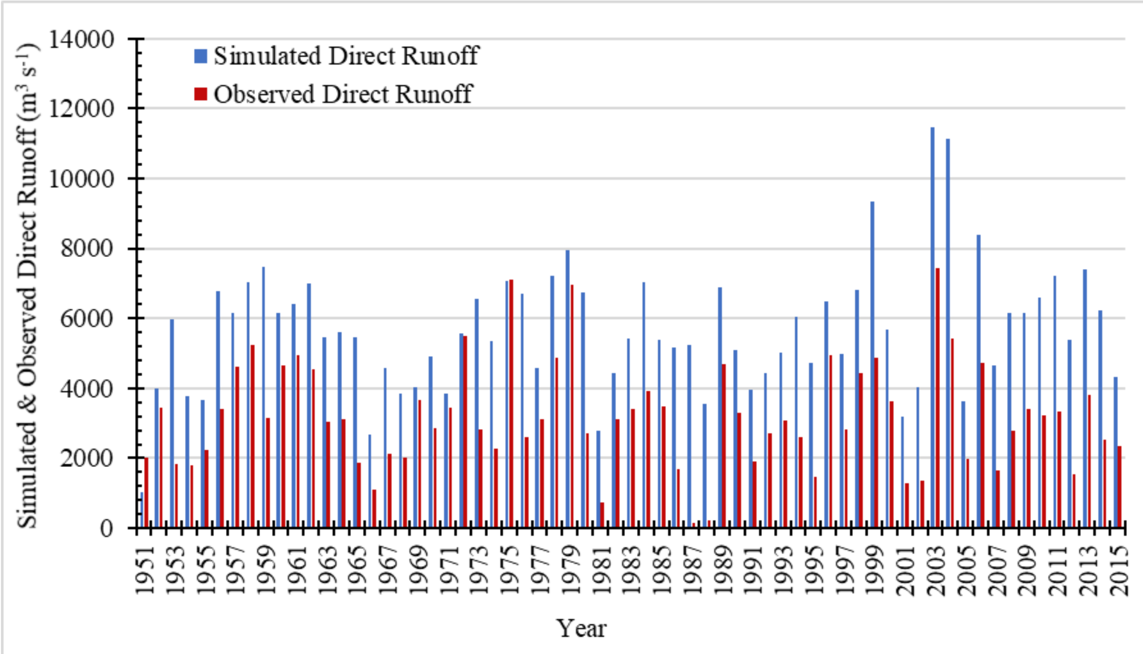

(a)

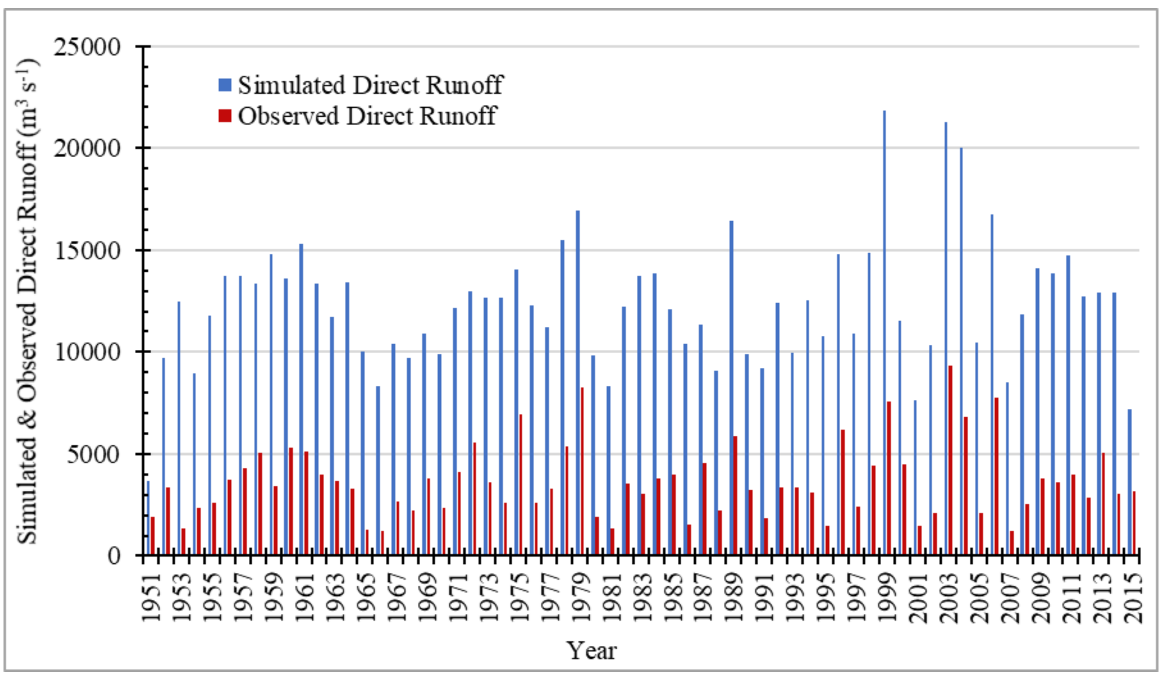

(b)

Figure 5.7. Plots of simulated and observed mean annual direct flow at: (a) Dendron; and (b) Franklin.

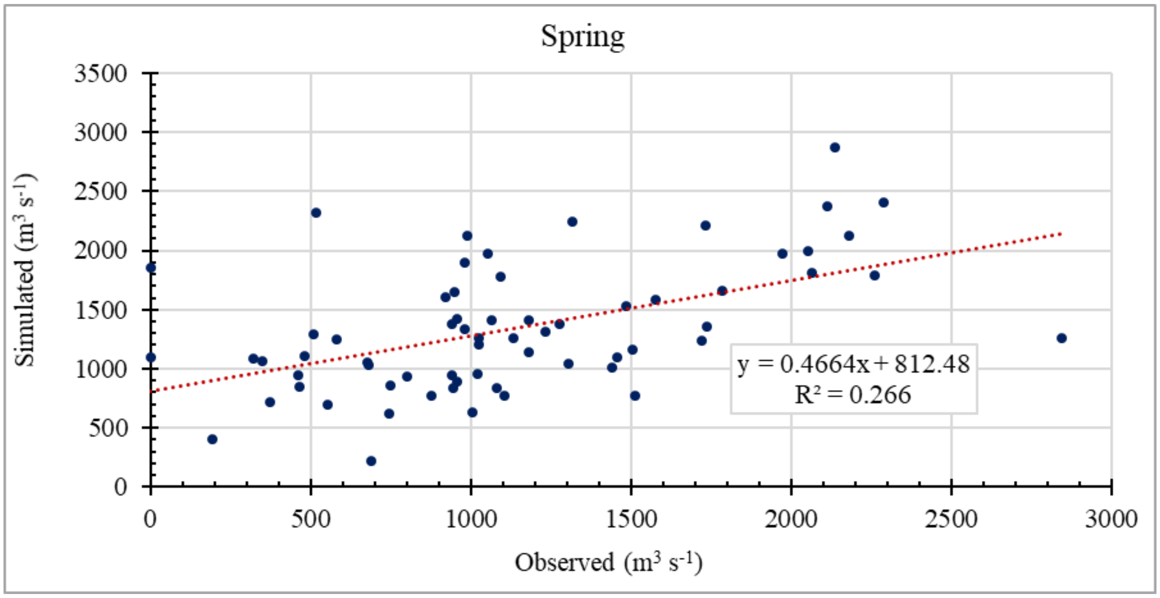

Spring
Simulated (m³ s⁻¹)
Observed (m³ s⁻¹)
0
500
1000
1500
2000
2500
3000
3500
0
500
1000
1500
2000
2500
3000
y = 0.4664x + 812.48
R² = 0.266

(a)

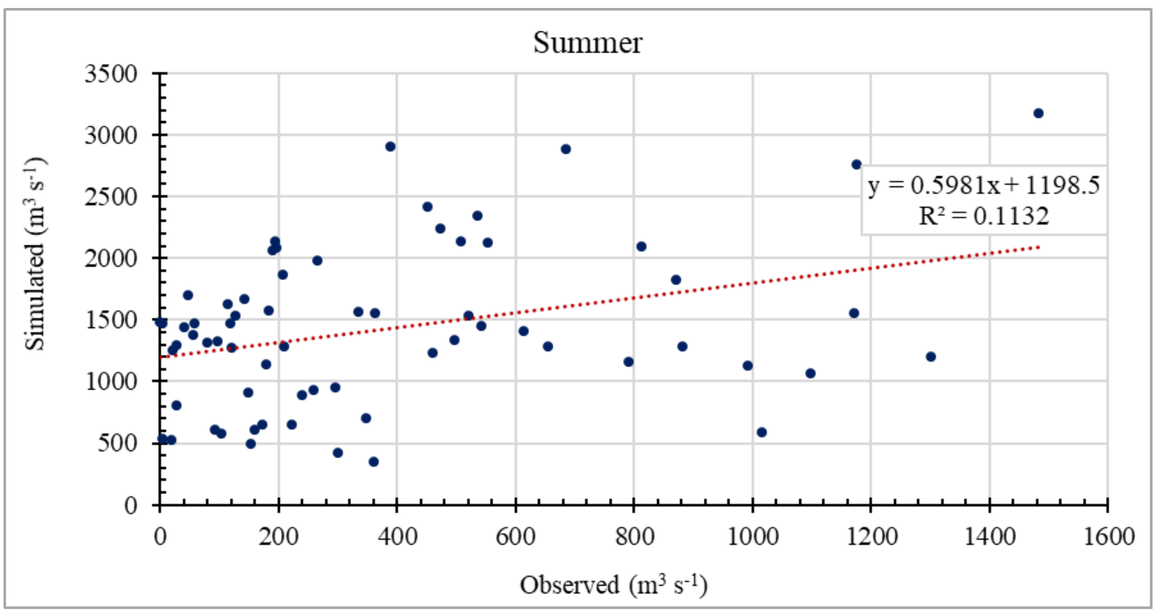

Summer
Simulated (m³ s⁻¹)
Observed (m³ s⁻¹)
0
500
1000
1500
2000
2500
3000
3500
0
200
400
600
800
1000
1200
1400
1600
y = 0.5981x + 1198.5
R² = 0.1132

(b)

[Figure 5.8]

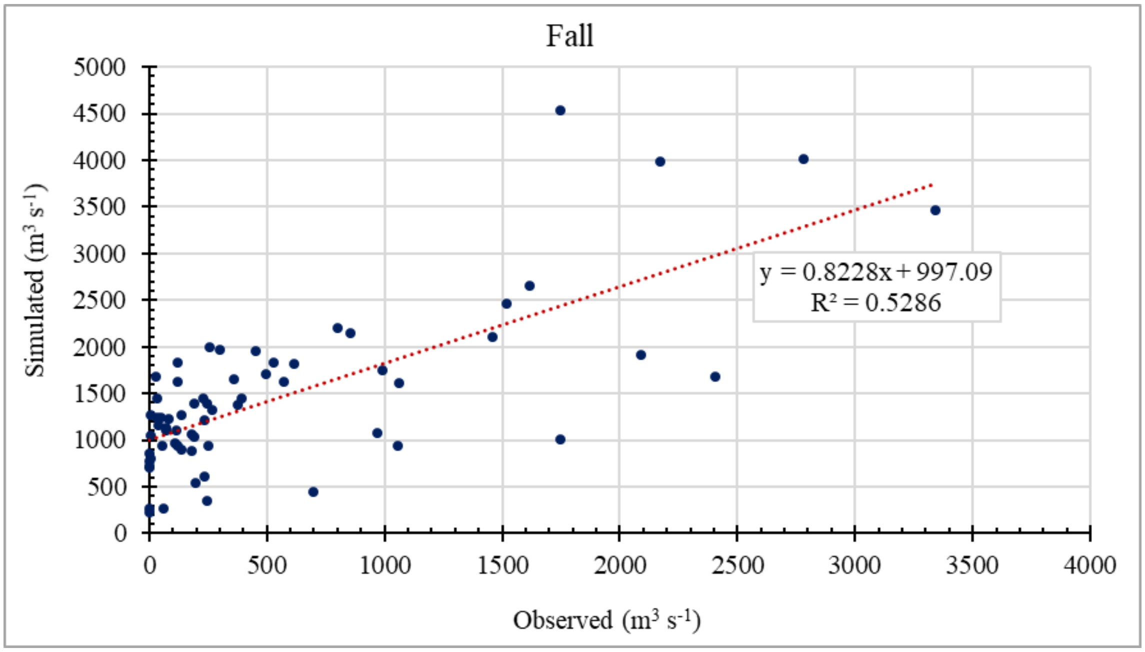

(c)

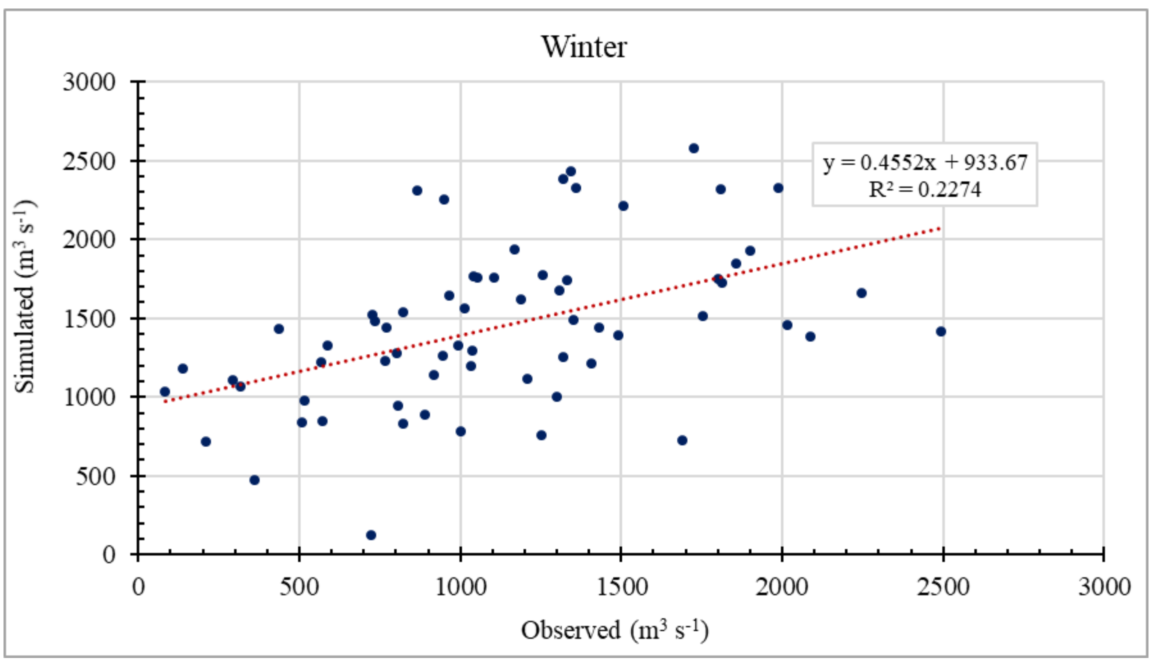

(d)

Figure 5.8. Plots of simulated versus observed mean seasonal direct flow at Dendron in: (a) spring; (b) summer; (c) fall; and (d) winter.

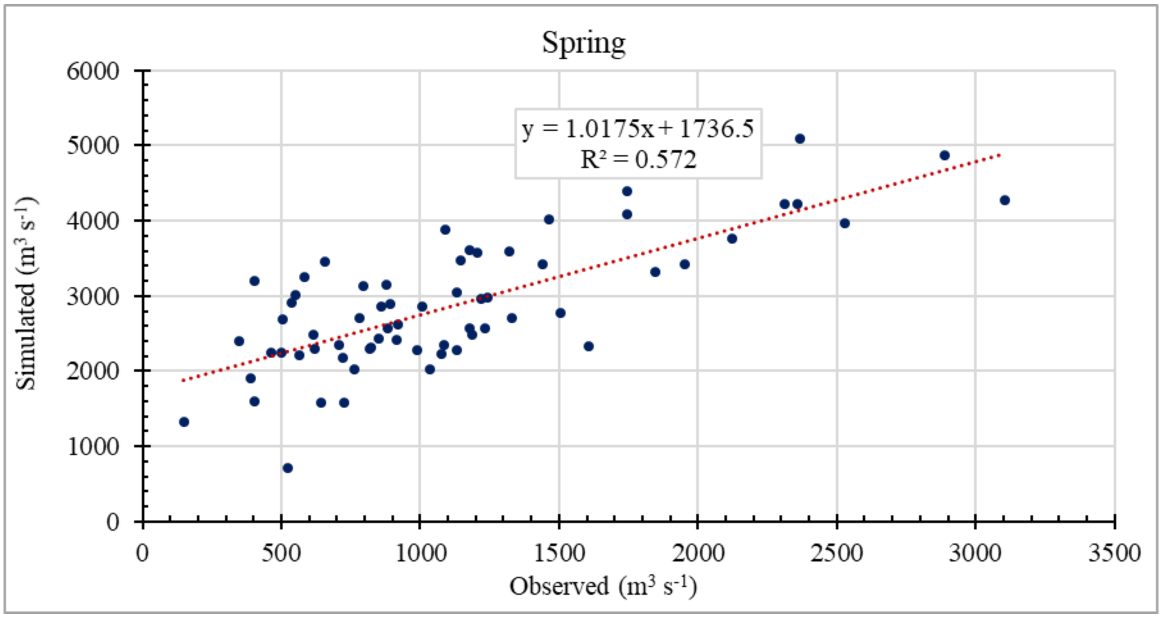

Spring
y = 1.0175x + 1736.5
R² = 0.572
Simulated (m³ s⁻¹)
Observed (m³ s⁻¹)
0
1000
2000
3000
4000
5000
6000
0
500
1000
1500
2000
2500
3000
3500

(a)

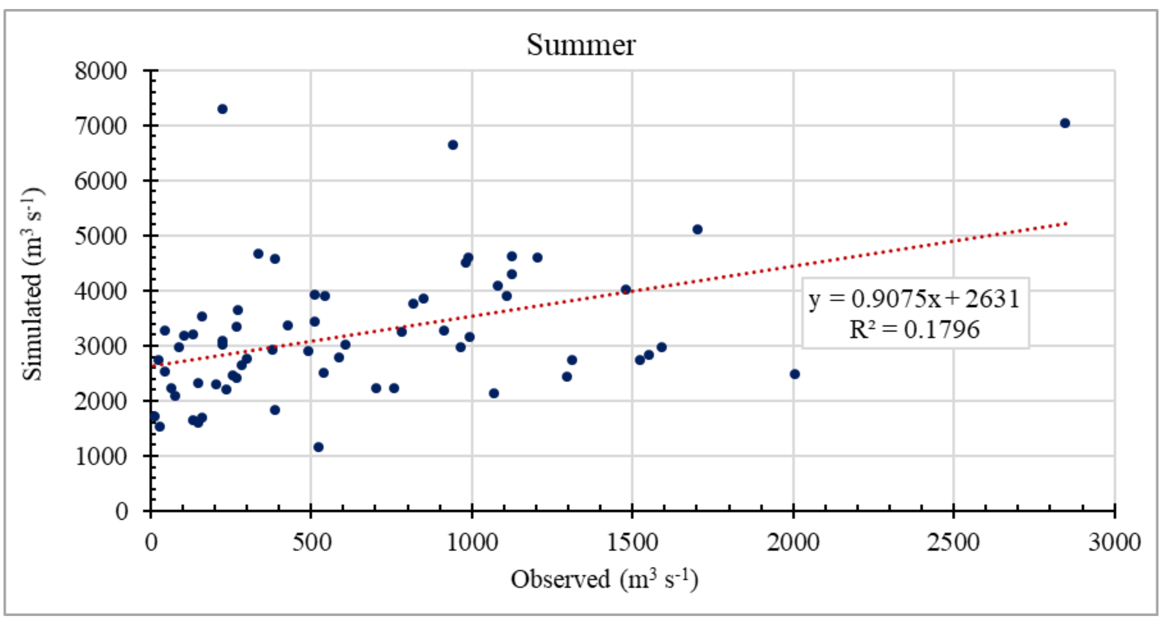

Summer
y = 0.9075x + 2631
R² = 0.1796
Simulated (m³ s⁻¹)
Observed (m³ s⁻¹)
0
1000
2000
3000
4000
5000
6000
7000
8000
0
500
1000
1500
2000
2500
3000

(b)

[Figure 5.9]

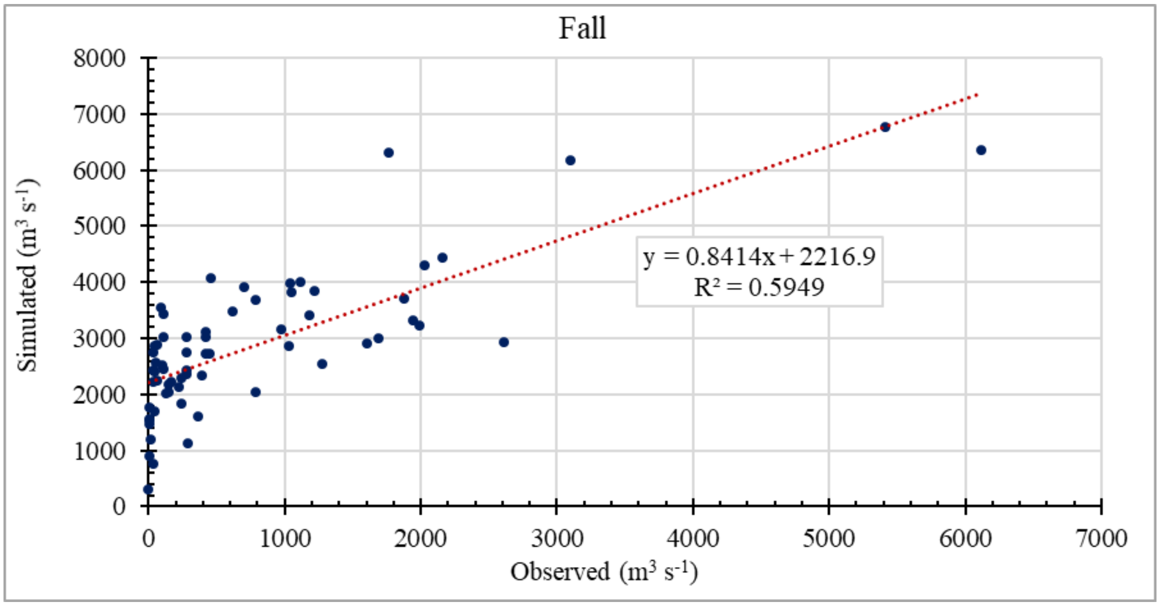

(c)

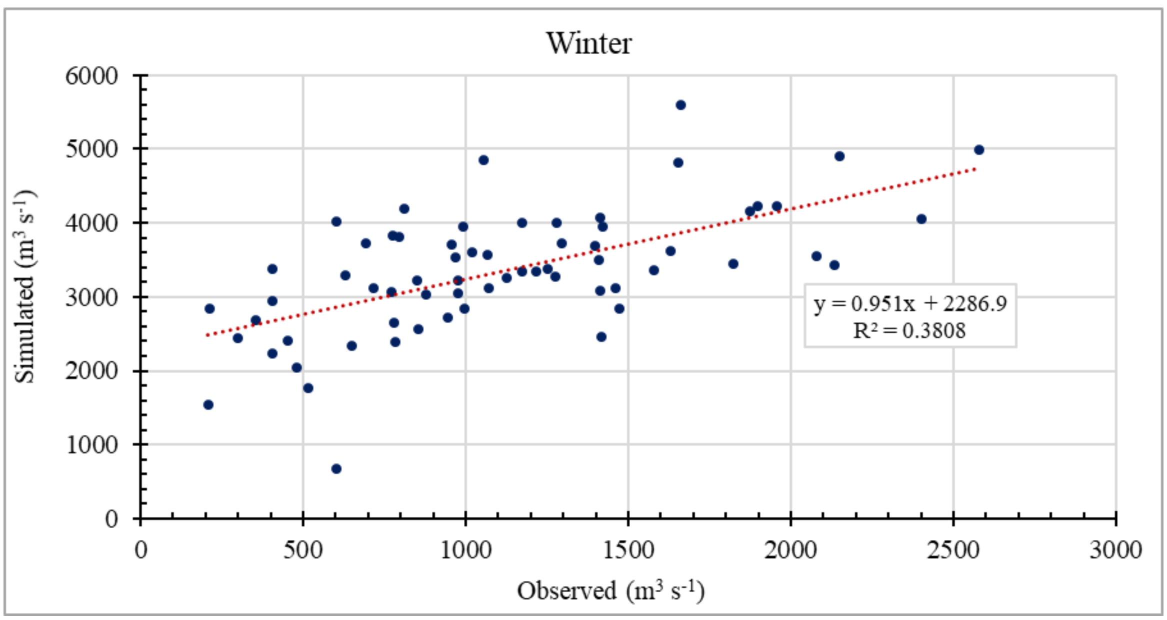

(d)

Figure 5.9. Plots of simulated versus observed mean seasonal direct flow at Franklin in: (a) spring; (b) summer; (c) fall; and (d) winter.

5.4 Discussion

Although the storage capacities provided by depressions, wetlands, channels, and soils might have a large spatial variability leading to spatially varied runoff coefficients (Figure 5.2), the rainfall-runoff relationship, when plotted as non-runoff coefficient versus precipitation, tended to follow a similar function regardless of the drainage areas within the watershed (Figures 5.3 through 5.5). This means that for a given storm, the generated runoff might be different from one drainage area to another if the localized storages were not antecedently filled, but it would become uniform across the watershed if the localized storages were completely full. The available spaces of the storages when a storm starts can play an important role in the resulting streamflow volume and peak. Thus, practical measures (e.g., installation of gated outlet structures) can be implemented to gradually lower water levels in the storages before the inception of a storm for the detention of the generated runoff. Depressional forested wetlands in urban areas can serve as essential storages for sediments and nutrients and have an important role on the landscape (Faulkner, 2004).

The not-very-good performance of the SWAT model (d = 0.62 to 0.67) was because it could not mimic the baseflow variations and represent the detention effects of the storages on runoff. In the future, a further investigation is needed to improve the model performance. However, the current model is still valuable for screening possible flood-mitigation scenarios for the Blackwater River Watershed because the screening process concerns the relative rather than absolute effects of the scenarios. The modelling errors can likely be crossed out when the relative effects are calculated from the simulation results of two compelling scenarios.

5.5 Sub-conclusions

Although the current SWAT model had limitations in mimicking the baseflow variations and representing the storages, it was judged to be good enough for the model to be used for screening possible flood-mitigation scenarios. Moreover, the historical floods incurred by the study watershed were primarily caused by storms with an above-normal intensity and/or duration, so will do in the future. Using gated outlet structures to regulate the water levels in the storages may be a cost-effective measure to mitigate floods in the Blackwater River Watershed and could elaborate here on other adaptations to increase storage and evapotranspiration not only storm water structural management. e.g., more forested wetland conservation, more conservation of natural depressions.

CHAPTER 6

ASSESSMENT OF POSSIBLE FLOOD MITIGATION MEASURES

The southeastern region of Virginia is very susceptible to the upward trend in sea level rise (SLR) and flash flooding, both of which are imposing economic impacts. In this regard, proper mitigation actions are required to sustain the future of this populated region. The mitigation actions should provide a comprehensive plan addressing the infrastructure design and community engagement. Practical experiences have indicated that enhancing zoning ordinances and land use regulations in accordance with increasing the resilience to SLR could be cost-effective. Also, the coordination and collaboration among residents, governments, and communities are crucial for implementing any mitigation actions. In addition, such a mitigation action should provide a series of procedures to avoid future intense events as well as to improve the flood resilience of buildings and neighborhoods while empowering the local economy. Further, proper federal and state resources should be allocated to implement resilience projects in preventing future damages. The Virginia Coastal Resilience Master Planning process is updating the stormwater rainfall data provide a greater degree of accuracy in assessing downstream impact and also to support accurate estimates of what communities can expect from storm events (Virginia, 2020)

6.1 Nonstructural Measures

Nonstructural measures decrease damage and destruction by excluding people and property out of hazard areas. They modify the influence of flooding (Douglas *et al.*,

2010) and require political efforts for implementation (Moore, 2018). The commonly used nonstructural measures include elevated structures, property buyouts, permanent relocation, land use planning and zoning, subdivision, and building codes.

6.1.1 Floodplain Policy and Management

Floodplain management is a program of preventive and protective measures to decrease the probability of current and future flooding. Accepting locality specific floodplain management plans can assist prioritize adaptation policies and programs and make Community Rating System Program (CRS) credit. To lower flood risk and make communities more resilient, state, and federal agencies, local communities and property owners have responsibility. Although, states must provide powerful model regulations, communities must adopt and enforce higher-standard building practices and property owners need to elevate their homes (Figure 6.1). Everyone can play a role in making communities safer and more resistant to floods.

Figure 6.1. Changes after Floyd 1999. (Gatley., 2015).

Another way is to increase open space in the floodplain that can contribute sustainability to environmental preservation (Figure 6.2). For instance, as a successful practice, restricting floodplain development or certain land use regulation can lead to the reduction of surface runoff. It is normally an optimal option in accordance to reducing flood damages and flood management costs (Olsen *et al.*, 2000). The third way is to buyout properties located in floodplains and then replacing them with sewage treatment plants and/or natural conservations (e.g., vegetated coverage).

Figure 6.2. Acquired and cleared homes in a flooded area. (FEMA511, 2005).

The City of Franklin in Blackwater River Watershed provides tools and resources to help communities and assist property owners and residents who have questions about the floodplain managements. The City of Franklin uses Flood Insurance Study (FIS) to update floodplain regulations as a part of the National Flood Insurance Program (NFIP). For floodplain management and flood insurance rates, flood events magnitude which are exceeded on the average during 10-, 50-, 100-, or 500-year period have been chosen by

10-, 2-, 1-, and 0.2-percent chance, respectively, of being exceeded during a year. Although recurrence interval represents long term average period between floods, few floods could happen at short intervals or within a year (FEMA, 2002).

To establish the peak discharge-frequency relationships for floods of the Blackwater River hydrologic analyses were used. River stages records and discharges on the Blackwater River have been preserved by the USGS and Virginia Department of Environmental Quality. Statistical analyses of stage-discharge data from the Blackwater River gaging stations were used for flood flow frequencies. To determine flood flow frequency the discharges for the 10-, 50-, 100-, and 500-year floods were developed. Table 6.1 reveals drainage area and peak discharge relationships for the Blackwater River (FEMA, 1992).

Table 6.1. Summary of discharges (FEMA, 1992) .

Flooding sources and location	Drainage area (km^2)	Peak discharges (cfs)			
		10-Years	50-Years	100-Years	500-Years
Blackwater River					
At the downstream corporate limits of the City of Franklin	1847	8,110	14,900	18,800	31,000
At the upstream corporate limits of the City of Franklin	1738	7,900	14,500	18,300	30,200
At USGS Gage 02049500	1598	7,630	14,000	17,700	29,200

Floodway is one of the floodplain management applications which used as a tool to help local communities to balance the economic earn from floodplain development against increasing flood damages. The floodway is the channel of a stream near floodplain fields which is free of encroachment so that the 100-year flood can be held with no significant increases in flood heights. The floodway widths will be computed at cross sections of specific stream segments from each side of the floodplain. Table 6.2 shows the result of the floodplain computations for specific cross sections. The floodway boundary of the

Table 6.2. Floodway data for Blackwater River.

Flooding Source		Floodway			Base Flood Water Surface Elevation (feet NGVD)			
Cross Section	Distance[1]	Width[2] (feet)	Section Area (square feet)	Mean Velocity (feet per second)	Regulatory	Without Floodway	With Floodway	Increase
Blackwater River								
A	57,516	831	13,353	1.4	16.9	16.9	17.8	0.9
B	63,221	1,100	17,132	1.1	18.1	18.1	18.8	0.7
C	66,391	1,200	19,196	1.0	18.7	18.7	19.5	0.8
D	68,186	1,500	24,562	0.8	18.9	18.9	19.7	0.8
E	70,616	1,700	14,137	1.3	19.2	19.2	20.1	0.9
F	72,466	1,300	19,208	1.0	19.6	19.6	20.5	0.9
G	73,166	1,500	18,029	1.0	20.3	20.3	20.9	0.6
H	73,716	1,500	20,670	0.9	20.4	20.4	21.1	0.7
I	74,366	1,550	23,863	0.8	20.6	20.6	21.2	0.6
J	78,115	2,750	51,297	0.4	20.8	20.8	21.5	0.7
K	83,501	3,200	37,200	0.5	21.0	21.0	21.7	0.7
L	90,682	2,850	43114	0.4	21.4	21.4	22.1	0.7
M	94,009	3,400	54,199	0.3	21.6	21.6	22.3	0.7

[1] Feet above confluence with Chowan River

[2] Width Extends beyond corporate limits (FEMA, 2002)

Blackwater River extends beyond the corporate limits of the City of Franklin. The community must limit development in regions outside the floodway to decrease the risk of property damage in areas where the velocities of stream are high. Also, a list of stream velocities at specific cross sections is presented in Table 6.2. The floodway fringe is the area between 100-year floodplain boundary and the floodway. The floodway fringe encompasses the part of the floodplain that could be completely obstructed without increasing the water-surface elevation of the 100-year flood by more than 1.0 foot at any point. Figure 6.3 illustrates the association between the floodway and floodway fringe and their function to floodplain development (FEMA, 2002).

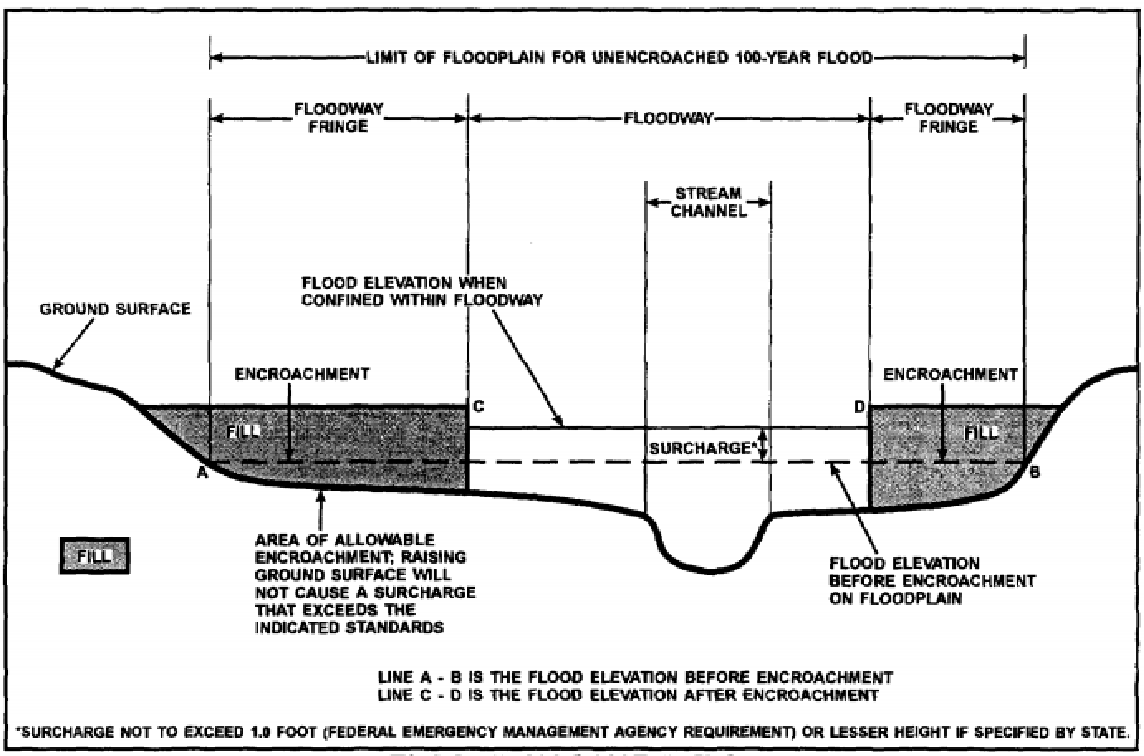

Figure 6.3. Floodway schematic. (FEMA, 2002).

6.1.2 Flood Forecasting and Warning

The most effective flood risk management strategy in reducing flooding is to monitor and forecast flood conditions. To date, a variety of weather information and its dissemination apps and websites have been developed and available for publics at no cost. For instance, the Emergency Alert System (EAS) and National Oceanic and Atmospheric Administration (NOAA) provide emergency alerts. During an emergency event, alerting and warning can be lifesaving.

National Weather Service (NWS) attempts to support the public safe from weather, water, and climate risks and protects lives and property. Figure 6.4 shows the NWS website to find weather information in each region. Wakefield, VA region includes weather story for all cities located in southeast VA (Blackwater River watershed and Franklin), northeast NC, and southeast MD. Based on the date and time and geographic location of issuance, for the latest weather information and potential threats are represented (https://www.weather.gov/wakefield). In Franklin and Blackwater River watershed communities are able to have access to weather forecast conditions which are based on statistical models of similar conditions from previous weather events. Temperature, size and shape of airborne moisture, cloudiness, and power of wind are all various elements of our weather. Being informed about threatening weather conditions and how to react to this situation can help protect lives.

The Wireless Emergency Alerts (WEAs) system approved national, state, or local government organizations send alarms for public safety emergencies such as severe weather, missing children, or the demand to evacuate. WEA alerts are sent through FEMA's Integrated Public Alert and Warning System (IPAWS) and it is just one of the

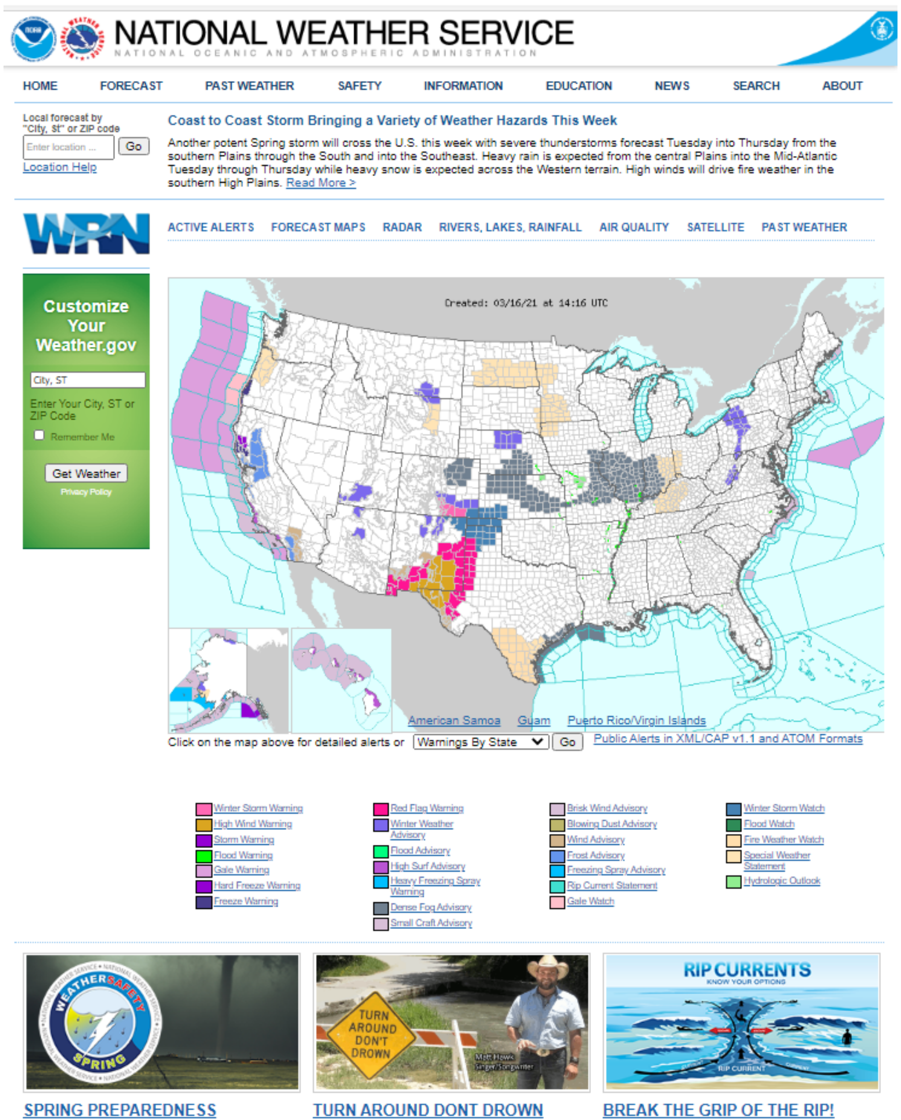

Figure 6.4. The National Weather Service. (Source: https://www.weather.gov).

ways public safety officials can quickly and effectively alert and warn the public about serious emergencies. WEA alerts cover four types of essential emergency situations. Alerts which issue by the president of the United State and contain forthcoming threats to safety or life. Also, alerts which are about missing children and expressing suggestions for saving lives and properties. In addition, the Public Safety and Homeland Security Bureau has reminded approved alert that the WEA system is accessible as a tool during the coronavirus COVID-19 pandemic (Figure 6.5).

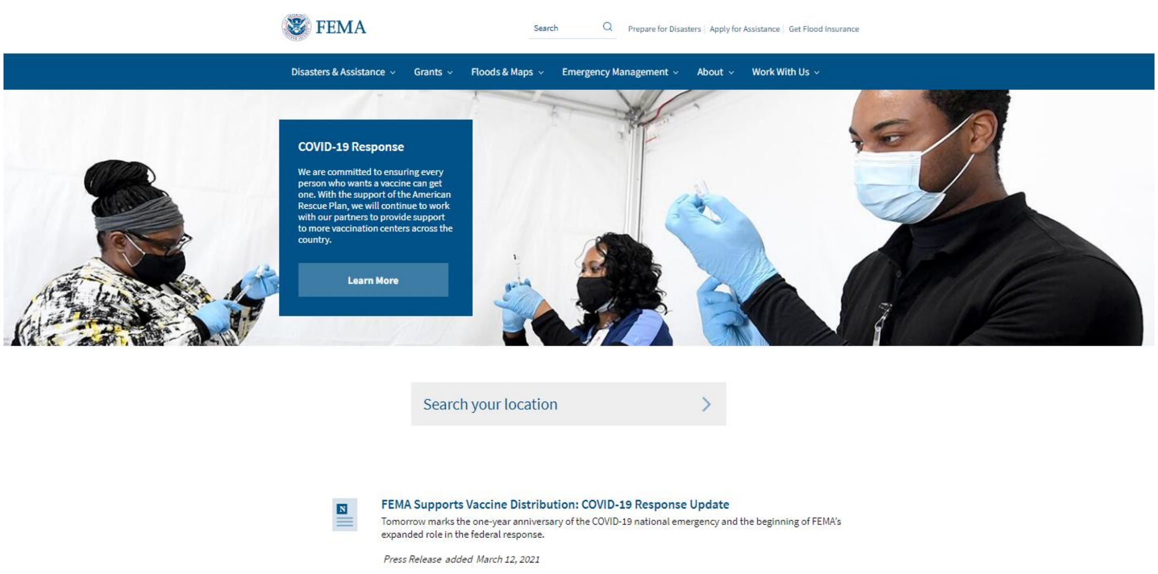

Figure 6.5. The emergency alert system. (Source: https://www.fema.gov).

6.1.3 Flood-proofing and Impact Reduction

Elevating service equipment, installing flood vents (Figure 6.6), and elevating house base (de Koning *et al.*, 2019) have been adopted for flood impact reduction.

Another flood proof approach is to maintain and/or expand drainage systems (Gimenez-Maranges *et al.*, 2020), such as constructing stormwater cisterns on residential property (Figure 6.7) and installing green infrastructure (Figure 6.8) to mitigate urban runoff. For properties that have to be located in a flood hazard area, it is essential to use flood damage resistant building materials to minimize flood damages (Balasbaneh *et al.*, 2019). Another way to generate less runoff from developed land is Low Impact Development (LID). It is the cost effective, lot-level stormwater management plan that integrate green space, native landscaping, and natural hydrologic tasks (figure 6.9).

Figure 6.6. Air conditioning compressor elevated on a cantilevered platform (FEMA 2017) and flood vent on brick home. (Source: https://www.crawlspacedoorscom/crawl-space-doors-articles/protect-your-home-with-flood-vents).

Figure 6.7. Stormwater cistern (Ediblecascadia, 2015)

Figure 6.8. Green infrastructure. (EPA, 2014).

Figure 6.9. Parking lot in Wasena Park constructed to allow water to infiltrate instead of producing runoff (Roanoke Valley Alleghany Regional Commission, 2007).

Basement infill floor, elevating lowest interior, and abandoning lowest floor are interior modifications that have proven to be effective in reducing damages to building components and contents placed below the Base Flood Elevation (BFE) since the lowest floor can potentially be re-located above the BFE, which is the elevation of surface water resulting from a flood that has a 1% chance of equaling or exceeding that level in any given year. In addition, dry flood-proofing of a residential building may minimize the risk of flooding damage during flood events (Botzen *et al.*, 2017). A dry flood-proofing system will perform best when all utility meters are higher than the BFE as well, and flap valves or passive backflow prevention devices are installed on building water and sewer lines. Further, barriers, such as floodwalls and levees, can be built around a residential building to control floodwaters (Figure 6.10) (Ziervogel *et al.*, 2016). Moreover, because flooding can cause sewage from sanitary sewer lines backups, sewer backflow valves can be installed.

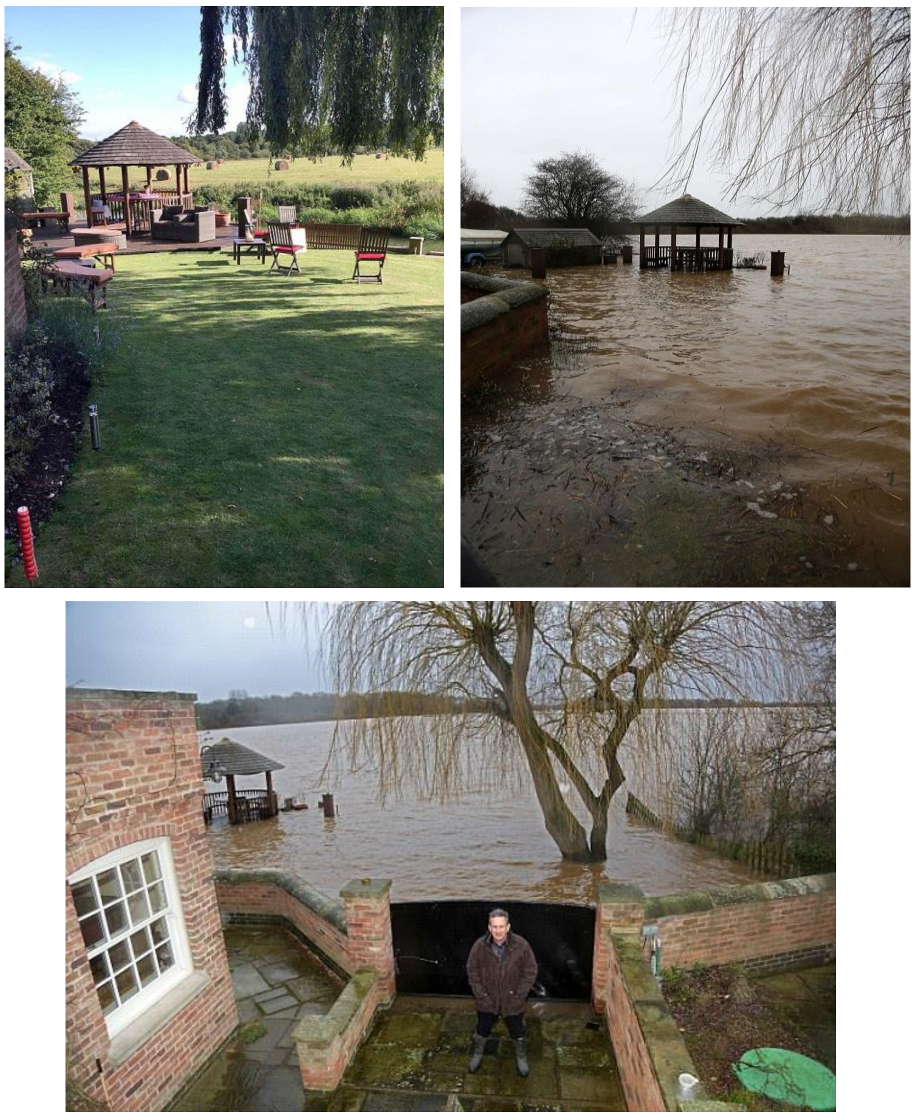

Figure 6.10. Permanent brick floodwall. (Smyth, 2015).

6.2 Hypothetical Measures and Evaluation

Although it is not possible to eliminate flooding in an area at a particular time, effective flood prevention and management in a flood zone are always needed. In such a general perspective, the role of river floodplains is one that also develops the resilience against climate as well as increasing flood safety and improving water quality (Kiedrzyńska *et al.*, 2015). When management expenses are contained with economic improvement and flood damages in a multi-objective formulation, the best policies consist of constructing more levees and expanding floodplain development (Olsen *et al.*, 2000).

In Franklin, the floodplains include much of the eastern section of the city that is adjacent to the Blackwater River. The wise land uses in the floodplains can protect people and property. The City of Franklin sweeps streets in the city and encourages residents to keep stormwater inlets, ditches, and natural watercourses free of trash, landscape debris, leaves, and other materials. Street cleaning makes drainage channels free of obstruction to decrease flooding possibility in the event of heavy storms. Residents can monitor the Blackwater River flood stage during the storm by applying two different River Gauges, namely Dendron and Franklin, which are managed by the National Weather Service. Stormwater management, urban forestry, low impact development, and open space and greenways are flood mitigation projects designed to reduce the frequency, duration and magnitude of flooding and hazards (Roanoke Valley Alleghany Regional Commission, 2007). To protect the quality and quantity of water from the potential harm of unmanaged stormwater runoff land-distributing activities, the

City of Franklin adopted the technical criteria for regulated land-distributing. National Flood Insurance Program (NFIP) helps to decrease the effect of flooding on private and public buddings by providing reasonable insurance and encouraging communities to accept floodplain management regulation. The NFIP regulations applies those residential buildings in zones A have the lowest floor (containing basement) elevated above the base flood elevation (BFE). To decrease costs and improving efficiency of services Southampton County and the City of Franklin executed a “shared services” Community Development Department including distributing a Building Official who is also a Certified Floodplain Manager (CFM). Also, to develop advancement outside of flood risk regions and generate preservation localities along shorelines Franklin started to interfere. Stormwater management regulations and drainage system protection rules declared at the state level and have been shown vigorously. In addition, flood warning systems in Southampton County and Franklin are affected and useful and Isle of Wight County recently shifted to a more vigorous procedure. Another method that is considered useful and protect from flood is sandbagging, however local governments are not participating in assisting property owners sandbag, with the exception of Franklin where a recent new rule permits downtown business owners to get sand and bags from the City (Hampton Roads Hazard Mitigation Plan, 2017).

6.3 Discussion

In Franklin, property owners who live in a high-risk zone must have an Elevation Certificate to obtain flood insurance. An Elevation Certificate is an essential tool that documents the building’s elevation. Currently, all new constructions and properties are required to be built two feet above the BFE shown in Figure 6.1.

All suggested improvements in the particular flood risk area (i.e., 100-year floodplain) need to be evaluated in compliance with the FEMA National Flood Insurance Program and the Floodplain District Ordinance, as required by Franklin City and Southampton County. If the cost of rebuilding, rehabilitation, or other improvements equals or exceeds 50% of the building's market value, the building must meet the same construction requirements as a new building; meaning that the structure may have to be elevated or flood proofed above the 100-year flood level. Substantially damaged buildings must be made up to the same standards as well, regardless of the cause of damage.

6.4 Sub-conclusions

To decrease flood risk and make communities resilient, the City of Franklin provides tools and resources to help communities and assist property owners and residents who have questions about the floodplain managements. Restricting floodplain development, buying out properties, and using floodplains wisely are good ways to the reduction of floods. The comprehensive approach for flood mitigation in Blackwater River Watershed and other similar coastal watersheds should consist of improving stormwater quality, seeping streets, maintaining storm drainage systems, increasing tree canopies in urban area, integrating green spaces, preserving natural hydrologic processes, and reserving open spaces and greenways.

CHAPTER 7

GENERAL CONCLUSIONS AND RECOMMENDATIONS

7.1 Overall Conclusions

This dissertation used a variety of data for setting up and running the SWAT model, namely temperature, precipitation, streamflow, soil data, land use and land cover, topography, and drainage network. The hydrological cycle is a dynamic process which has been affected by global climate change and human activities. Streamflow is affected by both the amount of precipitation as a significant role and temperature fluctuation. Although the effect of precipitation and sea level rise on streamflow is more significant to increase flood stage in coastal watershed. As a significant component of hydrologic cycle, runoff is affected by meteorological and geological factors in conjunction with land use. For simulation purposes, the Blackwater River Watershed was subdivided into six subbasins in terms of topography and 35 hydrologic response units (HRUs) in terms of unique combinations of topography, soil properties, and land use and land cover (LULC). Such long-term record of rainfall and runoff time series can provide a good opportunity to examining rainfall-runoff relationships in coastal watersheds.

For the Blackwater River Watershed, while both precipitation and runoff fluctuated annually and from season to season within a year, the data in the past 65 years did not indicate either a significant increasing or decreasing trend in precipitation. The weak increasing trends in precipitation and runoff over the 65 years were probably caused by the two outlier storms occurred in 1999 and 2006. Although human activities play an important role on the rainfall-runoff relationship, in this study rainfall-runoff relationship was not changed by human activities, as indicated by the linear double-mass curves (Figure 3.10). This means that for a given storm, the resulting streamflow hydrograph at a point of interest along the Blackwater River was expected to be same regardless of times (e.g., 1950s versus 1990s). The floods occurred in the watershed might primarily be caused by storms with an above-normal rainfall intensity and/or duration rather than by human activities. Also, the storage capacities provided by depressions, wetlands, channels, and soils might have a large spatial variability. Along the Blackwater River, the total streamflow consisted of a large fraction of baseflow, which accounted for more than 50%. Such a percentage was larger in spring and winter, whereas it was smaller in summer and fall. At both Franklin and Dendron, although precipitation increased in summer, the corresponding runoff decreased; and vice versa. Higher temperatures with steady precipitation tended to produce less runoff, whereas lower temperatures were favorite for producing more runoff. Streamflow can typically be divided into two components: direct runoff and baseflow. The portion of direct runoff is generally greater than that of baseflow.

In this dissertation, a seasonal transfer function model was implemented on runoff-rainfall time series, including temperature as an exogenous variable. The findings confirmed the existence of significant serial correlation in runoff observation in addition to cross-correlation between runoff and rainfall sequences. Moreover, the influence of temperature was investigated, which indicated a significant negative correlation between temperature and runoff. Furthermore, the proposed model was able to assess seasonality feature of runoff data. Finally, the model performance and adequacy were verified by several statistical criteria. In conclusion, the model proposed in this paper could be used as a well validated tool for modeling and forecasting rainfall-runoff time series by researchers in variety of fields such as water resource management, climate change, urban planning, and agriculture.

Although the storage capacities provided by depressions, wetlands, channels, and soils might have a large spatial variability leading to spatially varied runoff coefficients, the rainfall-runoff relationship, when plotted as non-runoff coefficient versus precipitation, tended to follow a similar function regardless of the drainage areas within the watershed. This means that for a given storm, the generated runoff might be different from one drainage area to another if the localized storages were not antecedently filled, but it would become uniform across the watershed if the localized storages were completely full. The available spaces of the storages when a storm starts can play an important role in the resulting streamflow volume and peak. Thus, practical measures (e.g., installation of gated outlet structures) can be implemented to gradually lower water levels in the storages before the inception of a storm for the detention of the generated runoff.

The not-very-good performance of the SWAT model (Nash-Sutcliffe efficiency = 0.62 to 0.67) was because it could not mimic the baseflow variations and represent the detention effects of the storages on runoff. In future studies, a further investigation is needed to improve the model performance. However, the current model is accurate enough for screening possible flood-mitigation scenarios for the Blackwater River Watershed because the screening process concerns the relative rather than absolute effects of the scenarios. The modelling errors can likely be crossed out when the relative effects are calculated from the simulation results of two compelling scenarios.

In Franklin, the property owners who live in a high-risk zone must have an Elevation Certificate to obtain flood insurance. An Elevation Certificate is an essential tool that documents the building's elevation. Currently, all new constructions and properties are required to be built two feet (i.e., 0.6 m) above the base (i.e., 100-year) flood elevation (BFE).

All suggested improvements in the regulated flood risk area (i.e., 100-year floodplain) need to be evaluated in compliance with the Federal Emergency Management Agency (FEMA) National Flood Insurance Program and the Floodplain District Ordinance, as required by Franklin City and Southampton County. If the cost of rebuilding, rehabilitation, or other improvements equals or exceeds 50% of the building's market value, the building must meet the same construction requirements as a new building; meaning that the structure may have to be elevated or flood proofed above the 100-year flood level. Substantially damaged buildings must be made up to the same standards as well, regardless of the cause of damage.

7.2 Recommendations for Future Research

Although the current SWAT model had limitations in mimicking the baseflow variations and representing the storages, it was judged to be good enough for the model to be used for screening possible flood-mitigation scenarios. Moreover, the historical floods incurred by the study watershed were primarily caused by storms with an above-normal intensity and/or duration, so will do in the future. Using gated outlet structures to regulate the water levels in the storages may be a cost-effective measure to mitigating floods in the Blackwater River Watershed.

To decrease flood risk and make communities resilient, the City of Franklin provides tools and resources to help communities as well as assists property owners and residents who have questions about the floodplain managements. Restricting floodplain development, buying out properties, and using floodplains wisely are good ways to the reduction of floods. The comprehensive approach for flood mitigation in Blackwater River Watershed and other similar coastal watersheds should consist of improving stormwater quality, sweeping streets, maintaining storm drainage systems, increasing tree canopies in urban area, integrating green spaces, preserving natural hydrologic processes, and reserving open spaces and greenways. In addition, preserving forest cover or facilitating marshes and afforestation will also help with flood mitigation (by increasing evapotranspiration). Future studies should be devised to quantify the effects of these improvements on flood mitigation.

REFERENCES

Acreman, M., & Holden, J. (2013). How wetlands affect floods. *Wetlands, 33*(5), 773-786.

Adam Terando, L. C., Kirstin Dow, Kevin Hiers, Kenneth E. Kunkel, Aranzazu Lascurain, Doug Marcy, Michael Osland, Paul Schramm. (National Climate Assessment). *Impacts, Risks, and Adaptation in the United States: Fourth National Climate Assessment, Volume II Southeast*.

Ahn, J., Cho, W., Kim, T., Shin, H., & Heo, J.-H. J. W. (2014). Flood frequency analysis for the annual peak flows simulated by an event-based rainfall-runoff model in an urban drainage basin. *6*(12), 3841-3863.

Allen, M. J., & Allen, T. R. (2019). Precipitation trends across the Commonwealth of Virginia (1947–2016). *Virginia Journal of Science, 70*(1), 4.

Amatya, D. M., Chescheir, G. M., Skaggs, R. W., & Fernandez, G. P. (2002). *Hydrology of poorly drained coastal watersheds in eastern North Carolina.* Paper presented at the 2002 ASAE Annual Meeting.

Areerachakul, S., & Junsawang, P. (2014). *Rainfall-Runoff relationship for streamflow discharge forecasting by ANN modelling.* Paper presented at the World Congress on Sustainable Technologies (WCST-2014).

Arnold, J., Allen, P., Muttiah, R., & Bernhardt, G. J. G. (1995). Automated base flow separation and recession analysis techniques. *33*(6), 1010-1018.

Arnold, J. G., Moriasi, D. N., Gassman, P. W., Abbaspour, K. C., White, M. J., Srinivasan, R., Santhi, C., Harmel, R., Van Griensven, A., & Van Liew, M. W. (2012). SWAT: Model use, calibration, and validation. *Transactions of the ASABE, 55*(4), 1491-1508.

ASCE, T. C. o. A. o. A. N. N. i. h. (2000). Artificial neural networks in hydrology. I: Preliminary concepts. *Journal of Hydrologic Engineering, 5*(2), 115-123.

Baker, J., & Laflen, J. (1982). Effects of corn residue and fertilizer management on soluble nutrient runoff losses. *Transactions of the ASAE, 25*(2), 344-0348.

Baker, J., Laflen, J., & Johnson, H. (1978). Effect of tillage systems on runoff losses of pesticides, a rainfall simulation study. *Transactions of the ASAE, 21*(5), 886-0892.

Balasbaneh, A. T., Marsono, A. K. B., & Gohari, A. (2019). Sustainable materials selection based on flood damage assessment for a building using LCA and LCC. *Journal of Cleaner Production, 222*, 844-855.

Band, L. E. (1986). Topographic partition of watersheds with digital elevation models. *Water Resources Research, 22*(1), 15-24.

Barszcz, M. P. J. P. J. o. E. S. (2016). Analysis of Probable Flows Based on the Rainfall-Runoff Model for Flood Scenarios: a Case Study of the Losse River Catchment (Germany). *25*(4).

Bergschneider, C. R. (2005). *Determining an appropriate organic matter loading rate for a created coastal plain forested wetland.* Virginia Tech,

Betson, R. P. (1964). What is watershed runoff? *Journal of Geophysical research, 69*(8), 1541-1552.

Bilskie, M., & Hagen, S. (2018). Defining flood zone transitions in low-gradient coastal regions. *Geophysical Research Letters, 45*(6), 2761-2770.

Bingner, R. (1996). Runoff simulated from Goodwin Creek watershed using SWAT. *Transactions of the ASAE, 39*(1), 85-90.

Blume, T., Zehe, E., & Bronstert, A. (2007). Rainfall—runoff response, event-based runoff coefficients and hydrograph separation. *Hydrological sciences journal, 52*(5), 843-862.

Boardman, J., Ligneau, L., de Roo, A., & Vandaele, K. (1994). Flooding of property by runoff from agricultural land in northwestern Europe. In *Geomorphology and Natural Hazards* (pp. 183-196): Elsevier.

Botzen, W. W., Monteiro, É., Estrada, F., Pesaro, G., & Menoni, S. (2017). Economic assessment of mitigating damage of flood events: Cost–benefit analysis of flood-proofing commercial buildings in Umbria, Italy. *The Geneva Papers on Risk and Insurance-Issues and Practice, 42*(4), 585-608.

Bouhia, H., Bouhia, H., Bouhia, H., Bouhia, H., Bouhia, H., Alaoui, M. B. E. H., Asad, M., Baumol, W. J., Blinder, A. S., & Bergman, L. (2001). Conclusions and Future Development. In *Water In The Macro Economy* (Vol. 20, pp. 1-6): Rapport de Mission Paris.

Box, G. E., & Cox, D. R. (1964). An analysis of transformations. *Journal of the Royal Statistical Society: Series B (Methodological), 26*(2), 211-243.

Box, G. E., & Jenkins, G. M. (1976). *Time series analysis: forecasting and control*: John Wiley & Sons.

Box, G. E., & Tiao, G. C. (1975). Intervention analysis with applications to economic and environmental problems. *Journal of the American Statistical association, 70*(349), 70-79.

Bracken, L., Cox, N., & Shannon, J. (2008). The relationship between rainfall inputs and flood generation in south–east Spain. *Hydrological Processes: An International Journal, 22*(5), 683-696.

Brocca, L., Melone, F., & Moramarco, T. J. H. p. (2011). Distributed rainfall-runoff modelling for flood frequency estimation and flood forecasting. *25*(18), 2801-2813.

Brockwell, P. J., Brockwell, P. J., Davis, R. A., & Davis, R. A. (2016). *Introduction to time series and forecasting*: Springer.

Brody, S. D., Highfield, W. E., Ryu, H.-C., & Spanel-Weber, L. (2007). Examining the relationship between wetland alteration and watershed flooding in Texas and Florida. *Natural Hazards, 40*(2), 413-428.

Bronstert, A. (1995). River flooding in Germany: influenced by climate change? *Physics and Chemistry of the Earth, 20*(5-6), 445-450.

Bronstert, A., Niehoff, D., & Bürger, G. (2002). Effects of climate and land-use change on storm runoff generation: present knowledge and modelling capabilities. *Hydrological Processes, 16*(2), 509-529.

Brun, S., & Band, L. (2000). Simulating runoff behavior in an urbanizing watershed. *Computers, Environment and Urban Systems, 24*(1), 5-22.

Burton, I., Kates, R. W., & White, G. F. (1968). The human ecology of extreme geophysical events.

Burton Jr, G. A., & Pitt, R. (2001). *Stormwater effects handbook: A toolbox for watershed managers, scientists, and engineers*: CRC Press.

Calder, I. (1993). Hydrologic effects of land-use change. Chapter 13 in Handbook of Hydrology (Maidment, DR Ed). In: McGraw-Hill, New York.

Caris, E. A. P., Kurtz, B. C., Cruz, C. B. M., & Scarano, F. R. (2013). Vegetation cover and land use of a protected coastal area and its surroundings, southeast Brazil. *Rodriguésia, 64*(4), 747-755.

Carleton, J. N., Grizzard, T. J., Godrej, A. N., Post, H. E., Lampe, L., & Kenel, P. P. (2000). Performance of a constructed wetlands in treating urban stormwater runoff. *Water Environment Research, 72*(3), 295-304.

Castillo, C. R., Güneralp, İ., & Güneralp, B. (2014). Influence of changes in developed land and precipitation on hydrology of a coastal Texas watershed. *Applied Geography, 47*, 154-167.

Castrucci, L., & Tahvildari, N. (2018). Modeling the impacts of sea level rise on storm surge inundation in flood-prone urban areas of Hampton Roads, Virginia. *Marine Technology Society Journal, 52*(2), 92-105.

CDC. (2017). *Coastal Flooding, Climate Change, and Your Health What You Can Do to Prepare*. Retrieved from https://toolkit.climate.gov/reports/coastal-flooding-climate-change-and-your-health-what-you-can-do-prepare

Chen, F., Zhang, M., Wang, S., Qiu, X., & Du, M. (2017). Environmental controls on stable isotopes of precipitation in Lanzhou, China: An enhanced network at city scale. *Science of the Total Environment, 609*, 1013-1022.

Cheng, Q.-B., Reinhardt-Imjela, C., Chen, X., Schulte, A., Ji, X., & Li, F.-L. (2016). Improvement and comparison of the rainfall–runoff methods in SWAT at the monsoonal watershed of Baocun, Eastern China. *Hydrological sciences journal, 61*(8), 1460-1476.

Chu, H., Wei, J., Qiu, J., Li, Q., & Wang, G. (2019). Identification of the impact of climate change and human activities on rainfall-runoff relationship variation in the Three-River Headwaters region. *Ecological Indicators, 106*, 105516.

Chu, X., Zhang, J., Chi, Y., & Yang, J. (2010). An improved method for watershed delineation and computation of surface depression storage. In *Watershed management 2010: innovations in watershed management under land use and climate change* (pp. 1113-1122).

Conversation and Recreation, D. (1999). Virginia stormwater management handbook. In. Richmond, VA: Virginia Department of Conservation and Recreation, Division of Soil and Water: Chapter.

Cooper, D., Wilkinson, W., & Arnell, N. J. H. s. j. (1995). The effects of climate changes on aquifer storage and river baseflow. *40*(5), 615-631.

Costa, V., & Fernandes, W. J. J. o. H. (2017). Bayesian estimation of extreme flood quantiles using a rainfall-runoff model and a stochastic daily rainfall generator. *554*, 137-154.

Crossett, K., Ache, B., Pacheco, P., & Haber, K. (2013). National coastal population report, population trends from 1970 to 2020. *NOAA State of the Coast Report Series, US Department of Commerce, Washington*.

Dahl, T. E. (1990). *Wetlands losses in the United States, 1780's to 1980's. Report to the Congress*. Retrieved from

Darboux, F., Davy, P., & Gascuel-Odoux, C. (2002). Effect of depression storage capacity on overland-flow generation for rough horizontal surfaces: water transfer distance and scaling. *Earth Surface Processes and Landforms: The Journal of the British Geomorphological Research Group, 27*(2), 177-191.

Dawson, R., Speight, L., Hall, J., Djordjevic, S., Savic, D., & Leandro, J. (2008). Attribution of flood risk in urban areas. *Journal of Hydroinformatics, 10*(4), 275-288.

de Koning, K., Filatova, T., Need, A., & Bin, O. (2019). Avoiding or mitigating flooding: Bottom-up drivers of urban resilience to climate change in the USA. *Global environmental change, 59*, 101981.

De Roo, A., Odijk, M., Schmuck, G., Koster, E., & Lucieer, A. (2001). Assessing the effects of land use changes on floods in the Meuse and Oder catchment. *Physics and Chemistry of the Earth, Part B: Hydrology, Oceans and Atmosphere, 26*(7-8), 593-599.

DeCatanzaro, R., Cvetkovic, M., & Chow-Fraser, P. (2009). The relative importance of road density and physical watershed features in determining coastal marsh water quality in Georgian Bay. *Environmental Management*, *44*(3), 456-467.

Desta, A. S. (2006). Modeling precipitation-runoff relationships to determine water yield from a ponderosa pine forest watershed. *Flagstaff, AZ: Northern Arizona University School of Forestry. 178 p. Thesis.*

Dibike, Y. B., & Coulibaly, P. (2005). Hydrologic impact of climate change in the Saguenay watershed: comparison of downscaling methods and hydrologic models. *Journal of Hydrology*, *307*(1-4), 145-163.

Dickey, D. A., & Fuller, W. A. (1979). Distribution of the estimators for autoregressive time series with a unit root. *Journal of the American Statistical association, 74*(366a), 427-431.

Douglas, I., Garvin, S., Lawson, N., Richards, J., Tippett, J., & White, I. (2010). Urban pluvial flooding: a qualitative case study of cause, effect and nonstructural mitigation. *Journal of Flood Risk Management*, *3*(2), 112-125.

Dunne, T., Zhang, W., & Aubry, B. F. (1991). Effects of rainfall, vegetation, and microtopography on infiltration and runoff. *Water Resources Research, 27*(9), 2271-2285.

Easton, Z. M., Fuka, D. R., Walter, M. T., Cowan, D. M., Schneiderman, E. M., & Steenhuis, T. S. J. J. o. h. (2008). Re-conceptualizing the soil and water assessment tool (SWAT) model to predict runoff from variable source areas. *348*(3-4), 279-291.

Ediblecascadia. (2015). Commercial Cistern.

El-Jabi, N., & Sarraf, S. (1991). Effect of maximum rainfall position on rainfall-runoff relationship. *Journal of Hydraulic Engineering*, *117*(5), 681-685.

Environment Agency, U. (2017). Retrieved from http://www.gov.uk/environment-agency

EPA. (1998). Your Coastal Watershed.

EPA. (2014). *Taking Action:*

A Guide for Homeowners. Retrieved from City of Franklin, VA: https://www.cnt.org/sites/default/files/uploads/RainReady-10-Actions-for-Homeowners.pdf

Fares, A. (2008). Overview of the hydrological modeling of small coastal watersheds on tropical islands. *Coastal Watershed Management, 13*, 1.

Fares, A., & El-Kadi, A. (2008). *Coastal Watershed Management*.

Faulkner, S. (2004). Urbanization impacts on the structure and function of forested wetlands. *Urban ecosystems, 7*(2), 89-106.

FEMA511. (2005). Reducing Damage from Localized Flooding: A Guide for Communities.

FEMA. (1992). *Floodplain Management in the United States: An Assessment Report (vol. 2)*. Retrieved from

FEMA. (2001). *Modernizing FEMAs flood hazard mapping program*. Retrieved from http://www.fema.gov/pdf/fhm/mm_fy01.pdf

FEMA. (2002). *Flood Insurance Study, City of Franklin, Virginia, Independent City*. Retrieved from

Ferguson, B. K., & Suckling, P. W. (1990). CHANGING RAINFALL-RUNOFF RELATIONSHIPS IN THE URBANIZING PEACHTREE CREEK WATERSHED, ATLANTA, GEORGIA 1. *JAWRA Journal of the American Water Resources Association, 26*(2), 313-322.

Frei, S., & Fleckenstein, J. H. (2014). Representing effects of micro-topography on runoff generation and sub-surface flow patterns by using superficial rill/depression storage height variations. *Environmental modelling & software, 52*, 5-18.

Fu, C., Chen, J., & Zeng, S. J. J. o. H. E. (2012). Observation and analysis of rainfall-runoff characteristics in a coastal granite catchment in Southern China. *17*(1), 138-149.

Gan, T. Y., Dlamini, E. M., & Biftu, G. F. (1997). Effects of model complexity and structure, data quality, and objective functions on hydrologic modeling. *Journal of Hydrology, 192*(1-4), 81-103.

Gassman, P. W., Reyes, M. R., Green, C. H., & Arnold, J. G. (2007). The soil and water assessment tool: historical development, applications, and future research directions. *Transactions of the ASABE, 50*(4), 1211-1250.

Gatley., F. D. (2015). Emergebcy Management.

Gesch, D. B., Oimoen, M. J., & Evans, G. A. (2014). *Accuracy assessment of the US Geological Survey National Elevation Dataset, and comparison with other large-area elevation datasets: SRTM and ASTER* (Vol. 1008): US Department of the Interior, US Geological Survey.

Ghorbani, K., Halaghi, M. M., Sohrabian, E., Golian, S., & Zakerinia, M. (2016). Evaluation of hydrological and data-based models in estimation of daily runoff in Galikesh watershed. *International Journal of Hydrology Science and Technology, 6*(1), 27-44.

Ghumman, A., Ghazaw, Y. M., Sohail, A., & Watanabe, K. (2011). Runoff forecasting by artificial neural network and conventional model. *Alexandria Engineering Journal, 50*(4), 345-350.

Gimenez-Maranges, M., Breuste, J., & Hof, A. (2020). Sustainable Drainage Systems for transitioning to sustainable urban flood management in the European Union: A review. *Journal of Cleaner Production, 255*, 120191.

Goel, N., Kurothe, R., Mathur, B., & Vogel, R. (2000). A derived flood frequency distribution for correlated rainfall intensity and duration. *Journal of Hydrology, 228*(1-2), 56-67.

Golmohammadi, G., Prasher, S., Madani, A., & Rudra, R. J. H. (2014). Evaluating three hydrological distributed watershed models: MIKE-SHE, APEX, SWAT. *1*(1), 20-39.

Guhathakurta, P., Sreejith, O., & Menon, P. (2011). Impact of climate change on extreme rainfall events and flood risk in India. *Journal of earth system science, 120*(3), 359-373.

Gunn, J. R. (2016). *Urban Patterns and Flood Damage in Texas Coastal Watersheds.* Texas A & M University,

Hallegatte, S., Green, C., Nicholls, R. J., & Corfee-Morlot, J. (2013). Future flood losses in major coastal cities. *Nature climate change, 3*(9), 802-806.

Hampton Roads Hazard Mitigation Plan. (2017). *Hampton Roads Hazard Mitigation Plan*

Retrieved from https://www.franklinva.com/media/161116/2017-hampton-roads-hazard-mitigation-plan-update-final.pdf

Heath, R. C. (1984). *Ground-water regions of the United States* (Vol. 2242): US Department of the Interior, Geological Survey.

Hey, D. L., & Philippi, N. S. (1995). Flood reduction through wetland restoration: the Upper Mississippi River Basin as a case history. *Restoration Ecology, 3*(1), 4-17.

Hipel, K. W., & McLeod, A. I. (1994). *Time series modelling of water resources and environmental systems*: Elsevier.

Holman-Dodds, J. K., Bradley, A. A., & Potter, K. W. (2003). Evaluation of hydrologic benefits of infiltration based urban storm water management 1. *JAWRA Journal of the American Water Resources Association, 39*(1), 205-215.

Homer, C. H., Fry, J. A., & Barnes, C. A. (2012). *The national land cover database*. Retrieved from

Howitt, J. A., Baldwin, D. S., Rees, G. N., & Williams, J. L. (2007). Modelling blackwater: predicting water quality during flooding of lowland river forests. *Ecological Modelling, 203*(3-4), 229-242.

Hunt, R. J., Walker, J. F., & Krabbenhoft, D. P. (1999). Characterizing hydrology and the importance of ground-water discharge in natural and constructed wetlands. *Wetlands, 19*(2), 458-472.

Huntington, T. G. (2010). Chapter One - Climate Warming-Induced Intensification of the Hydrologic Cycle: An Assessment of the Published Record and Potential Impacts on Agriculture. In D. L. Sparks (Ed.), *Advances in Agronomy* (Vol. 109, pp. 1-53): Academic Press.

Hyndman, R. J., & Koehler, A. B. (2006). Another look at measures of forecast accuracy. *International journal of forecasting, 22*(4), 679-688.

Ibarra-Zavaleta, S., Landgrave, R., Romero-López, R., Poulin, A., & Arango-Miranda, R. J. W. (2017). Distributed hydrological modeling: Determination of theoretical hydraulic potential & streamflow simulation of extreme hydrometeorological events. *9*(8), 602.

Joel, A., Messing, I., Seguel, O., & Casanova, M. (2002). Measurement of surface water runoff from plots of two different sizes. *Hydrological Processes, 16*(7), 1467-1478.

Jung, Y., Shin, Y., Won, N.-I., & Lim, K. J. (2016). Web-based BFlow system for the assessment of streamflow characteristics at national level. *Water, 8*(9), 384.

Kalcic, M. M., Chaubey, I., & Frankenberger, J. (2015). Defining Soil and Water Assessment Tool (SWAT) hydrologic response units (HRUs) by field boundaries. *International Journal of Agricultural and Biological Engineering, 8*(3), 69-80.

Kang, H., & Nielsen, P. (1997). Watertable dynamics in coastal areas. In *Coastal Engineering 1996* (pp. 4601-4612).

Kang, I. S., Park, J. I., & Singh, V. P. (1998). Effect of urbanization on runoff characteristics of the On-Cheon Stream watershed in Pusan, Korea. *Hydrological Processes, 12*(2), 351-363.

Kannan, N., White, S., Worrall, F., & Whelan, M. (2007). Sensitivity analysis and identification of the best evapotranspiration and runoff options for hydrological modelling in SWAT-2000. *Journal of Hydrology, 332*(3-4), 456-466.

Kasei, R. A., Ampadu, B., & Sapanbil, G. S. (2013). Relationship between Rainfall-Runoff on the White Volta River at Pwalugu of the Volta Basin in Ghana. *Journal of Environment and Earth Science, 3*(11), 92-99.

Kiedrzyńska, E., Kiedrzyński, M., & Zalewski, M. (2015). Sustainable floodplain management for flood prevention and water quality improvement. *Natural Hazards, 76*(2), 955-977.

Kim, N. W., & Lee, J. (2008). Temporally weighted average curve number method for daily runoff simulation. *Hydrological Processes: An International Journal, 22*(25), 4936-4948.

Kreibich, H., Thieken, A. H., Petrow, T., Müller, M., & Merz, B. (2005). Flood loss reduction of private households due to building precautionary measures--lessons learned from the Elbe flood in August 2002.

Kwiatkowski, D., Phillips, P. C., Schmidt, P., & Shin, Y. (1992). Testing the null hypothesis of stationarity against the alternative of a unit root: How sure are we that economic time series have a unit root? *Journal of econometrics, 54*(1-3), 159-178.

Labat, D., Goddéris, Y., Probst, J. L., & Guyot, J. L. (2004). Evidence for global runoff increase related to climate warming. *Advances in water resources, 27*(6), 631-642.

Leavesley, G., Lichty, R., Troutman, B., & Saindon, L. (1983). Precipitation-runoff modeling system: User’s manual. *Water-resources investigations report, 83*(4238), 207.

Lee, J., Kim, J., Jang, W., Lim, K., & Engel, B. J. W. (2018). Assessment of baseflow estimates considering recession characteristics in SWAT. *10*(4), 371.

Legates, D. R., & McCabe Jr, G. J. (1999). Evaluating the use of “goodness-of-fit” measures in hydrologic and hydroclimatic model validation. *Water Resources Research, 35*(1), 233-241.

Legret, M., Colandini, V., & Le Marc, C. J. S. o. t. t. e. (1996). Effects of a porous pavement with reservoir structure on the quality of runoff water and soil. *189*, 335-340.

Li, R. (2018). *Predicting Effects of Climate Change and Sea Level Rise on Hydrologic Processes in a Mid-Atlantic Coastal Watershed.*

Line, D., & White, N. (2007). Effects of development on runoff and pollutant export. *Water Environment Research, 79*(2), 185-190.

Liu, B. M., Collick, A. S., Zeleke, G., Adgo, E., Easton, Z. M., & Steenhuis, T. S. J. H. P. A. I. J. (2008). Rainfall-discharge relationships for a monsoonal climate in the Ethiopian highlands. *22*(7), 1059-1067.

Liu, C., & Zheng, H. (2004). Changes in components of the hydrological cycle in the Yellow River basin during the second half of the 20th century. *Hydrological Processes, 18*(12), 2337-2345.

Ljung, G. M., & Box, G. E. (1978). On a measure of lack of fit in time series models. *Biometrika, 65*(2), 297-303.

Loaiciga, H. A., Valdes, J. B., Vogel, R., Garvey, J., & Schwarz, H. (1996). Global warming and the hydrologic cycle. *Journal of Hydrology, 174*(1-2), 83-127.

Lu, J., Sun, G., Amatya, D. M., Harder, S., & McNulty, S. G. (2006). *Understanding the hydrologic response of a coastal plain watershed to forest management and climate change in South Carolina, USA.* Paper presented at the Hydrology and Management of Forested Wetlands, Proceedings of the International Conference, April 8-12, 2006, New Bern, North Carolina.

Luna, M. C. d. M., Parteli, E. J., Durán, O., & Herrmann, H. J. (2011). Model for the genesis of coastal dune fields with vegetation. *Geomorphology, 129*(3-4), 215-224.

Lyne, V., & Hollick, M. (1979). *Stochastic time-variable rainfall-runoff modelling.* Paper presented at the Institute of Engineers Australia National Conference.

Magilligan, F., Nislow, K., Fisher, G., Wright, J., Mackey, G., & Laser, M. (2008). The geomorphic function and characteristics of large woody debris in low gradient rivers, coastal Maine, USA. *Geomorphology, 97*(3-4), 467-482.

Mallin, M. A., Williams, K. E., Esham, E. C., & Lowe, R. P. (2000). Effect of human development on bacteriological water quality in coastal watersheds. *Ecological applications, 10*(4), 1047-1056.

Manguerra, H., & Engel, B. (1998). HYDROLOGIC PARAMETERIZATION OF WATERSHEDS FOR RUNOFF PREDICTION USING SWAT 1. *JAWRA Journal of the American Water Resources Association, 34*(5), 1149-1162.

Marchi, L., Brunetti, M. T., Cavalli, M., & Crema, S. (2019). Debris-flow volumes in northeastern Italy: Relationship with drainage area and size probability. *Earth Surface Processes and Landforms, 44*(4), 933-943.

Marquínez, J., Lastra, J., & García, P. J. J. o. h. (2003). Estimation models for precipitation in mountainous regions: the use of GIS and multivariate analysis. *270*(1-2), 1-11.

Marsalek, J., W. E. Watt, E. Zeman, & Sieker, F. (2000). Overview of flood issues in contemporary water management. In *Flood Issues in Contemporary Water Management* (pp. 1-16): Springer.

Martin, E. H., & Smoot, J. L. (1986). *Constituent-load changes in urban stormwater runoff routed through a detention pond-wetlands system in central Florida* (Vol. 85): US Department of the Interior, Geological Survey.

Martz, L. W., & Garbrecht, J. (1993). Automated extraction of drainage network and watershed data from digital elevation models 1. *JAWRA Journal of the American Water Resources Association, 29*(6), 901-908.

McCabe, G. J., & Wolock, D. M. (2011). Independent effects of temperature and precipitation on modeled runoff in the conterminous United States. *Water Resources Research, 47*(11).

Miller, J. D., & Hutchins, M. (2017). The impacts of urbanisation and climate change on urban flooding and urban water quality: A review of the evidence concerning the United Kingdom. *Journal of Hydrology: Regional Studies, 12*, 345-362.

Mitsch, W. J., Reeder, B. C., & Klarer, D. M. (1989). The role of wetlands in the control of nutrients with a case study of western Lake Erie. *JOHN WILEY, NEW YORK, NY(USA).* 129-158.

Modarres, R., & Ouarda, T. B. (2013). Modeling rainfall–runoff relationship using multivariate GARCH model. *Journal of Hydrology, 499*, 1-18.

Molnar, P., & Ramírez, J. A. (2001). Recent trends in precipitation and streamflow in the Rio Puerco Basin. *Journal of climate, 14*(10), 2317-2328.

Moore, S. (2018). The political economy of flood management reform in China. *International Journal of Water Resources Development, 34*(4), 566-577.

Moravej, M., & Khalili, K. (2015). Hydrological time series analysis and modelling using statistical tests and linear time series models (case study: West Azerbaijan province of Iran). *International Journal of Hydrology Science and Technology, 5*(4), 349-371.

Moriasi, D. N., Arnold, J. G., Van Liew, M. W., Bingner, R. L., Harmel, R. D., & Veith, T. L. (2007). Model evaluation guidelines for systematic quantification of accuracy in watershed simulations. *Transactions of the ASABE, 50*(3), 885-900.

Mu, W., Yu, F., Li, C., Xie, Y., Tian, J., Liu, J., & Zhao, N. (2015). Effects of rainfall intensity and slope gradient on runoff and soil moisture content on different growing stages of spring maize. *Water, 7*(6), 2990-3008.

Nash, J. E., & Sutcliffe, J. V. (1970). River flow forecasting through conceptual models part I—A discussion of principles. *Journal of Hydrology, 10*(3), 282-290.

National Research Council. (2007). *Elevation data for floodplain mapping*: National Academies Press.

Nayak, P., Sudheer, K., & Ramasastri, K. (2005). Fuzzy computing based rainfall–runoff model for real time flood forecasting. *19*(4), 955-968.

Neitsch, S. (2005). Soil and water assessment tool. *476*.

Neitsch, S. L., Arnold, J. G., Kiniry, J. R., & Williams, J. R. (2011). *Soil and water assessment tool theoretical documentation version 2009*. Retrieved from

Nicholls, R. J., Hoozemans, F. M., & Marchand, M. (1999). Increasing flood risk and wetland losses due to global sea-level rise: regional and global analyses. *Global environmental change, 9*, S69-S87.

Niedzielski, T. (2007). A data-based regional scale autoregressive rainfall-runoff model: a study from the Odra River. *Stochastic Environmental Research and Risk Assessment, 21*(6), 649-664.

Nigam, R., Nigam, S., & Mittal, S. K. (2014). Stochastic modelling of rainfall and runoff phenomenon: a time series approach review. *International Journal of Hydrology Science and Technology, 4*(2), 81-109.

Niroomandi, A., Ma, G., Ye, X., Lou, S., & Xue, P. (2018). Extreme value analysis of wave climate in Chesapeake Bay. *Ocean Engineering, 159*, 22-36.

NOAA. (2017). What is high tide flooding?

Nourani, V., Kisi, Ö., & Komasi, M. (2011). Two hybrid artificial intelligence approaches for modeling rainfall–runoff process. *Journal of Hydrology, 402*(1-2), 41-59.

Nourani, V., Komasi, M., & Mano, A. J. W. r. m. (2009). A multivariate ANN-wavelet approach for rainfall–runoff modeling. *23*(14), 2877.

NRCS, N. R. C. S. (2017). Part 630 Hydrology National Engineering Handbook - Chapter 10: Estimation of Direct Runoff from Storm Rainfall. Washington D.C.: U.S. Department of Agriculture. In.

NRCS, N. R. C. S., USDA (United States Department of Agriculture). (2000). Climate Narrative for Franklin County, Virginia. Retrieved from https://www.wcc.nrcs.usda.gov/legacy/ftp/support/climate/soil-nar/va/

O'Connell, P., Ewen, J., O'Donnell, G., & Quinn, P. (2007). Is there a link between agricultural land-use management and flooding?

Ogawa, H., & Male, J. W. (1986). Simulating the flood mitigation role of wetlands. *Journal of Water Resources Planning and Management, 112*(1), 114-128.

Oki, T., & Kanae, S. (2006). Global hydrological cycles and world water resources. *science, 313*(5790), 1068-1072.

Olivera, F., & DeFee, B. B. (2007). Urbanization and Its Effect On Runoff in the Whiteoak Bayou Watershed, Texas 1. *JAWRA Journal of the American Water Resources Association, 43*(1), 170-182.

Olsen, J. R., Beling, P. A., & Lambert, J. H. (2000). Dynamic models for floodplain management. *Journal of Water Resources Planning and Management, 126*(3), 167-175.

Oppenheimer., M., Bruce C. Glavovic (New Zealand, S. A., (Germany), J. H., (Netherlands), R. V. D. W., (France), A. K. M., (Egypt), A. A.-E., (China), R. C., Rica), M. C.-J. C., States), R. M. D. U., (India), T. G., Is.), J. H. C., (Argentina), F. I., (Germany), B. M., (France), B. M., Zita Sebesvari (Hungary, G., (Netherlands), R. B., States), M. K. B. U., Kingdom), R. S. d. C. U., (France), G. L. C., (Australia), C. D., (Germany), S. D., (Germany), P. D., (France), V. K. E. D., Kingdom), T. E. U., (Russia), A. E., (Canada), D. F., Kingdom), J. F. U., (Philippines), M. D. F., (Netherlands), T. F., (France), J.-P. G., States), R. K. U., (Netherlands), E. L., Zealand), J. L. N., Andrew Mackintosh (Australia, N. Z., (France), A. M., States), E. M. U., States), M. M. U., States), S. N. U., States), R. J. N. U., Kingdom), F. R. U., Kingdom), J. S. U., Africa), A. S. S., Africa), C. S. S., (Vietnam), N. M. T., States), J. W. U., (Singapore), P. P. W., & States), S. X. U. (2016). *Special Report on the Ocean and Cryosphere in a Changing Climate*. Retrieved from

Orupabo, S., Hart, L., Okwere, A. J. E. J. o. E. S., & Management. (2015). Flood prediction using rainfall–runoff spatial variation: An overview of flood prediction models. *8*(4), 377-386.

Pektaş, A. O., & Cigizoglu, H. K. (2013). ANN hybrid model versus ARIMA and ARIMAX models of runoff coefficient. *Journal of Hydrology, 500*, 21-36.

Peña-Arancibia, J. L., Bruijnzeel, L. A., Mulligan, M., & van Dijk, A. I. (2019). Forests as ‘sponges’ and ‘pumps’: Assessing the impact of deforestation on dry-season flows across the tropics. *Journal of Hydrology, 574*, 946-963.

Peng, T., & Wang, S.-j. (2012). Effects of land use, land cover and rainfall regimes on the surface runoff and soil loss on karst slopes in southwest China. *Catena, 90*, 53-62.

Pielke, R. A., Downton, M. W., & Miller, J. B. (2002). *Flood damage in the United States, 1926-2000: a reanalysis of National Weather Service estimates*. Retrieved from

Pilgrim, D. H., Cordery, I., & Baron, B. C. (1982). Effects of catchment size on runoff relationships. *Journal of Hydrology, 58*(3-4), 205-221.

Potter, K. W. J. W. R. R. (1991). Hydrological impacts of changing land management practices in a moderate-sized agricultural catchment. *27*(5), 845-855.

Pugh, A. L., & Westerman, D. A. (2014). *Mean annual, seasonal, and monthly precipitation and runoff in Arkansas, 1951-2011* (2014-5006). Retrieved from Reston, VA: http://pubs.er.usgs.gov/publication/sir20145006

Qi, S., Sun, G., Wang, Y., McNulty, S., & Myers, J. M. (2009). Streamflow response to climate and landuse changes in a coastal watershed in North Carolina. *Transactions of the ASABE, 52*(3), 739-749.

Rafter, G. W. (1903). *The relation of rainfall to run-off*. Retrieved from

Rahimi, R., Tavakol-Davani, H., Graves, C., Gomez, A., & Fazel Valipour, M. (2020). Compound Inundation Impacts of Coastal Climate Change: Sea-Level Rise, Groundwater Rise, and Coastal Watershed Precipitation. *Water, 12*(10), 2776.

Rajurkar, M., Kothyari, U., & Chaube, U. (2004). Modeling of the daily rainfall-runoff relationship with artificial neural network. *Journal of Hydrology, 285*(1-4), 96-113.

Rao, K., Steenhuis, T., Cogle, A., Srinivasan, S., Yule, D., & Smith, G. (1998). Rainfall infiltration and runoff from an Alfisol in semi-arid tropical India. II. Tilled systems. *Soil and tillage research, 48*(1-2), 61-69.

Roanoke Valley Alleghany Regional Commission. (2007). *Flood Prone Roadway Study*. Retrieved from www.rvarc.org

Rosim, S., de Oliveira Ortiz, J., de Freitas Oliveira, J. R., Jardim, A. C., & Abreu, E. S. (2015). Drainage Network Definition for Low Resolution DEM Obtained from Drainage Network Extracted from High Resolution DEM Using Upscaling Processes. In *Engineering Geology for Society and Territory-Volume 3* (pp. 271-274): Springer.

Rostamian, R., Jaleh, A., Afyuni, M., Mousavi, S. F., Heidarpour, M., Jalalian, A., & Abbaspour, K. C. (2008). Application of a SWAT model for estimating runoff and sediment in two mountainous basins in central Iran. *Hydrological sciences journal, 53*(5), 977-988.

Santhi, C., Arnold, J. G., Williams, J. R., Dugas, W. A., Srinivasan, R., & Hauck, L. M. J. J. J. o. t. A. W. R. A. (2001). Validation of the swat model on a large rwer basin with point and nonpoint sources 1. *37*(5), 1169-1188.

Schmitt, T. G., Thomas, M., & Ettrich, N. (2004). Analysis and modeling of flooding in urban drainage systems. *Journal of Hydrology, 299*(3-4), 300-311.

Seaburn, G. (1969). *Effects of urban development on direct runoff to East Meadow Brook, Nassau County, Long Island, New York*: US Government Printing Office.

Şen, Z. (1998). Average areal precipitation by percentage weighted polygon method. *Journal of Hydrologic Engineering, 3*(1), 69-72.

Shen, Y., Morsy, M. M., Huxley, C., Tahvildari, N., & Goodall, J. L. (2019). Flood risk assessment and increased resilience for coastal urban watersheds under the combined impact of storm tide and heavy rainfall. *Journal of Hydrology, 579*, 124159.

Shutes, R., Revitt, D., Lagerberg, I., & Barraud, V. J. S. o. t. T. E. (1999). The design of vegetative constructed wetlands for the treatment of highway runoff. *235*(1-3), 189-197.

Singh, K. P. (1968). Some factors affecting baseflow. *Water Resources Research, 4*(5), 985-999.

Sitterson, J., Knightes, C., Parmar, R., Wolfe, K., Muche, M., & Avant, B. (2017). An Overview of Rainfall-Runoff

Model Types Retrieved from FINAL_RUNOFF_MODELS_SITTERSON 508 REVISED.PDF

Sklash, M. G., & Farvolden, R. N. (1979). The role of groundwater in storm runoff. In *Developments in water science* (Vol. 12, pp. 45-65): Elsevier.

Smith, J., Welsh, S. A., Anderson, J. T., & Fortney, R. H. J. S. N. (2015). Water quality trends in the Blackwater River watershed, West Virginia. *14*(sp7), 103-112.

Smyth, S. (2015). Why wait for ministers? I built my own £20,000 flood defence: Engineer fitted walls, gates and pumps around his cottage to realise his dream of living by the river. *Daily mail*. Retrieved from www.dailymail.co.uk/news/article-3380743/Why-wait-ministers-built-20-000-flood-defence-Engineer-fitted-walls-gates-pumps-cottage-realise-dream-living-river.html

Sohail, A., Watanabe, K., & Takeuchi, S. (2008). Runoff analysis for a small watershed of Tono area Japan by back propagation artificial neural network with seasonal data. *Water resources management, 22*(1), 1-22.

Strecker, E. W. (1992). The use of wetlands for controlling stormwater pollution.

Sun, Z., Li, X., Fu, W., Li, Y., & Tang, D. (2013). Long-term effects of land use/land cover change on surface runoff in urban areas of Beijing, China. *Journal of Applied Remote Sensing, 8*(1), 084596.

Syed, K. H., Goodrich, D. C., Myers, D. E., & Sorooshian, S. (2003). Spatial characteristics of thunderstorm rainfall fields and their relation to runoff. *Journal of Hydrology, 271*(1-4), 1-21.

Tahvildari, N., & Castrucci, L. (2020). Relative Sea Level Rise Impacts on Storm Surge Flooding of Transportation Infrastructure. *Natural Hazards Review, 22*(1), 04020045.

Talchabhadel, R., Shakya, N. M., Dahal, V., & Eslamian, S. J. J. o. F. E. (2015). Rainfall Runoff Modelling for Flood Forecasting (A Case Study on West Rapti Watershed). *6*(1), 53-61.

Tankersley, C. D., Graham, W. D., & Hatfield, K. (1993). Comparison of univariate and transfer function models of groundwater fluctuations. *Water Resources Research, 29*(10), 3517-3533.

Tasdighi, A., Arabi, M., & Harmel, D. (2018). A probabilistic appraisal of rainfall-runoff modeling approaches within SWAT in mixed land use watersheds. *Journal of Hydrology, 564*, 476-489.

Teegavarapu, R. S., & Chandramouli, V. J. J. o. H. (2005). Improved weighting methods, deterministic and stochastic data-driven models for estimation of missing precipitation records. *312*(1-4), 191-206.

Todini, E. (1988). Rainfall-runoff modeling—Past, present and future. *Journal of Hydrology, 100*(1-3), 341-352.

Tokar, A. S., & Johnson, P. A. (1999). Rainfall-runoff modeling using artificial neural networks. *Journal of Hydrologic Engineering, 4*(3), 232-239.

Ullah, W., & Dickinson, W. (1979). Quantitative description of depression storage using a digital surface model: I. Determination of depression storage. *Journal of Hydrology, 42*(1-2), 63-75.

van der Valk, A. G., Squires, L., & Welling, C. (1994). Assessing the impacts of an increase in water level on wetland vegetation. *Ecological Applications, 4*(3), 525-534.

Van Dijk, A., Meesters, A., Schellekens, J., & Bruijnzeel, L. (2005). A two-parameter exponential rainfall depth-intensity distribution applied to runoff and erosion modelling. *Journal of Hydrology, 300*(1-4), 155-171.

Van Liew, M., Arnold, J., & Garbrecht, J. J. T. o. t. A. (2003). Hydrologic simulation on agricultural watersheds: Choosing between two models. *46*(6), 1539.

Vicente-Serrano, S. M., Saz-Sánchez, M. A., & Cuadrat, J. M. (2003). Comparative analysis of interpolation methods in the middle Ebro Valley (Spain): application to annual precipitation and temperature. *Climate research, 24*(2), 161-180.

Vieux, B. E. (2001). Distributed hydrologic modeling using GIS. In *Distributed Hydrologic Modeling Using GIS* (pp. 1-17): Springer.

Virginia, O. o. G. C. o. (2020). VIRGINIA COASTAL RESILIENCE MASTER PLANNING FRAMEWORK, Principles and Strategies for Coastal Flood

Protection and Adaptation. Retrieved

Vörösmarty, C. J., Green, P., Salisbury, J., & Lammers, R. B. J. s. (2000). Global water resources: vulnerability from climate change and population growth. *289*(5477), 284-288.

Wan, H., McLaughlin, D., Shao, Y., van Eerden, B., Ranganathan, S., & Deng, X. (2021). Remotely-sensed evapotranspiration for informed urban forest management. *Landscape and Urban Planning, 210*, 104069.

Wang, W.-c., Chau, K.-w., Xu, D.-m., & Chen, X.-Y. (2015). Improving forecasting accuracy of annual runoff time series using ARIMA based on EEMD decomposition. *Water resources management, 29*(8), 2655-2675.

Wang, X., & Melesse, A. M. (2006). Effects of statsgo and ssurgo as inputs on swat model's snowmelt simulation 1. *JAWRA Journal of the American Water Resources Association, 42*(5), 1217-1236.

Wang Xixi, Li, R., Jalaeian Taghadomi, H., Pedram, S., & Zhao, X. (2017). Effects of sea level rise on hydrology: case study in a typical mid-Atlantic coastal watershed. *Journal of Water and Climate Change, 8*(4), 730-754.

Wei, W., Chen, L., Fu, B., Huang, Z., Wu, D., & Gui, L. (2007). The effect of land uses and rainfall regimes on runoff and soil erosion in the semi-arid loess hilly area, China. *Journal of Hydrology, 335*(3-4), 247-258.

Wheater, H., & Evans, E. (2009). Land use, water management and future flood risk. *Land use policy, 26*, S251-S264.

White, G. F. (1937). Notes on flood protection and land-use planning. *The Planners' Journal, 3*(3), 57-61.

Winchell, M., Srinivasan, R., Di Luzio, M., Arnold, J. J. S., & Water Research Laboratory, U. A. R. S., Texas. (2013). ArcSWAT interface for SWAT2012: user's guide. Blackland Research and Extension Center, Texas Agrilife Research. Grassland. *3*.

Windham-Myers, L., Marvin-DiPasquale, M., Kakouros, E., Agee, J. L., Kieu, L. H., Stricker, C. A., Fleck, J. A., & Ackerman, J. T. (2014). Mercury cycling in agricultural and managed wetlands of California, USA: Seasonal influences of vegetation on mercury methylation, storage, and transport. *Science of the Total Environment, 484*, 308-318. Retrieved from https://www.sciencedirect.com/science/article/abs/pii/S0048969713005706?via%3Dihub

Winkler, R. D., Moore, R., Redding, T. E., Spittlehouse, D. L., Carlyle-Moses, D. E., & Smerdon, B. D. (2010). Hydrologic processes and watershed. *Compendium of forest hydrology and geomorphology in British Columbia. BC Min. For. Range, 66*, 133.

Winter, T. C., Harvey, J. W., Franke, O. L., & Alley, W. M. (1998). *Ground water and surface water: a single resource* (Vol. 1139): DIANE Publishing Inc.

Wittenberg, H. J. H. P. (2003). Effects of season and man-made changes on baseflow and flow recession: case studies. *17*(11), 2113-2123.

Wong, T. H., Breen, P. F., & Somes, N. L. (1999). *Ponds vs wetlands–performance considerations in stormwater quality management.* Paper presented at the Proceedings of the 1st South Pacific Conference on Comprehensive Stormwater and Aquatic Ecosystem Management.

Woodruff, J. D., Irish, J. L., & Camargo, S. J. (2013). Coastal flooding by tropical cyclones and sea-level rise. *Nature, 504*(7478), 44-52.

Wooldridge, S. A., Franks, S. W., & Kalma, J. D. (2001). Hydrological implications of the Southern Oscillation: variability of the rainfall-runoff relationship. *Hydrological sciences journal, 46*(1), 73-88.

Wu, M., Shi, P., Chen, A., Shen, C., & Wang, P. (2017). Impacts of DEM resolution and area threshold value uncertainty on the drainage network derived using SWAT. *Water Sa, 43*(3), 450-462.

Wu, S., Yu, M., & Chen, L. (2017). Nonmonotonic and spatial-temporal dynamic slope effects on soil erosion during rainfall-runoff processes. *Water Resources Research, 53*(2), 1369-1389.

Xu, J. (2011). Variation in annual runoff of the Wudinghe River as influenced by climate change and human activity. *Quaternary International, 244*(2), 230-237.

Xu, K., Ma, C., Lian, J., & Bin, L. (2014). Joint probability analysis of extreme precipitation and storm tide in a coastal city under changing environment. *PLoS One, 9*(10), e109341.

Yang, W.-Y., Li, D., Sun, T., & Ni, G.-H. (2015). Saturation-excess and infiltration-excess runoff on green roofs. *Ecological Engineering, 74*, 327-336.

Yao, L., Wei, W., & Chen, L. J. E. I. (2016). How does imperviousness impact the urban rainfall-runoff process under various storm cases? *, 60*, 893-905.

Yao, Q., & Brockwell, P. J. (2006). Gaussian maximum likelihood estimation for ARMA models. I. time series. *Journal of time series analysis, 27*(6), 857-875.

Zeng, Q., Chen, H., Xu, C.-Y., Jie, M.-X., & Hou, Y.-K. J. H. R. (2016). Feasibility and uncertainty of using conceptual rainfall-runoff models in design flood estimation. *47*(4), 701-717.

Zhang, A., Zhang, C., Fu, G., Wang, B., Bao, Z., & Zheng, H. (2012). Assessments of impacts of climate change and human activities on runoff with SWAT for the Huifa River Basin, Northeast China. *Water resources management, 26*(8), 2199-2217.

Zhang, R., Li, Q., Chow, T. L., Li, S., & Danielescu, S. (2013). Baseflow separation in a small watershed in New Brunswick, Canada, using a recursive digital filter calibrated with the conductivity mass balance method. *Hydrological Processes, 27*(18), 2659-2665.

Zhang, S., Hua, D., Meng, X., & Zhang, Y. (2011). Climate change and its driving effect on the runoff in the "Three-River Headwaters" region. *Journal of Geographical Sciences, 21*(6), 963.

Zhao, W., & Khalil, M. (1993). The relationship between precipitation and temperature over the contiguous United States. *Journal of climate, 6*(6), 1232-1236.

Zhou, M., Qu, S., Chen, X., Shi, P., Xu, S., Chen, H., Zhou, H., & Gou, J. J. W. (2019). Impact Assessments of Rainfall–Runoff Characteristics Response Based on Land Use Change via Hydrological Simulation. *11*(4), 866.

Ziervogel, G., Waddell, J., Smit, W., & Taylor, A. (2016). Flooding in Cape Town's informal settlements: barriers to collaborative urban risk governance. *South African Geographical Journal, 98*(1), 1-20.

Zurbuch, P. E. (1963). Dissolving limestone from revolving drums in flowing water. *Transactions of the American Fisheries Society, 92*(2), 173-178.

VITA

Homa Jalaeian Taghadomi
Department of Civil and Environmental Engineering
Old Dominion University, 5115 Hampton Blvd, Norfolk, VA 23529

EDUCATION

- Master of Environmental Science (2012), University Putra Malaysia, Malaysia
- Bachelor's Degree in environmental science (2007), University of Birjand, Iran
- Associated Degree in Environmental Science (2003), University of Birjand, Iran

FELLOWSHIP

- Commonwealth of Virginia Engineering and Science (COVES) Policy Fellowship (May 17-August 6, 2021), funded by Virginia Academy of Science, Engineering and Medicine (VASEM).

PUBLICATIONS

- **Homa Jalaeian Taghadomi**, Xixi Wang, Mujde Erten-Unal, and Vazifedan Turaj. (Accepted for Publication) "Assessment of Rainfall-Runoff Time Series Data Using Transfer Function Modelling with Exogenous Variable." International Journal of Hydrology Science and Technology.
- Vazifedan, Turaj, **Homa Jalaeian Taghadomi**, Xixi Wang and Mujde Erten-Unal. (2020). "Parameter Estimation of a Seasonal Poisson INAR (1) Model with Different Monthly Means." *Journal of Data Science* 18(4):697-717.
- Wang, Xixi, Rui Li, **Homa Jalaeian Taghadomi**, Shohreh Pedram and Xiao Zhao. (2017). "Effects of Sea Level Rise on Hydrology: Case Study in a Typical Mid-Atlantic Coastal Watershed." *Journal of Water and Climate Change* 8(4):730-54.
- **Jalaeian Taghadomi, Homa**. (2012). "Assessment of Household Electrical and Electronic Waste Management: A Case Study in Putrajaya (Malaysia)." LAP LAMBERT Academic Publishing.

CONFERENCES

- **Jalaeian Taghadomi, Homa**, Xixi Wang, Mujde Ertan Unal and Turaj Vazifedan. 2018. "Rainfall-Runoff Modeling in a Virginian Coastal Watershed Using an ARMA Model." AGUFM 2018:H22I-01.
- **Homa Jalaeian Taghadomi** and Hamid Sharifan. 2005. "Assessing water resources using GIS in Birjand." Environment, Biotechnology and Industry, First symposium on environmental research, Tehran.